INFORMATION TO USERS

This was produced from a copy of a document sent to us for microfilming. While the most advanced technological means to photograph and reproduce this document have been used, the quality is heavily dependent upon the quality of the material submitted.

The following explanation of techniques is provided to help you understand markings or notations which may appear on this reproduction.

1. The sign or "target" for pages apparently lacking from the document photographed is "Missing Page(s)". If it was possible to obtain the missing page(s) or section, they are spliced into the film along with adjacent pages. This may have necessitated cutting through an image and duplicating adjacent pages to assure you of complete continuity.

2. When an image on the film is obliterated with a round black mark it is an indication that the film inspector noticed either blurred copy because of movement during exposure, or duplicate copy. Unless we meant to delete copyrighted materials that should not have been filmed, you will find a good image of the page in the adjacent frame.

3. When a map, drawing or chart, etc., is part of the material being photographed the photographer has followed a definite method in "sectioning" the material. It is customary to begin filming at the upper left hand corner of a large sheet and to continue from left to right in equal sections with small overlaps. If necessary, sectioning is continued again—beginning below the first row and continuing on until complete.

4. For any illustrations that cannot be reproduced satisfactorily by xerography, photographic prints can be purchased at additional cost and tipped into your xerographic copy. Requests can be made to our Dissertations Customer Services Department.

5. Some pages in any document may have indistinct print. In all cases we have filmed the best available copy.

University
Microfilms
International

300 N. ZEEB ROAD, ANN ARBOR, MI 48106
18 BEDFORD ROW, LONDON WC1R 4EJ, ENGLAND

7916988

MA, CHENG-QUINN
STUDY OF THE INHOMOGENEOUS ELECTRON GAS AT SURFACES.

CITY UNIVERSITY OF NEW YORK, PH.D., 1979

University Microfilms International 300 N. ZEEB ROAD, ANN ARBOR, MI 48106

PLEASE NOTE:

In all cases this material has been filmed in the best possible way from the available copy. Problems encountered with this document have been identified here with a check mark ✓.

1. Glossy photographs _____
2. Colored illustrations _____
3. Photographs with dark background _____
4. Illustrations are poor copy _____
5. Print shows through as there is text on both sides of page _____
6. Indistinct, broken or small print on several pages ✓ throughout _____
7. Tightly bound copy with print lost in spine _____
8. Computer printout pages with indistinct print _____
9. Page(s) _____ lacking when material received, and not available from school or author _____
10. Page(s) _____ seem to be missing in numbering only as text follows _____
11. Poor carbon copy _____
12. Not original copy, several pages with blurred type _____
13. Appendix pages are poor copy _____
14. Original copy with light type _____
15. Curling and wrinkled pages _____
16. Other _____

University Microfilms International

300 N. ZEEB RD., ANN ARBOR, MI 48106 (313) 761-4700

STUDY OF THE INHOMOGENEOUS ELECTRON GAS AT SURFACES

by

CHENG-QUINN MA

A dissertation submitted to the Graduate Faculty in Physics in partial fulfillment of the requirements for the degree of Doctor of Philosophy, The City University of New York.

1979

This manuscript has been read and accepted for the Graduate Faculty in physics in satisfaction of the dissertation requirement for the degree of Doctor of Philosophy.

Jan 18, 1979.
date

V. Sahni
Prof. V. Sahni
Chairman of Examining Committee

Feb 9, 1979
date

Prof. F. Martino - Frank Martino, Jr.
Executive Officer

Prof. J.B. Krieger Joseph B Krieger

Prof. G. Skorinko George Skorinko

Prof. C.R. Fischer C. R. Fischer

Dr. H.F. Budd Herbert F Budd
Supervisory Committee

The City University of New York

Abstract

STUDY OF THE INHOMOGENEOUS ELECTRON GAS AT SURFACES

Cheng-Quinn Ma

Adviser: Professor Viraht Sahni

The system of an interacting neutrally charged electron gas at a jellium surface is studied for a wide range of densities including those for the metallic range. Both the fully correlated as well as the inhomogeneous Hartree-Fock gas interacting only via Pauli correlation are examined. In addition, certain aspects of the density functional formalism are investigated for density profiles such as those existing at surfaces, and the applicability of a new variational formalism for the density to the inhomogeneous many-body problem at surfaces demonstrated. The various properties determined are the electronic density variation at surfaces, surface dipole barriers, work functions, electrostatic potentials, and surface energies.

One of the techniques employed to study the inhomogeneous electron gas is the use of model potentials to represent the effective potential seen by electrons at a surface in conjunction with the application of certain theoretical and physical constraints. The use of such model potentials permit the calculations to be primarily analytic, and the application of meaningful constraints lead to accurate results. These model potentials also permit the easy incorporation of non-local effects. Typical contraints applied are the condition of charge neutrality, the requirement of the self-consistency of the surface dipole barrier, the satisfaction of the constraint set on the electrostatic potential by the Budd-Vannimenus theorem, and the energy minimum criterion set by the Rayleigh-Ritz variational principle.

The fully correlated system is investigated within the finite linear potential approximation for which the potential varies linearly over a finite region and is a constant beyond some point. Results for the work function are derived for metallic and higher densities within this model effective potential by application of appropriate constraints. Metallic and lower density surface energies are determined both by the component Kohn-Sham method within the local density approximation for exchange-correlation, and by application of the Vannimenus-Budd theorem in conjunction with the physical criterion of the vanishing of the surface energy in the low density limit.

The surface properties of the inhomogeneous Hartree-

Fock gas are studied within the linear potential approximation, for which the effective potential is linear in the positive half space and constant elsewhere, and the non-local surface exchange energy determined exactly. The requisite convergence of the local density approximation value of this property to the exact value as the density is made slowly varying is demonstrated. The surface dipole barriers and work functions are determined by use of the Budd-Vannimenus Theorem constraint for this system. Rigorous upper bounds to the surface energy are obtained by variational minimization of the exactly known Kohn-Sham total surface energy functional with each component of this functional being determined exactly. Finally, the variation of these surface properties of the inhomogeneous Hartree-Fock gas as correlation is gradually introduced are also examined.

The density-gradient expansion for the kinetic energy within the density functional theory is studied by application of the expansion to an inhomogeneous system of noninteracting fermions. The requisite convergence of this expansion as the density is made slowly varying is demonstrated for density profiles generated by the linear potential approximation of a surface. It is shown that the original von Weisacker coefficient of the first density-gradient correction is inappropriate for both rapidly and slowly varying densities. The quantum mechanically determined coefficient, which is the von Weisacker coefficient reduced by a factor of nine,is shown to be appropriate for all density profiles provided that the the second density-gradinet correction is included for the rapidly varying case. The applicability of the expansion to the metal surface problem is dicussed, and the inclusion of the second density-gradient correction with its nonlinear response contributions shown to be of major significance in such calculations.

The applicability of recently developed variational principles for the determination of single-particle expectation values and density matrices correct to second order is demonstrated by application of the formalism to the operator $W=\Sigma_i \delta(\vec{r}_i-\vec{r})$ to determine the charge density variation at metallic surfaces. A single-particle Hamiltonian in the sense of Kohn-Sham is assumed, and the trial wave functions employed are those generated by the linear potential model. The auxiliary function within this formalism is determined analytically and leads to semi-analytical expressions for the density and all other surface related properties. The stationary property of the variational formalism is first demonstrated with respect to the specific property of the surface dipole barrier, and work functions and surface energies determined by use of these accurately calculated densities. The extension of this formalism to determine crystal face dependent densities by incorporating into the Hamiltonian local ionic pseudopotentials representing the crystal lattice is also indicated.

Acknowledgements

I would like to express my sincere thanks to Prof. V. Sahni who proposed this thesis topic. It is through his continuous encouragement, assistance, and patience that this work has been possible. I am also indebted to Prof. J. B. Krieger for extremely valuable discussions, especially at the early stages of this thesis. And I wish to acknowledge the constructive comments of J. Flamholz with respect to certain aspects of this work. Finally, I wish to thank my wife Ayling for her many sacrifices over the years which have enabled me to concentrate fully on this work.

Computer facilities provided by the Computer Center and financial support by the Physics Department, Graduate Center, and Research Foundation of the City University of New York are gratefully acknowledged.

TABLE OF CONTENTS

TABLE OF CONTENTS
(continued)

LIST OF ILLUSTRATIONS

ed to the Fermi momemtum by the BVT.

Fig.11 The full line is the variation of the correspondence between r_s and the slope parameter y_F as determined by the BVT for self-consistent barrier height. The dashed curve is the variation of the self-consistent barrier height parameter y_b versus y_F.

Fig.12 The full curve is the variation of the universal function $\Delta\phi/k_F$, where $\Delta\phi$ is the surface dipole barrier, versus the barrier height parameter β for the step potential model. The dashed curve is a plot of r_s as a function of the self-consistent barrier height parameter.

Fig.13 Plot of the universal functions of the exact surface kinetic energy E_k/k_F^4 (denoted by E_k), and those of the Thomas-Fermi (TF) contribution $E_k^{(1)}$, TF plus first gradient correction $E_k^{(1)}+E_k^{(2)}$ (λ =1 and 1/9), and TF plus first and second gradient corrections $E_k^{(1)}+E_k^{(2)}(\lambda=1/9)+E_k^{(3)}$ (γ =1), as a function of the slope parameter y_F.

Fig.14 The full line is a plot of the correspondence between r_s and the slope parameter y_F as determined by the Budd-Vannimenus theorem. The dashed curve is the correspondence as determined by the variational principle for the energy.

Fig.15 The figure caption is the same as that of Fig. 13. The range of the slope parameter y_F considered, however, is different.

Fig.16 Variation of the coefficient λ of the first gradient correction which leads to the exact result for the kinetic energy when only the first two terms of the expansion are considered, as a function of the slope parameter y_F.

Fig.17 Plot of the universal functions of the exact surafce kinetic energy E_k/k_F^4 (denoted by E_k), and the energy as obtained by the gradient expansion E_k^{GE} for both γ =1 and 1.336, as a function of the slope parameter y_F.

Fig.18 Plot of the variation of the total surface dipole barrier $\Delta\phi$ and that due to the trial system $(\Delta\phi)_0$ as a function of the barrier height parameter y_b for r_s=2.5. The horizontal line represents the fully self-consistent Lang-Kohn result.

Fig.19 Plot of the spatial variation of the correction

charge density $n_1(y)$ for $r_s=2.5$. The full curve corresponds to a value for the barrier height parameter y_b of 1.82, and the dashed curve to a value of $y_b=1.20$.

Fig.20 Plot of the universal function E_x/k_F^3, where E_x is the surface exchange energy as obtained exactly and within the local density approximation (LDA), versus the slope parameter y_F.

Fig.21 Plot of the percent error between the local density approximation for the surface exchange energy E_x^{LDA} and the exact value E_x versus the slope parameter y_F.

Fig.22 Plot of the rigorous upper bounds to the total surface energy of an inhomogeneous Hartree Fock gas, and the bounds obtained within the local density approximation (LDA) as a function of the Wigner-Seitz radius r_s. The crosses represent the self-consistently determined results of Lang and Kohn.

Fig.23 Plot of the variation of the work function Φ as a function of the correlation factor α for different values of the Wigner-Seitz radius r_s.

Fig.24 Plot of the variation of the surafce dipole barrier $\Delta\phi$ as a function of the correlation factor α for different values of the Wigner-Seitz radius r_s.

I. INTRODUCTION

It has long been recognized that an understanding of the electron charge distribution near metal surfaces is crucial for the determination of many surface sensitive properties and for an understanding of experiments related to these properties. The tailing-off of the electron density near the solid surface is responsible for the existence of an electrostatic dipole layer which contributes to the work function (1,2), the different electron density on different single crystal faces of the same material being responsible for the crystal face dependence of the work function (3). Similarly, the surface energy of a crystal, i.e., the energy required per unit area of new crystal formed to split the crystal in two along a plane (4) evidently depends on the energy density of the electron gas near the resulting surface (5). Many experiments including those using low energy electron diffraction (LEED) have been performed to investigate the structure of solid surfaces (6), and theoretical calculations have been performed to enable interpretation of the data (7). The most recent theoretical models assume that the incoming electrons have a mean free path of only a few lattice constants. Thus even for a clean metallic surface, the variation of the electron density near the surface and the consequent change in the screening of these surface atoms is an important complication which will affect the

LEED intensity distribution (8) and must be understood if quantitative conclusions are to be inferred from LEED experiment. Electrons not only play a crucial role in the binding of the atoms in a lattice but also in the binding of foreign materials to the surface layer of atoms, e.g., the formation of adsorbed or chemisorbed layers. Atomic and molecular properties are altered when in the presence of a nearby surface due to the existence of the surface charge distribution and this accounts for the well known catalytic effect of surfaces. Any realistic calculation of surface states on metals must recognize and take into account the fact that the conduction band electron charge density, and hence, the potential, varies near the surface instead of simply assuming that the periodic crystal potential remains unchanged right up to the bounding surface (9,10). Finally a knowledge of the electron distribution near solid surfaces aids in our understanding of tunneling, field emission and field ionization, and size effect in galvanomagnetic properties of solids among many other phenomena. It is also an important input for the determination of both surface plasmon and surface phonon dispersion relations.

Until recently the development of a quantitative theory of metal surfaces lagged far behind theoretical treatments of bulk properties of solids. This was due primarily to the fact that the electron charge density near metal surfaces is highly inhomogeneous as compared to that in the bulk and thus the extension of the usual bulk theories to solid sur-

faces is not entirely straightforward or completely understood. As early as 1936, Bardeen (2) discussed how the work function could be obtained from the self-consistent solutions of the Hartree-Fock (HF) equation. However, due to the lack of computing facilities at that time, he was unable to carry out the calculation completely self-consistently and was forced to make a choice of exchange potentials at the outset which were held fixed throughout the calculation. For a real three dimensional crystal, a Hartree-Fock calculation is still a formidable computational problem, partly because of the long rang of the Coulomb potential and partly due to the lack of simple spherical symmetry as found in atoms.

Several years ago, significant progress in formulating methods for the treatment of the ground state of an interacting electron gas in an external potential was made by Hohenberg and Kohn (11), and Kohn and Sham (12). Based on the variational principle for the energy, they showed that the ground state could be exactly written in terms of an integral of the product of the external potential and the electron density plus a term which is a universal functional of the true density. The exact form of this functional, which includes both exchange and correlation effects, is not known at present but results in the limit of high density and in the limit of slowly varying density have been obtained (11) and methods for solving the resultant equations discussed (12). The variational principle establishing the

minimal properties of this energy functional leads to an Euler equation for the density. Two approaches for the solution of this equation have been formulated: the density gradient expansion method and the Kohn-Sham self-consistent method, the former being similar to extended Thomas-Fermi and the latter to the Hartree method. A brief review of the density functional formalism including recent developments is given in Section A of Chap. II. In Section II.B we present definitions of various properties of the inhomogeneous electron gas at surfaces based on this formalism together with various sum rules which are to be employed in this work.

A fully self-consistent numerical solution of the Kohn-Sham equations for the one-dimensional jellium model, in which the positive ions are replaced by a uniform semi-infinite positive charge density, has been performed by Lang and Kohn (13,14) for metallic densities within the local density approximation (LDA) for exchange and correlation. They then included the effects of the ionic lattice on the work function and surface energy perturbatively. Although various computer proprams for the iterative procedure described by Kohn and Sham exist, the extension of the fully self-consistent formalism to a three dimensional lattice is still a formidable task. There do, however, exist non-fully self-consistent three dimensional calculations of certain selected faces of a few metals (15-22). These calculations employ diverse treatments of the ionic pseudopotential, al-

ways employ the LDA for exchange and correlation, and achieve varying degrees of self-consistency. The principle additional approximation beyond the LDA in the majority of these calculations is a variational restriction on the number density arising from the use of a finite wave function basis. Thus these calculations are not fully self-consistent in the same sense as the work of Lang and Kohn.

Using parametrized densities, the extended Thomas-Fermi approach with only the first density gradient correction for the kinetic energy functional has been employed by Smith (23) to study the jellium model, and by Paasch and Heitschold (24) who also considered the effects of the ionic lattice. A considerable amount of work has thus already been done on understanding both the jellium model as well as the real metal surface. The various formalisms employed in the above calculations and the conclusions derived are detailed in several recent review articles (25-31). However, there are many aspects of both the ideal as well as the realistic surface problem which are as yet not well understood or which in the past have been derived on the basis of approximations which themselves have yet to be fully understood and proved conclusively to be valid. In addition, the most accurate of the existing methods require heavy numerical computations and are difficult to apply to the realistic three dimensional metal surface problem.

One of the primary aims of this work, therefore, is the development and application of simpler methods for the study

of the inhomogeneous electron gas at surfaces. These methods overcome, in several ways, some of the difficulties of previous calculations of others, and thus also permit a study not only of metallic surfaces but also of systems with densities both higher and lower than those existing in metals. Furthermore, these techniques tend in general to be primarily analytic and thus obviate the necessity of heavy numerical computations. They also permit the easy incorporation of non-local effects, and are in principle easily extendable to three dimensions.

One of the approaches that we have examined for the study of the inhomogeneous electron gas at surfaces including metallic surfaces is the use of analytic model potentials in conjunction with various constraints to represent the effective potential at a jellium surface. The principle advantage of such model potential calculations is the elimination of the requirement of a numerical solution of the Schrodinger equation for particles moving in a self-consistently obtained effective potential. Together with the requirement of charge neutrality (2), typical constraints applicable to such calculations are those of the self-consistency of the surface dipole barrier, the application of the sum rule due to Budd and Vannimenus (32), and that of the Rayleigh-Ritz variational principle for the energy (33). The choice and number of these constraints to be satisfied would of course depend upon the complexity of the model potential employed. The use of the Budd-Vannimenus

theorem (BVT) allows the exact determination of the contribution to the surface dipole barrier from charge inside the metal. This contribution, particularly for high density metals, can be as large as 40% of the total dipole moment. Thus application of this theorem leads to accurate results for the surface dipole barrier. On the other hand, application of the variational principle for the energy, leads not only to a determination of the energy correct to second order but also to an upper bound for that specific choice of energy functional of the density. Such model potentials are also a means of generating single-particle wave functions which may then be employed in more complex variational or perturbational schemes as the unperturbed ground state wave function. The use of analytic potentials with constraints has previously been studied (34-37), the most accurate of these potentials to date being the linear potential model (36,37). In Chap. III we examine a more sophisticated version of the LP model, one which is linear over a finite region and constant beyond some point with its value being determined self-consistently, i.e., its value is the sum of the exchange-correlation potential plus the electrostatic dipole barrier that it generates. Since the effective potential must asymptotically approach a finite value outside the surface (26), this model potential is a far more accurate representation of the actual potential than either the step or linear potential models, and this fact is born out by the results. It is also interesting to note that in com-

parison with experimental values for the work function of polycrystalline metals, the results of this model potential calculations are superior to those of Lang and Kohn (14) for the majority of simple metals considered. Of course, it is important to recognize that although the Lang-Kohn calculations are exact, they are so only within the LDA for exchange and correlation. Thus our procedure is accurate and justified. As in the linear potential (LP) case the calculation of all properties within this finite linear potential (FLP) model are primarily analytic. Since the application of this model to jellium is easy and proven accurate, it is possible to extend the calculations for various properties beyond the metallic density range towards both the high as well as the low density limits, thus gleaning additional information with regard to the inhomogeneous electron gas system. The results of such a calculation within the FLP model for the high density behavior of the work function, and results for the surface energy as obtained by application of the Vannimenus-Budd theorem (VBT) (38) for which no local density approximation need be made are also given in Chap. III.

In Chap. IV we present a study of the density gradient expansion formalism for the kinetic energy (39-43) functional as applied to the surface physics problem. There exist a substantial sum of literature on both paramagnetic and ferromagnetic surfaces (44-47,23,24) in which the extended Thomas-Fermi approach with only the first density gradient

correction has been employed. The accuracy of this approximation for surfaces has, however, only recently been tested in published work of ours (48,49). In this work (48) (which comprises the subject matter of Chap. IV) we have demonstrated the convergence of this gradient expansion by including the second density gradient correction term. In addition we have shown that the original von Weisacker coefficient (50) of the first density gradient correction is inappropriate for both rapidly and slowly varying densities. However, the coefficient reduced by a factor of nine (a result obtained on the basis of quantum mechanical considerations) is appropriate for all density profiles provided the second density gradient correction is included for the rapidly varying case. We have also examined the applicability of the expansion to the metal surface problem and shown that the inclusion of the second density gradient correction with its non-linear response contribution is of major significance is such calculations. These conclusions have thus enabled a better understanding of the statistical results of Smith, Paasch and Heitschold, and others.

The determination of quantum mechanical properties without an accurate knowledge of the wave function of the interacting system is a problem of considerable interest. A second approach to the surface physics problem which we have investigated, and which achieves this end, is the use of variational principles for obtaining highly accurate single-particle expectation values (51-55) and density ma-

trices (56,57) as developed by Sahni and Krieger. Employing only crude approximations to the exact wave function, these variational principles lead to results for the density and all the other single-particle expectation values correct to second order, as is the case for the energy on application of the Rayleigh-Ritz variational principle (33). A generalization of these variational principles to the reduced single-particle density matrix (56,57) leads to accurate results not only for the density but also the momentum density. When applied to atomic systems, these variational principles have led to results which in all cases have been as accurate as numerical Hartree-Fock calculations even though the technique is entirely analytic. For example, the single-parameter analytic expression for the coherent atomic scattering factor (the Fourier transform of the density) derived (53,54) for the highly inhomogeneous ground state of the helium isoelectronic sequence and valid for all momentum transfer, leads to results which are within 1.2% of a 120-parameter configuration-interaction wave function treatment (58), and are equivalent to those of a 6-parameter analytic Hartree-Fock calculation (59). The least accurate of the analytic results for the expectations $\langle r^n \rangle$, n=2,1,-1,-2 and $\langle \delta(r) \rangle$ for the helium ground state is the expectation $\langle r^2 \rangle$ which is within 0.66% (60) of a 1078-parameter Hylleraas wave function calculation (61) due to Pekeris. The corresponding error in the results obtained by Tong and Sham (62) for the same quantity using the density functional

method in the LDA is 9%. A similar local density functional calculation by Shore et al. (63) for the negative ion of atomic hydrogen, H^-, leads to an unbound state and thus to erroneous values for other expectations, whereas the variational results for the interior of the ion are in error by only 3.5%, 1.35%, and 0.6% respectively for $\langle\delta(r)\rangle$, $\langle r^{-2}\rangle$, and $\langle r^{-1}\rangle$ in comparison with the results of Pekeris. The results (57) of the analytic expressions derived for the momentum density of the helium ground state isoelectronic sequence together with the expectations of the operators p^4, p^2, $|p|$ and $|p|^{-1}$, and the Compton profile in the impulse approximation (64) are highly accurate and closely approximate those of analytic Hartree-Fock and many-parameter correlated wave function calculations. Other applications of these variational principles have been to the 2^3S and 2^1S isoelectronic sequences of the helium atom and the results of various expectations are again observed to closely approximate the results of a 2300-parameter correlated wave function calculation (65). We note, however, that in all the above applications, the trial wave functions employed in these variational calculations have always been appropriately antisymmeterized product by hydrogenic functions. The successful application of these variational principles to few particle atomic systems thus motivated their application to the many-body system. However, since the many-electron system at a surface is considerably more complex, we deemed it necessary to first demonstrate its applicability to the

simplest model of a surface viz. that of jellium, by determining the electron density variation at the surface. Furthermore, as this is the first application of the Sahni-Krieger formalism to the many-body problem, we assume as in the work of Kohn and Sham, that the electrons at the surface move in some single-particle effective potential. This simplification was made strictly for purposes of analytical simplicity. The use of the exact non-relativistic Hamiltonian is not precluded in this method. In Section V.A we give a description of this variational principle with appropriate modifications to incorporate the fact that a semi-infinite lattice is being considered and that a single-particle effective potential is being assumed. The trial wave functions in these variational calculations were chosen to be those generated by the linear potential model (36,37). In Section V.B we apply the variational formalism to the inhomogeneous gas at a surface to determine the electron density and from it properties such as the surface dipole barrier, work function, and surface energy. In Section V.C and V.D we demonstrate both the stationary property of the variational formalism and discuss the accuracy of the results obtained. Since in this work it is the density rather than the single-particle wave functions which are determined accurately, the kinetic energy contribution to the surface energy is obtained via the density gradient expansion as discussed in Chap. IV. We conclude Chap. V by indicating how the crystal lattice may be incorporated into

the variational scheme by employing local ionic pseudopotentials in order to determine accurately the electronic density at real metal surfaces.

A simple example of two fundamental properties which have yet to be derived accurately for the realistic inhomogeneous electron gas at a surface are the exchange and correlation energy contributions to the surface energy. Calculations for these properties employing the infinite barrier model (IBM) densities have, however, been performed (66,67), with the surface exchange energy determined exactly and the surface correlation energy being obtained within the random phase approximation (RPA). These results, as discussed in Chap. VI, are physically unrealistic and should be considered with care. On the other hand, the attempt by Bardeen (2) at a self-consistent solution of the Hartree-Fock (HF) equations is fraught with approximations. In Chap. VI we present a study of the surface properties of the inhomogeneous HF gas within the realistic linear potential approximation. Employing these wave functions we have determined the non-local surface exchange energy exactly and demonstrated the convergence of the LDA result for this property. We have also derived rigorous upper bounds for the total surface energy of a HF gas which we believe to be essentially exact since not only are we employing very accurate wave functions but in addition are doing so in conjunction with the Rayleigh-Ritz variational principle for the energy. Accurate results for the work function are also

derived by application of the Budd-Vannimenus theorem constraint. Finally, in the last section of this chapter, we investigate the effects of introducing correlation on the surface properties of a HF gas.

II. DENSITY FUNCTIONAL FORMALISM

A. General Theory and Recent Developments

In the density functional formalism of Hohenberg and Kohn (HK) (11), and Kohn and Sham (KS) (12), the ground state Ψ of a system of electrons moving under the influence of their mutual Coulomb interaction in a given static external potential $v(\vec{r})$ is a unique functional of the electron density $\rho(\vec{r})$. The ground state energy of this interacting inhomogeneous electron gas is then a universal functional of the density defined as

$$\mathcal{E}[\rho] = \int v(\vec{r})\rho(\vec{r})d\vec{r} + 1/2 \int \frac{\rho(\vec{r})\,\rho(\vec{r}')}{|\vec{r}-\vec{r}'|} d\vec{r}d\vec{r}'$$

$$+ E_k[\rho(\vec{r})] + E_{xc}[\rho(\vec{r})], \qquad (2.1)$$

where the first term corresponds to the interaction between the external potential and the electrons and the second to the Coulomb self-energy of the electrons. $E_k[\rho]$ in the above expression is the kinetic energy of a system of non-interacting electrons having the same density $\rho(\vec{r})$, and $E_{xc}[\rho]$ the exchange-correlation energy of the interacting system. It has been shown (11,12) that this energy functional is stationary and a minimum for the correct density, subject to the constraint that all the densities considered

conserve the total number of electrons. Employing a Lagrange multiplier μ (which can be shown to correspond to the chemical potential of the system) to incorporate the constraint that the total number of particles be conserved, this variational principle implies that for the correct density

$$\mu = \frac{\delta \mathcal{E}[\rho]}{\delta \rho(r)} = V_{es}(\vec{r}) + \frac{\delta E_k[\rho]}{\delta \rho(\vec{r})} + \frac{E_{xc}[\rho]}{\delta \rho(\vec{r})} , \qquad (2.2)$$

where $V_{es}(\vec{r})$ is the total electrostatic potential of the system due to all the charges i.e.

$$V_{es}(\vec{r}) = v(\vec{r}) + \int \frac{\rho(\vec{r}')}{|\vec{r}-\vec{r}'|} d\vec{r}' . \qquad (2.3)$$

Thus the density may be obtained by solution of Eq. 2.2 in conjunction with Eq. 2.3.

However, since the kinetic energy $E_k[\rho]$ within this formalism corresponds to a system of non-interacting electrons, solution of Eq. 2.2 is equivalent to solving self-consistently a set of single-particle Schrodinger-like equations for non-interacting electrons moving in an effective potential $V_{eff}(\vec{r})$ whose solution gives the exact ground state density, and hence the energy, of the system. The single-particle equations to be solved self-consistently are

$$[-1/2\ \nabla^2 + v_{eff}(\vec{r})]\ \psi_i(\vec{r}) = \epsilon_i \psi_i(\vec{r}) \qquad (2.4)$$

with

$$\rho(\vec{r}) = \sum_i |\psi_i(\vec{r})|^2 , \qquad (2.5)$$

and where the effective potential is defined as

$$V_{eff}(\vec{r}) = V_{es}(\vec{r}) + \frac{\delta E_{xc}[\rho]}{\delta \rho(\vec{r})} . \qquad (2.6)$$

The kinetic energy within this self-consistent scheme is then given exactly as

$$E_k[\rho(\vec{r})] = \sum_i \epsilon_i - \int V_{eff}(\vec{r})\rho(\vec{r})\, d\vec{r}. \qquad (2.7)$$

Thus all the many-body complexity is contained in the functional $E_{xc}[\rho]$ and since, at present, the exact form of this functional is unknown, it must be approximated.

For the case in which the density is slowly varying, Kohn-Sham expand $E_{xc}[\rho]$ in the series of density gradients. Within linear response theory to terms of $O(\nabla^4)$ this expansion may be expressed as (68,11)

$$E_{xc}[\rho] = \int d\vec{r}\{ \epsilon_{xc}[\rho(\vec{r})]\rho(\vec{r}) + \epsilon_{xc}^{(2)}[\rho(\vec{r})]|\vec{\nabla}\rho(\vec{r})|^2$$

$$+ \varepsilon_{xc}^{(3)}[\rho(\vec{r})]\,\vec{\nabla}\rho(\vec{r}).\vec{\nabla}[\nabla^2\rho(\vec{r})]\}, \qquad (2.8)$$

where $\varepsilon_{xc}=\varepsilon_x+\varepsilon_c$ is the sum of the average exchange ε_x and correlation ε_c energy per particle of a uniform electron gas with density $\rho(\vec{r})$, and $\varepsilon_{xc}^{(2)}$ and $\varepsilon_{xc}^{(3)}$ are the coefficients of the first and second density gradient corrections respectively. In terms of the Wigner-Seitz radius r_s ($4\pi r_s^3/3=1/\bar{\rho}$), the average exchange energy per particle (69) for the uniform gas is

$$\varepsilon_x(\bar{\rho}) = -0.458/r_s(\bar{\rho}),$$

whereas for metallic densities, the average correlation energy is usually assumed to be that given by the Wigner (W) (70) interpolation formula

$$\varepsilon_c^W(\bar{\rho}) = -0.44/(r_s(\bar{\rho})+7.8). \qquad (2.9)$$

If all the gradient terms in Eq. 2.8 are neglected, the exchange-correlation energy is said to be determined within the so-called local density approximation (LDA):

$$E_{xc}^{LDA}[\rho] = \int d\vec{r}\ \varepsilon_{xc}(\rho)\rho(\vec{r}). \qquad (2.10)$$

It has been shown (71-74) that this approximation is mean-

ingful provided it is made for the combined exchange and correlation contributions. In Eq. 2.8, the coefficients $\varepsilon_{xc}^{(2)}$ of the first gradient term have recently been derived for the metallic range of densities from a calculation of the energy within the random phase approximation (RPA) by Geldart and Rasolt (75). Both the coefficients $\varepsilon_{xc}^{(2)}$ and $\varepsilon_{xc}^{(3)}$ of the first and second density gradient corrections have also been derived by Gupta and Singwi (68) using a slightly modified version of the theory of Vashista and Singwi (76) and based on an expansion of the dielectric function. The coefficients thus obtained are therefore very sensitive to the choice of dielectric function employed (77). Lau and Kohn (78) have also obtained $\varepsilon_{xc}^{(2)}$ by equating the surface energy of two adjacent jellium metals as determined in terms of the static electronic polarizability of Vashista and Singwi (76) and that obtained using the density functional formalism. A discussion of the probable sources of error in these coefficients is given in Ref. 68.

Another approach to the use of the Hohenberg-Kohn-Sham theorem has been to perform variational calculations by employing parametrized trial densities in the energy functional of Eq. 2.1 (23,24). If the energy functionals $E_k[\rho]$ and $E_{xc}[\rho]$ were known, the results of such calculations would constitute rigorous upper bounds to the exact ground state energy. However, both these functionals of the density are as yet undefined and must be approximated. One approximation to the kinetic energy functional for the non-

interacting inhomogeneous electron gas is that determined within a density gradient expansion formalism similar to the one discussed with respect to $E_{xc}[\rho]$. The density gradient expansion for the kinetic energy to terms of $O(\nabla^4)$ may be written as

$$E_k^{GE}[\rho(\vec{r})]=E_k^{(1)}[\rho(\vec{r})]+E_k^{(2)}[\rho(\vec{r})]+E_k^{(3)}[\rho(\vec{r})], \qquad (2.11)$$

where

$$E_k^{(1)}[\rho(\vec{r})] = 3/10\ (3\pi^2)^{2/3} \int \rho(\vec{r})\rho^{2/3}(\vec{r})d\vec{r} \qquad (2.12)$$

and

$$E_k^{(2)}[\rho(\vec{r})] = \lambda/8 \int |\vec{\nabla}\rho(\vec{r})|^2/\rho(\vec{r})d\vec{r} \qquad (2.13)$$

and

$$E_k^{(3)}[\rho(\vec{r})] = \frac{\gamma}{(3\pi^2)^{2/3}} \frac{1}{540} \int d\vec{\pi}\, \rho(\vec{\pi})^{1/3} \left\{ \left(\frac{\nabla^2\rho(\vec{\pi})}{\rho(\vec{\pi})}\right)^2 \right. \qquad (2.14)$$

$$\left. -\frac{9}{8}\left(\frac{\nabla^2\rho(\vec{\pi})}{\rho(\vec{\pi})}\right)\left(\frac{\vec{\nabla}\rho(\vec{\pi})}{\rho(\vec{\pi})}\right)^2+\frac{1}{3}\left(\frac{\vec{\nabla}\rho(\vec{\pi})}{\rho(\vec{\pi})}\right)^4 \right\}$$

In the above e equations $E_k^{(1)}$ is the Thomas-Fermi (TF) con-

bution (26) to the kinetic energy. With the coefficient $\lambda = 1$, $E_k^{(2)}$ is the first gradient correction originally proposed by von Weisacker (50). Subsequent rigorous derivations (39-42) of this first gradient correction valid for slowly varying densities have led to a value of the coefficient λ reduced by a factor of nine. $E_k^{(3)}$ with the coefficient $\gamma = 1$ is the second density gradient correction valid for slowly varying densities as obtained originally by Kirzhnits (40) and modified by Hodges (43). The first term of $E_k^{(3)}$ is the linear response theory contribution to fourth order in the gradient operator. The last two terms arise from non-linear response theory and their inclusion should shed light on the importance of such contributions to the metal surface problem.

The criterion for the validity of these density gradient expansions is that $|\vec{\nabla} \rho / \rho|$ is smaller than both the Fermi wave number k_F and the Thomas-Fermi screening wave number $k_{TF}=(8k_F/3\pi)^{1/2}$. However, for metallic surfaces the density variation is fairly rapid over a distance of approximately half a Fermi wavelength, and thus an investigation of these expansions for metallic systems together with a study of their applicability to higher and more slowly varying density systems is particularly meaningful. The results of such a study (48) for the kinetic energy density gradient expansion are discussed in Chap. IV.

Recently, a different approach to the determination of the correction to the LDA value of exchange-correlation has

been performed by Langreth and Perdew (72,73). In their wave-vector decomposition-interpolation scheme they analyze the exchange-correlation energy of a metal surface in terms of the wavelength of the fluctuations which contribute to it and interpolate between the exact plasmon dominated behavior at large wavelengths and the LDA which is exact at short wavelengths. Studies and comparisons of the wave-vector analysis method and the various density gradient expansion schemes for the exchange-correlation energy have also recently been performed by Perdew, Langreth and Sahni (79), and Sahni and Gruenebaum (80).

More recently a non-local approximation to the exchange energy and potential of an inhomogeneous electron gas has been proposed by Alonso and Girifalco (81) and Gunnarsson et al. (82). This approximation is based on an expression for the exchange charge density that conserves total exchange charge, satisfies the limiting conditions at the center of and far from the exchange hole, and reduces to the free-electron form for the homogeneous electron gas. Employing the same correlation factor as in their non-local approximation to the exchange energy, Alonoso and Girifalco (81) have also proposed a new kinetic energy functional within the Hartree-Fock (HF) approximation, and both these approximate exchange and kinetic energy functionals tested on atoms. In Chap. VI of this work we present an <u>exact</u> non-local calculation of the exchange energy within the linear potential model of a metal surface (36), and also determine <u>rigorous</u>

upper bounds to the surface energy of an inhomogeneous HF gas. On the basis of the accuracy of the wave functions employed (36,37), and the fact that in these calculations the variational principle for the energy is applied, we conclude that the bounds obtained are very close approximations to those that might be determined by a fully self-consistent HF calculation.

B. Definitions of Jellium Surface Properties and Sum Rules

In this section we present definitions and discuss various properties of interest as applied to the jellium model in which the positive ions are assumed to be replaced by a uniform semi-infinite positive charge background. Because of the reduction in symmetry in the surface physics problem, the Hamiltonian of the system is different inside and outside the surface and the momentum perpendicular to the surface is no longer a good quantum number. Furthermore, since jellium has no structure parallel to the surface, the electronic wave function can be written as

$$\psi_{\vec{k}}(\vec{r}) = \psi_k(x)\exp(i\vec{k}_{\parallel}\cdot\vec{x}_{\parallel}),$$

where $\vec{k}_{\parallel}$ and $\vec{x}_{\parallel}$ are respectively the projections of the momentum $\vec{k}$ and position $\vec{r}$ of the electron on the surface plane and k and x are measured along the surface normal. The translational invariance in the direction parallel to the surface thus reduces the complex three-dimensional calculation to one which is one-dimensional. Away from the surface region in the bulk, the wave function must have the asymptotic form

$$\psi_k(x) = \sin[kx-\delta(k)],$$

where $\delta(k)$, the asymptotic phase shift, is a continuous

function of k.

The fundamental quantities from which all other surface properties may be obtained are the electronic $\rho(x)$ and total charge densities $\rho_T(x)$ defined as

$$\rho(x) = \frac{L}{2\pi^2} \int_0^{k_F} (k_F^2 - k^2) |\psi_k(x)|^2 dk \qquad (2.15)$$

and

$$\rho_T(x) = \rho(x) - \rho_+(x), \qquad (2.16)$$

where $\rho_+ = k_F^3/3\pi^2\theta(x)$ is the jellium background density which ends abruptly at the surface position and where $k_F = (9\pi/4)^{1/3}/r_s$ (83) is the Fermi momentum.

Total charge neutrality for the system requires that

$$\int_{-\infty}^{+\infty} \rho_T(x)dx = 0. \qquad (2.17)$$

It has been shown (84) that for arbitrary effective potential this charge neutrality condition is equivalent to a phase shift sum rule due to Sugiyama (85,5), according to which the weighted Fermi surface average of the asymptotic phase shift $\delta(k)$ of the electronic wave function must equal $-\pi/4$:

$$\int_0^{k_F} k\delta(k)dk \Big/ \int_0^{k_F} kdk = -\pi/4. \qquad (2.18)$$

In our work we do not treat the jellium edge position as fixed at the origin but rather treat it as a variable quantity ending abruptly at some arbitrary position 'a'. This position is then determined by either ensuring charge neutrality via Eq. 2.17 or equivalently by employing the Sugiyama sum rule. Application of the latter condition leads to a simple expression for the jellium edge position in terms of the asymptotic phase shift $\delta(k)$ which is

$$a = -3\pi/(8k_F) - 3/k_F^3 \int_0^{k_F} k\delta(k)dk. \qquad (2.19)$$

Symmetry does not require that the electron charge distribution be symmetric along the direction normal to the surface plane. Furthermore, based on quantum mechanical considerations, this electron charge distribution does not end abruptly at the surface position but spreads out beyond the jellium edge background in order to lower its kinetic energy. This density decays exponentially well outside the jellium edge and exhibits Friedel oscillations at and inside the surface as it approaches its bulk value. A double layer is thus formed in the region about the surface and an electron trying to escape from the metal will experience a dipole barrier of height

$$\Delta\phi = 4\pi \int_{-\infty}^{+\infty} x\, \rho_T(x)dx. \qquad (2.20)$$

The corresponding electrostatic potential $V_{es}(x)$ due to the total charge distribution of the system is then the solution to Poisson's equation

$$d^2V_{es}/dx^2 = -4\pi \rho_T(x). \tag{2.21}$$

With the choice of boundary conditions $V_{es}(-\infty)=V'_{es}(-\infty)=0$, together with the charge neutrality condition, the solution to the Poisson's equation may be written as

$$V_{es}(x) = \Delta\phi - 4\pi\int_{\infty}^{x} dx'\int_{\infty}^{x'} dx'' \rho_T(x''). \tag{2.22}$$

The most important electronic properties of a surface that may be derived from the density are the work function and surface energy. The work function Φ is defined as the minimum amount of work required to remove an electron from the metal at 0°K (14) and is given by an expression reminiscent of Koopmans' theorem for the removal energy of an electron from an atom:

$$\Phi = -\mu ,$$

where μ is the highest occupied eigenvalue of the Kohn-Sham self-consistent single-particle equations. This leads to

the separation of Φ into its surface $\Delta\phi$ and bulk $\bar{\mu}$ contributions such that

$$\Phi = \Delta\phi - \bar{\mu} , \tag{2.23}$$

where $\bar{\mu}$, the bulk chemical potential relative to the mean interior electrostatic potential, is defined as

$$\bar{\mu} = 1/2\ k_F^2 + \mu_{xc}. \tag{2.24}$$

In the above equation μ_{xc} is just the exchange-correlation part of the chemical potential of a uniform electron gas i.e.

$$\mu_{xc} = d(\bar{\rho}\epsilon_{xc})/d\bar{\rho} , \tag{2.25}$$

where $\bar{\rho}=k_F^3/3\pi^2$ is the mean interior electronic density. A generalization of the Koopmans' theorem expression of Eq. 2.23 for the work function to real metals incorporating appropriate local ionic pseudopotentials and including band structure effects has recently been derived by Sahni and Gruenebaum (80).

Yet another expression for the work function of jellium metal has also been derived by Mahan and Schaich (86), according to which

$$\Phi = V_{es}(\infty) - V_{es}(a) - \varepsilon_T, \qquad (2.26)$$

where $\varepsilon_T = 3k_F^2/10 + \varepsilon_{xc}(\bar{\rho})$ is the sum of the kinetic, exchange and correlation energies per particle for a uniform electron gas of density $\bar{\rho}$. For a fully self-consistent calculation within the LDA, these two definitions for the work function lead to the same result (86). The generalization of Eq. 2.26 for the case when the ions are replaced by local pseudopotentials is straightforward (87). Both this generalized expression for the work function, and thus Eq. 2.26, have also been derived by Monnier et al. (88) by considering the difference in surface energies between the neutral and infinitesimally charged surface, the latter surface charge density occurring due to the removal of one or more electrons from the metal. However, more importantly, it has been shown that these expressions, although as simple to use as Koopmans' theorem, are much more accurate when the density is obtained from variational calculations of the surface energy. The variational accuracy of Eq. 2.26 has recently been demonstrated by Perdew and Sahni (89).

The surface energy of a metal E_s, which is the energy required per unit area formed to split the crystal in two along a plane, may be determined by two completely different methods. The component method requires knowledge of the individual kinetic, electrostatic, and exchange-correlation energy contributions. The kinetic energy contribution to the surface energy E_k in terms of the asymptotic phase shift

$\delta(k)$ is given within the Kohn-Sham scheme via Eq. 2.7 as (5,26,36)

$$E_k[\rho] = \frac{k_F^4}{160\pi}\{1+\frac{80}{k_F^4}[3/5\, k_F^2\int_0^{k_F} k\delta(k)dk-\int_0^{k_F} k3\delta(k)dk]\}$$

$$-\int_{-\infty}^{+\infty}\{V_{eff}[\rho;x]-V_{eff}[\rho;-\infty\,]\}\rho(x)dx. \qquad (2.27)$$

Implicit in this definition for $E_k[\rho]$ is the fact that one is here dealing with single-particle wave functions from which the density is obtained. If on the other hand, we had knowledge only of the density (see Chap. V), then one choice for the surface kinetic energy functional would be to represent it by its density gradient expansion. The electrostatic contribution to the surface energy E_{es} is

$$E_{es}[\rho] = 1/2\int_{-\infty}^{+\infty}\rho_T(x)V_{es}(x)dx, \qquad (2.28)$$

and the sum of the surface exchange-correlation contributions E_{xc} which must be taken together within the LDA (71-74) is given as (26)

$$E_{xc}^{LDA}[\rho] = \int_{-\infty}^{+\infty}[\varepsilon_{xc}(\rho(x))-\varepsilon_{xc}(\bar{\rho})]\rho(x)dx. \qquad (2.29)$$

In this work we will restrict ourselves to determining the exchange-correlation energy strictly within the LDA and

neglect all density gradient terms. The total surface energy functional is then the sum of the individual components discussed above i.e.

$$E_s[\rho] = E_k[\rho] + E_{es}[\rho] + E_{xc}^{LDA}[\rho]. \qquad (2.30)$$

A second method for the determination of surface energy is to employ an exact sum rule due to Vannimenus and Budd (38). The Vannimenus-Budd theorem (VBT) relates the derivative of the surface energy E_s with respect to the density to an integral of the electrostatic potential inside the metal. In terms of the Wigner-Seitz radius r_s, the BVT states that

$$dE_s/dr_s = -9/(4\pi r_s^4) \int_{-\infty}^{a} [V_{es}(-\infty) - V_{es}(x)]dx, \qquad (2.31)$$

Thus it is possible to obtain the surface energy of jellium metal directly by a simple integration over r_s together with a suitable choice for the constant of integration. The accuracy of the method thus depends on the accuracy of the electrostatic potential inside the metal and on the reasonableness of the criterion for the determination of the constant of integration. The principle advantage of the method is that no approximations with regard to any component energy functional have to be made.

Another fundamental sum rule (to be used extensively in this work) derived by Budd and Vannimenus (32) relates the

difference in electrostatic potential between that at the surface and in the bulk, to the total energy per particle ϵ_T of a uniform electron gas. According to the Budd-Vannimenus theorem (BVT)

$$\Delta V = V_{es}(a) - V_{es}(-\infty) = \bar{\rho} d\epsilon_T / d\bar{\rho} \cdot \qquad (2.32)$$

The significance of this theorem lies in the fact that it relates a surface property to those of the more well understood bulk. In model potential calculations, this theorem can thus be used as a constraint on the electrostatic potential.

Mahan and Schaich (86) have also recently derived an integral condition, which can be shown to be equivalent to the differential sum rule of the BVT within the LDA. For an arbitrary effective potential, the Mahan-Schaich theorem (MST) states that

$$1/\bar{\rho} \int_{-\infty}^{+\infty} V_{eff}(x)(-d\rho/dx)dx = 2/5\ E_F + V_{eff}(-\infty). \qquad (2.33)$$

For a fully self-consistent or model potential calculation this condition is always satisfied. For fully self-consistent calculation within the LDA, this thus implies that the BVT must always be satisfied (86). However, for non-self-consistently obtained densities such as those determined by variational principles for the density itself

(see Chap. V) this theorem can be used as an additional constraint. Since in such variational calculations, the density is obtained correct to second order, the use of the MST in this manner precludes the determination of any higher order terms in the series for the density.

Throughout this work we employ the Wigner interpolation formula (Eq. 2.9) for the average correlation energy per particle for all $r_s \geq 1$ and the Gell Mann-Brueckner (GB) expression (90) for $r_s \leq 1$;

$$\varepsilon_c^{GB} = 0.0311 \ln r_s - 0.048. \qquad (2.34)$$

The justification for the above choice is that at $r_s=1$ the difference $\varepsilon_c^W - \varepsilon_c^{GB} = 0.05$ eV only, and the fact that the GB expression becomes more accurate for higher densities whereas the Wigner expression is appropriate for both metallic and lower densities. Employing the Wigner and Gell Mann-Brueckner expressions for ε_c we have ΔV in units of the free-electron Fermi energy $E_F = k_F^2/2$ to be

$$\Delta V^W = 0.4 - 0.0829 r_s - 0.0796 r_s^3/(r_s+7.8)^2 , \qquad (2.35)$$

and

$$\Delta V^{GB} = 0.4 - 0.0829 r_s - 0.005629 r_s^2 , \qquad (2.36)$$

respectively.

III. USE OF MODEL POTENTIALS WITH THEORETICAL AND PHYSICAL CONSTRAINTS FOR THE STUDY OF A NEUTRALLY CHARGED ELECTRON GAS WITH A SURFACE

In this chapter we present the results of a study over a wide range of densities, including the metallic range, of a charge neutral electron gas system with a surface. The inhomogeneity in the electronic density at the surface is created by assuming the electrons move in a model effective potential in the presence of a positive uniform charge (jellium) background which ends abruptly at a well defined point. The properties derived from these calculations are metallic surface dipole barriers, work functions and surface energies, the behavior of the work function for densities higher than those existing in metals, and low density surface energies. The appropriate use of various theoretical and physical constraints coupled with the fact that the choice of effective potential employed here leads to results which are primarily analytic permits the study of such an inhomogeneous electron system over a substantial range of densities. The model potential considered is one which varies linearly over a finite region and is constant beyond some point (see Fig. 1), and we refer to it as the finite linear potential (FLP) model. The parameters in this model potential system are the edge of the neutralizing positive charge background, the field strength and the barrier

height. In all the calculations presented here, the jellium edge and barrier height parameters are always determined by the requirements of charge neutrality (2) and self-consistency respectively. It is the field strength parameter which is adjusted so as to either satisfy the BVT or varied until the energy is minimized. Thus not only is this model effective potential a realistic approximation to that which exists at such a surface, it has more physically meaningful constraints applied simultaneously than any other analytic potentials studied (34-37) previously. The effective potential $V_{eff}(x)$ at the surface of the electron gas is assumed to be (see Fig. 1)

$$V_{eff} = Fx[\Theta(x)-\Theta(x-b)] + V\Theta(x-b), \qquad (3.1)$$

where the field strength F is defined in terms of the barrier height and slope parameters b and x_F as $F=V/b=E_F/x_F$, and where V is the barrier height, $E_F=k_F^2/2$ is the Fermi energy and $\Theta(x)$ the step function. We also specify the variation of the barrier height in terms of the parameter β where $\beta^2=E_F/V=x_F/b$. For the effective potential of Eq. 3.1, the solution of the Schrodinger equation for the electronic wave function is

$$\psi_k(x) = \begin{cases} A \sin[kx+\delta(k)] & \text{for} \quad x \leq 0 \\ B_k Ai(\zeta)+C_k Bi(\zeta) & \text{for} \quad 0 \leq x \leq b \\ D_k \exp(-\kappa x) & \text{for} \quad b \leq x \end{cases} \qquad (3.2)$$

where $k=(2E)^{1/2}$, $\kappa=(2(V-E))^{1/2}$, $\zeta=(x-E/F)(2F)^{1/3}$, E is the energy, and where $Ai(\zeta)$ and $Bi(\zeta)$ are the linearly independent solutions of the Airy differential equation (91). The constant A in the above equation is obtained by the normalization condition whereas the phase factor $\delta(k)$ and the coefficients B_k, C_k and D_k are determined by the requirement of the continuity of the wave function and its logarithmic derivative at both x=0 and x=b. Thus

$$A = -(2/L)^{1/2} \quad , \quad B_k = (2/L)^{1/2}(\zeta_o/\Lambda(-\zeta_o))^{1/2}$$

$$C_k = -B_k\, X(\zeta_b)/Y(\zeta_b)$$

$$D_k = B_k\, M(\zeta_b)\exp[(\zeta_b+\zeta_o)\zeta_b^{1/2}]$$

$$\cot\delta(k) = N(-\zeta_o)/(\zeta_o^{1/2}M(-\zeta_o))$$

where

$$X(\zeta_b) = Ai'(\zeta_b) + (\zeta_b)^{1/2}Ai(\zeta_b)$$
$$Y(\zeta_b) = Bi'(\zeta_b) + (\zeta_b)^{1/2}Bi(\zeta_b)$$
$$M(\zeta) = Ai(\zeta) - Bi(\zeta)X(\zeta_b)/Y(\zeta_b)$$
$$N(\zeta) = Ai'(\zeta) - Bi'(\zeta)X(\zeta_b)/Y(\zeta_b)$$
$$\Lambda(\zeta) = N^2(\zeta) - \zeta M^2(\zeta)$$
$$\zeta_o = k^2(b/2V)^{2/3} = (k^2/k_F^2)(k_Fx_F)^{2/3}$$
$$\zeta_b = b(2V/b)^{1/3} - \zeta_o = bk_F(k_Fx_F)^{-1/3} - \zeta_o$$

and where $Ai'(\zeta)$ and $Bi'(\zeta)$ are the derivatives (91) of the Airy functions.

The various properties of interest determined with the above wave functions are the electronic density $\rho(x)$, the jellium edge position at $x=a$, the total charge density $\rho_T(x)$, the surface dipole barrier $\Delta\phi$, the work function Φ, the electrostatic potential $V_{es}(x)$, the kinetic E_k (26), electrostatic E_{es} and exchange-correlation (13) E_{xc} components of the surface energy E_s as obtained within the LDA, and the derivative of the surface energy with respect to the Wigner-Seitz radius dE_s/dr_s as stated by VBT. The mathematical definitions of these properties are all given in Chap. II.

For the present choice of effective potential, all the spatial integrals of the above defined properties, with the sole exception of the exchange-correlation contribution to the surface energy, can be performed analytically, since it has been possible to derive analytic expressions for indefinite integrals involving products of Airy functions, products of their derivatives and various moments of these products. These integral expressions are given in Appendix A. With a change of variables to $y=xk_F$ and $q=k/k_F$, such that the jellium edge, slope and barrier height parameters are now defined to be $y_a=ak_F$, $y_F=x_Fk_F$ and $y_b=bk_F$, the determination of all these properties thus reduces to simple numerical computations of momentum space integrals from 0 to 1. With the density normalized with respect to its bulk value,

we have $n(y)=\rho(y)/\overline{\rho}$, $\zeta_o=q^2y_F^{2/3}$, $\zeta_b=y_by_F^{-1/3}-\zeta_o$, and $\zeta=yy_F^{-1/3}-\zeta_o$. The resulting semi-analytic expressions for the various properties in terms of these variables are given below.

Phase Shift

With the definition

$$K(q) = y_F^{1/3}\, M(-\zeta_o)/N(-\zeta_o), \tag{3.3}$$

so that

$$K(0) = y_F^{1/3}\, \frac{Ai(0)-Bi(0)X(y_by_F^{-1/3})/Y(y_by_F^{-1/3})}{Ai'(0)-Bi'(0)X(y_by_F^{-1/3})/Y(y_by_F^{-1/3})} \tag{3.4}$$

the phase shift is

$$\delta(q) = \cot^{-1}[1/qK(q)]. \tag{3.5}$$

Electronic Density

For $y \geq y_b$

$$n(y) = 3\int_0^1 dq(1-q^2)\zeta_o\, M^2(\zeta_b) \cdot \exp[2(\zeta_b-\zeta)\zeta_b^{1/2}]/\Lambda(-\zeta_o). \tag{3.6}$$

For $0 \leq y \leq y_b$

$$n(y) = 3 \int_0^1 dq(1-q^2)\zeta_o M^2(\zeta)/\Lambda(-\zeta_o). \qquad (3.7)$$

For $y \leq 0$

$$n(y) = 3 \int_0^1 dq(1-q^2)\sin^2[qy+\delta(q)]. \qquad (3.8)$$

Jellium Edge Position

The jellium edge position as determined by the phase shift rule of Sugiyama (Eq. 2.19) may be written as

$$y_a = -3\pi/8 - 3 \int_0^1 q\delta(q)dq, \qquad (3.9)$$

whereas the charge neutrality condition of Eq. 2.17 leads to the expression

$$y_a = 2/5\ y_F - 3\pi/8 + 3/2\ y_F^{1/3} \int_0^1 dq(1-q^2)[\zeta_o M^2(\zeta_b)/\zeta_b{}^{1/2} - M(-\zeta_o)N(-\zeta_o)]/\Lambda(-\zeta_o). \qquad (3.10)$$

The specific analytic equivalence of the charge neutrality condition to that of the phase shift rule for the FLP model is proved in Appendix B.

Surface Dipole Barrier

$$\Delta\phi/k_F = 1/\pi + K(0)/2 - 2y_a^2/(3\pi) + 16y_F^2/(105\pi)$$

$$+ y_F^{2/3}\, J(y_F, y_b)/\pi \qquad (3.11)$$

where

$$J(y_F, y_b) = \int_0^1 dq\,(1-q^2)\frac{M^2(-s_0)}{\Lambda(-s_0)} + \int_0^1 dq\,(1-q^2)\frac{s_0}{\Lambda(-s_0)}\left\{\frac{4}{3}\left[M(s_b)N(s_b) - M(-s_0)N(-s_0)\right] + M^2(s_b)\left[\frac{1}{s_b} + 2\frac{s_0+s_b}{\sqrt{s_b}}\right]\right\}$$

Electrostatic Potential

For $y \geq y_b$

$$\frac{V_{es}(y)}{k_F} = \frac{\Delta\phi}{k_F} - \frac{y_F^{2/3}}{\pi}\int_0^1 dq\,(1-q^2)\frac{s_0}{s_b}\frac{M^2(s_b)}{\Lambda(-s_0)}\, e^{2\sqrt{s_b}(s_b - s)} \qquad (3.12)$$

For $0 \leq y \leq y_b$

$$\frac{V_{es}(y)}{k_F} = \frac{1}{\pi} + \frac{1}{2}K(0) + \frac{16}{105}\frac{y_F^2}{\pi} + \left(\frac{1}{2} - \frac{8}{15}\frac{y_F}{\pi}\right)y \qquad (3.13)$$

$$+ \frac{2}{3\pi}\left\{y_a(2y - y_a)\,\theta(y - y_a) + y\,\theta(y_a - y)\right\}$$

$$+\frac{y_F^{1/3}}{\pi}\int_0^1 dq\,(1-q^2)\frac{M(-s_0)}{\Lambda(-s_0)}\left\{y_F^{1/3}\,M(-s_0)+2y\,N(-s_0)\right\}$$

$$+\frac{4}{3}\frac{y_F^{2/3}}{\pi}\int_0^1 dq\,(1-q^2)\frac{s_0}{\Lambda(-s_0)}\left\{2s\,\Lambda(s)+M(s)N(s)-M(-s_0)N(-s_0)\right\}$$

For $y\leq 0$

$$\frac{V_{es}(y)}{k_F}=\frac{1}{\pi}+\frac{1}{2}K(0)+\frac{1}{2}y-\frac{2}{3\pi}(y-y_a)^2\,\theta(y-y_a) \qquad (3.14)$$

$$+\frac{1}{\pi}\int_0^1 dq\,(1-q^2)\frac{1}{q^2}\sin^2(qy+\delta)$$

Kinetic Energy

$$\frac{\pi^2}{k_F^4}E_k=-\frac{\pi}{32}+\frac{y_F}{35}-\frac{y_a}{10}+\frac{y_F^{1/3}}{8}\int_0^1 dq\,(1-q^4)\frac{1}{\Lambda(-s_0)}\left\{\frac{s_0}{\sqrt{s_b}}M^2(s_b)\right. \qquad (3.15)$$

$$\left.-M(-s_0)N(-s_0)\right\}-\frac{1}{4}\int_0^1 dq\,(1-q^2)\frac{q^2}{\Lambda(-s_0)}\left\{\frac{y_b}{\sqrt{s_b}}M^2(s_b)\right.$$

$$\left.+\frac{2}{3}y_F^{1/3}\left[M(s_b)N(s_b)-M(-s_0)N(-s_0)\right]\right\}$$

The above equation for the kinetic energy is derived from Eq. 2.27 by using the equivalence of the charge neutrality

condition to the Sugiyama phase shift rule.

Electrostatic Energy

$$E_{es}/k_F^3 = P(y_F,y_b) + R(y_F,y_b)$$

$$+1/(6\pi^2)\int_0^{y_b} dy\, n(y) V_{es}(y)/k_F, \qquad (3.16)$$

where

$$P(y_F,y_b) = \frac{y_F}{4\pi^2}\int_0^1 dq(1-q^2)\frac{q^2}{\Lambda(-\beta_0)} M^2(\beta_b)\left\{\frac{\Delta\phi}{k_F}\frac{1}{\sqrt{\beta_b}}\right.$$
$$\left. - \frac{y_F^{2/3}}{\pi}\int_0^1 dq'(1-q'^2)\frac{\beta_0'}{\Lambda(-\beta_0')}\frac{M^2(\beta_b')}{\beta_b'}\frac{1}{\sqrt{\beta_b}+\sqrt{\beta_b'}}\right\}$$

$$R(y_F,y_b) = \frac{1}{4\pi^2}\left\{-\frac{1}{12} + y_a\left[\frac{4}{27}\frac{y_a^2}{\pi} - \frac{y_a}{6} - \frac{2}{3}\left(\frac{1}{\pi}+\frac{1}{2}K(0)\right)\right]\theta(-y_a)\right.$$
$$+\int_0^1 dq(1-q^2)\left[\frac{\sin^2\delta}{q^2} - \left(\frac{1}{\pi}+\frac{1}{2}K(0)\right)\frac{\sin 2\delta}{q}\right]$$
$$\left. +\frac{1}{4\pi}\int_0^1 dq(1-q^2)\frac{1}{q^2}\int_0^1 dq'(1-q'^2)\left[\frac{\sin 2\delta_-}{2q_-} + \frac{\sin 2\delta_+}{2q_+} - \frac{\sin 2\delta'}{q'}\right]\right\}$$
$$+\frac{1}{6\pi^3} y_a\left[\int_0^1 dq(1-q^2)\left(\frac{\sin^2\delta}{q^2} + y_a\frac{\sin 2\delta}{2q}\right)\right]\theta(-y_a)$$
$$-\frac{1}{6\pi^3}\int_0^1 dq(1-q^2)\frac{1}{q^2}\left[y_a + \frac{1}{2q}(\sin 2\delta - \sin 2(qy_a+\delta))\right]\theta(-y_a)$$

In the above expressions all the primed quantities are functions of the variable q', and $q_-=q-q'$, $q_+=q+q'$, $\delta_-=\delta-\delta'$, and $\delta_+=\delta+\delta'$.

Derivative of Surface Energy

For $y_a \leq 0$

$$\frac{4\pi}{9}\kappa_s^4\frac{dE_s}{d\kappa_s} = \mathcal{S}(y_F,y_b)+\frac{1}{2\pi}\int_0^1 dq\,(1-q^2)\frac{1}{q^2}\left\{ y_a+\frac{1}{2q}\sin 2\delta - \frac{1}{2q}\sin 2(qy_a+\delta)\right\} \tag{3.17}$$

For $y_a \geq 0$

$$\begin{aligned}\frac{4\pi}{9}\kappa_s^4\frac{dE_s}{d\kappa_s} &= \mathcal{S}(y_F,y_b)+\frac{2}{9}\frac{y_a^3}{\pi}-\frac{4}{15}\frac{y_F}{\pi}y_a^2+\frac{16}{105}\frac{y_F^2}{\pi}y_a \\ &+ y_a\frac{y_F^{2/3}}{\pi}\int_0^1 dq\,(1-q^2)\frac{M(-\mathcal{S}_0)}{\Lambda(-\mathcal{S}_0)}\left\{M(-\mathcal{S}_0)+y_a y_F^{1/3}N(-\mathcal{S}_0)\right\} \\ &+\frac{4}{3}\frac{y_F}{\pi}\int_0^1 dq\,(1-q^2)\frac{\mathcal{S}_0}{\Lambda(-\mathcal{S}_0)}\left\{\frac{4}{5}\left[\mathcal{S}_a^2\Lambda(\mathcal{S}_a)-\mathcal{S}_0^2\Lambda(-\mathcal{S}_0)\right]\right. \\ &+\frac{3}{10}\left[M^2(\mathcal{S}_b)-M^2(-\mathcal{S}_0)\right]-(\mathcal{S}_0+\mathcal{S}_a)M(-\mathcal{S}_0)N(-\mathcal{S}_0) \\ &\left.+\frac{2}{5}\left[\mathcal{S}_a M(\mathcal{S}_a)N(\mathcal{S}_a)+\mathcal{S}_0 M(-\mathcal{S}_0)N(-\mathcal{S}_0)\right]\right\}\end{aligned} \tag{3.18}$$

where $\zeta_a = y_a y_F^{-1/3} - \zeta_o$, $\Lambda(\zeta_a) = N^2(\zeta_a) - \zeta_a M^2(\zeta_a)$, and where

$$\mathcal{S}(y_F, y_b) = \frac{1}{8} + \frac{1}{4} y_a^2 + \left(y_a + \frac{1}{2}K(0)\right)\left(\frac{1}{\pi} + \frac{1}{2}K(0)\right) - \frac{1}{2\pi}\int_0^1 dq \frac{1}{q^2}\left\{(1-q^2)\frac{K(q)}{1+q^2K^2(q)} - K(0)\right\}$$

We note that the VBT expression of Eq. 2.31 is derived on the assumption that for a slab of length L, the electrostatic potential at the center (relative to the value at the surface) differs from the value in the L goes to ∞ limit by terms of higher order than L^{-1}. This assumption can be shown to be equivalent to the requirement that the electrostatic potential approaches its value at the center faster than L^{-1}. In Appendix C we prove this to be the case and demonstrate that for the electrostatic potential generated by the FLP model this condition is satisfied.

It may be observed from these expressions that the quantities $n(y)$, y_a, $\Delta\phi/k_F$, E_k/k_F^4, E_{es}/k_F^3 and $r_s^4\, dE_s/dr_s$ are functions of the barrier height and slope parameters. Since in our calculations, the barrier height is always determined by the requirement of the self-consistency of the surface dipole barrier, each of these quantities is a universal function of the slope parameter for a given density. Note that in order to determine the barrier height the

density must be specified. In Figs. 2-6 we plot the universal functions of y_a, $\Delta\phi/k_F$, $(160\pi/k_F^4)E_k$, E_{es}/k_F^3, and $(4\pi/9)r_s^4\, dE/dr_s$ versus the slope parameter y_F for r_s=2,4 and 6 with the barrier height determined self-consistently for each point on the graphs. In Fig. 7 we plot the variation of the self-consistently obtained barrier height parameter y_b versus the slope parameter y_F for the same values of r_s. Thus, if for a given density, the slope parameter is known by application of some constraint, these five properties may be determined directly from Figs. 2-6 and the corresponding self-consistent value of the barrier height parameter from Fig. 7. In Section A we present the values for metal surface dipole barriers and work functions as obtained by application of BVT, and extend these calculations to plot the variation of the work function for higher densities. The results of a variational self-consistent calculation of metal surface energies within the LDA are given in Section B. In Section C we determine the surface energy for metallic and lower densities via the VBT (Eq. 2.31) without having to determine any individual kinetic, electrostatic and exchange-correlation components of the energy. The constant of integration in the application of VBT is determined by the physical criterion of the vanishing of the surface energy in the low density limit. For purposes of comparison, the results of a LDA calculation over the same range of densities with the same choice of effective potential are also included. Finally we conclude this last section by indicat-

ing further use of such model potentials in the study of other aspects of the inhomogeneous electron gas problem and in the determination of more realistic metal surfaces properties.

A. Surface Dipole Barriers and Work Functions for Metallic and Higher Densities by Application of the Budd-Vannimenus Theorem

The model potential employed in the present calculations is a two-parameter one, the parameters being the barrier height and field strength. In addition, a third parameter, the jellium edge position must be introduced in order that the electronic system under consideration be charge neutral. The surface of the system is defined to be at the jellium edge. In all the calculations to follow, the barrier height is always determined by the requirement of the self-consistency of the surface dipole barrier. In this section the results for metallic and higher density surface dipole barriers and work functions are presented, with the field strength adjusted so as to satisfy the BVT (Eq. 2.32). The principle advantage of this constraint is that it leads to accurate results for the work function since ΔV consitiutes a substantial fraction of the surface dipole barrier. In particular for high densities this contribution can be as large as 40%. For densities such that $r_s \leq 4.3$ all three constraints, viz. that of the BVT, self-consistency of $\Delta\phi$ and charge neutrality are satisfied exactly whereas for $r_s > 4.3$ only those of the self-consistency of the surface dipole barrier and charge neutrality can be satisfied. Further details are given in Appendix D.

In Table I we present results for the surface dipole barrier and work function in the density range $r_s = 1\text{-}6$ employing the Wigner expression for the correlation energy.

TABLE I

Results for metallic and higher density (r_s=1-6) surface dipole barriers $\Delta\phi$ and work functions ϕ. The slope, barrier height and jellium edge parameters y_F, y_b and y_a quoted are determined by application of the BVT, self-consistency of $\Delta\phi$ and charge neutrality respectively employing the Wigner function for the correlation energy. The results for the barrier height written in terms of the parameter β are given in parenthesis in the y_b column.

r_s	$y_F=k_F z_F$	$y_b=k_F b$ ($\beta=k_F/\sqrt{2W}$)	$y_a=k_F a$	Dipole barrier $\Delta\phi$ (eV)		Work Function ϕ(eV)		$\lvert\phi_{LK}-\phi\rvert$ (eV)
				Present Work	Lang-Kohn[a]	Present Work	Lang-Kohn[a]	
1.0	6.60	7.31(0.95)	2.64	37.51		5.43		
1.5	4.91	5.97(0.91)	1.95	14.66		4.82		
2.0	3.74	4.99(0.87)	1.48	7.10	6.80	4.19	3.89	0.30
2.5	2.79	4.07(0.83)	1.10	3.82	3.83	3.71	3.72	0.01
3.0	1.94	3.11(0.79)	0.76	2.16	2.32	3.34	3.50	0.16
3.5	1.16	2.02(0.76)	0.39	1.21	1.43	3.04	3.26	0.22
4.0	0.13	0.25(0.73)	-0.28	0.64	0.91	2.79	3.06	0.27
4.5	0.00	0.00(0.68)	-0.46	0.50	0.56	2.81	2.87	0.06
5.0	0.00	0.00(0.65)	-0.50	0.42	0.35	2.80	2.73	0.07
5.5	0.00	0.00(0.57)	-0.54	0.35	0.16	2.73	2.54	0.19
6.0	0.00	0.00(0.55)	-0.57	0.30	0.04	2.67	2.41	0.26

a. see Ref. 14.

Included for purposes of comparison are the completely self-consistent LDA values of Lang and Kohn (LK) (13,14). Note that the FLP model gives rise to approximately the same results for both medium and high metallic densities, in particular reproducing the large values of $\Delta\phi$ required for higher densities. The corresponding charge densities are also very similar to those of Lang-Kohn. For example, for r_s=2.5 the FLP electronic density differs by 0.2% at the surface and is within 1.8% inside the metal, and within 4% up to half a Fermi wavelength outside where the density has fallen to a fortieth of its bulk value. For low metallic densities (for which the dipole barriers are of considerably less significance) our work functions differ by at most a quarter of an electron volt from those of LK. Although for these densities the LK results also do not satisfy the BVT, the values of our electrostatic potentials at the surface are more in error than those of LK. In the last column of Table I we give the magnitude of the difference between LK and our results for the work function and note that over the entire metallic range these values lie within three tenths of an electron volt.

A comparison of these results and those of LK with experimental values (26) for polycrystalline metals is made in Fig. 8. Note that for the majority of the simple metals considered, the results of our model potential calculation more closely approximate the experimental results than do those of LK.

It has been conjectured by Lang and Kohn (14) that in the high density limit the work function in the jellium model tends to a finite value in the vicinity of 4 eV as the leading terms of both the dipole barrier and bulk chemical potential relative to the mean electrostatic potential in the interior diverge as the Fermi energy and thus cancel each other. More recently a Green's function analysis by Peuckert (92) has yielded a value of 1.2 eV for the work function in the high density limit. This result suggests that the work function must decrease from its metallic value as the density is increased saturating at the above value for infinite density.

In order to determine the continuous behavior of the work function as the density is increased beyond the metallic range, we have extended the calculations of the dipole barrier and work function to higher densities employing the same constraints as discussed above. The results using both the Gell Mann-Brueckner and Wigner expressions for the correlation energy are given in Table II. In Fig. 9 we plot the variation of the high density work functions with the density. A study of the graph indicates that initially the work function increases as the density is increased, reaches a maximum at about $r_s=1$, and then rapidly diminishes vanishing at approximately $r_s=0.4$ in contrast to the conclusions of both Peuckert and Lang and Kohn. The results for the dipole barrier for the two different correlation functions differ by at most 0.7 eV, the work functions being within

TABLE II

Results for high density ($r_s \leq 1$) surface dipole barriers $\Delta\phi$ and work functions Φ. The slope, barrier height and jellium edge parameters y_F, y_b and y_a quoted are determined by application of the BVT, self-consistency of $\Delta\phi$ and charge neutrality respectively employing the Gell Mann-Brueckner (GB) expression for the correlation energy. The results for $\Delta\phi$ and Φ employing the Wigner (W) expression are also quoted.

r_s	$y_F=k_F x_F$	$y_b=k_F b$	$y_a=k_F a$	Dipole barrier $\Delta\phi$(eV)		$\frac{1}{2}k_F^2$(eV)	$-\mu_{xc}$(eV)	Work Function Φ(eV)	
	GB	GB	GB	GB	W		GB	GB	W
0.43	10.99	11.04	4.42	231.3	232.0	271.0	41.0	1.23	1.09
0.44	10.85	10.91	4.36	220.3	221.0	258.8	40.1	1.55	1.41
0.45	10.71	10.79	4.30	210.1	210.8	247.5	39.2	1.85	1.72
0.50	10.09	10.24	4.05	168.0	168.7	200.4	35.4	3.01	2.92
0.55	9.54	9.76	3.83	137.1	137.7	165.7	32.3	3.78	3.74
0.60	9.06	9.34	3.64	113.8	114.3	139.2	29.7	4.31	4.30
0.65	8.64	8.98	3.46	95.7	96.3	118.6	27.5	4.65	4.69
0.70	8.25	8.65	3.31	81.5	82.1	102.3	25.6	4.89	4.97
0.80	7.59	8.09	3.04	60.9	61.4	78.3	22.6	5.14	5.30
0.90	7.02	7.62	2.82	46.0	47.4	61.9	20.1	5.20	5.43
1.00	6.55	7.22	2.62	37.0	37.5	50.1	18.2	5.14	5.43

three tenths of an electron volt of each other. The vanishing of the work function occurs due to the fact that for the densities concerned, the surface dipole barrier is not a large enough fraction of the Fermi energy ($\Delta\phi/E_F=0.85$ for $r_s=0.43$) and thus the cancellation referred to by Lang and Kohn does not occur (93). Furthermore, there is no substantial increase in the magnitude of the exchange and correlation contribution to the chemical potential although the density at which the work function vanishes is three orders of magnitude greater than those which occur in metals. In the range from $r_s=2$-0.4, μ_{xc} changes by a factor of approximately 4 in sharp contrast to $\Delta\phi$ which changes by a factor of over 30. Thus, as the density is increased, the Fermi energy approaches the barrier height with the net result that the work function vanishes.

B. Variational Self-Consistent Calculation of Metal Surface Energies in the Local Density Approximation

In this section we present the results of a variational self-consistent calculation of metal surface energies as determined within the LDA. The barrier height parameter is determined as usual by the self-consistency requirement set for the dipole barrier. It is the field strength or the slope parameter which is varied till the total energy is minimized. The values obtained thus constitute an upper bound to the surface energy for this choice of energy functional of the density. The results for the surface energy E_s, together with its individual kinetic E_k, electrostatic E_{es}, and LDA exchange-correlation E_{xc}^{LDA} components are given in Table III. Since Lang and Kohn employed the same energy functional, a comparison with their work is meaningful and we include their results in the table. Note that for $r_s \geq 2.5$ our values for E_s are within 5 ergs/cm^2 of those of LK, the result for $r_s=2$ differing by less than 3%. Thus with the same local density approximation for the surface energy our model potential results are equivalent to those of a completely self-consistent calculation. We have also included in this table the values of the dipole barrier obtained using these energy minimized wave functions. As may be observed, these results though good are in general not as accurate as those of the previous section. This is consistent with the fact that this property is determined only to the same order of accuracy as that of the wave function employed

TABLE III

Results for metallic density (r_s=2-6) surface energies E_s as obtained within the local density approximation. The barrier height and jellium edge parameters y_b and y_a quoted are determined by the self-consistency of the surface dipole barrier and charge neutrality conditions respectively, whereas the slope parameter y_F is obtained by variational minimization of the total energy. The Wigner expression for the correlation energy is employed.

r_s	$y_F=k_F x_F$	$y_b=k_F b$	$y_a=k_F a$	$\Delta\phi$ (eV)	Surface Energy Components (ergs/cm^2)			Surface Energies E_s (ergs/cm^2)		$\lvert E_{s(LK)}-E_s\rvert$ (ergs/cm^2)
					E_k	E_{es}	E_{xc}	Present Work	Lang-Kohn[a]	
2.0	3.34	4.21	1.33	6.17	-5416	1265	3171	-980	-1008	28
2.5	2.66	3.84	1.06	3.64	-1809	420	1430	41	36	5
3.0	2.13	3.48	0.84	2.35	- 720	172	749	201	199	2
3.5	1.70	3.13	0.65	1.61	- 321	82	435	196	194	2
4.0	1.37	2.82	0.49	1.16	- 156	44	274	162	158	4
4.5	1.11	2.54	0.36	0.87	- 81	26	183	128	124	4
5.0	0.91	2.30	0.24	0.68	- 44	17	128	101	98	3
5.5	0.76	2.10	0.15	0.55	- 24	11	94	81	77	4
6.0	0.64	1.92	0.06	0.45	- 14	8	71	65	60	5

a. see Refs. 13 and 37.

and not correct to second order as is the energy.

C. Surface Energies for Metallic and Lower Densities by Application of the Vannimenus-Budd Theorem

We present here results for the surface energy for metallic and lower densities as obtained by application of the VBT. According to this theorem, the derivative of the surface energy with respect to the Wigner-Seitz radius r_s can be determined exactly by integration of the electrostatic potential over the interior of the system. The surface energy is thus obtained to within a constant. For the determination of this constant of integration we apply the physical condition that the surface energy vanishes in the limit of vanishing density. Thus for a specific value of the Wigner-Seitz radius the surface energy is given by

$$E_s(r_s) = \int_{\infty}^{r_s} \frac{dE_s}{dr_s'} dr_s',$$

where dE_s/dr_s is obtained from the sum rule of Eq. 2.31. The parameters in this model calculation are again determined by application of the BVT, self-consistency of $\Delta\phi$ and charge neutrality for $r_s \leq 4.3$ and by satisfaction of the latter two constraints for all $r_s > 4.3$. For $r_s = 14$, the self-consistent barrier height is so large that there is negligible difference between the value for dE_s/dr_s thus obtained and the value for the infinite barrier potential.

Therefore for $r_s \geq 14$ the analytic expression for dE_s/dr_s derived in Ref. 35 is valid, the surface energies for these densities being given as $E_s = 4.689 \times 10^3/r_s^3$ ergs/cm^2. The results for $r_s = 2$-14 are given in Table IV. For purposes of comparison we include in the table results for the surface energy as obtained in the LDA with the same choice of parameters. Thus the single-particle Hamiltonian is the same for the two different calculations of the surface energy. We first observe that these LDA results closely approximate the variational self-consistent calculations of the previous section (and hence of LK). This is due to the fact that the energy variation near its minimum is fairly flat and variations in the parameters lead to only small changes in the energy. Furthermore, we note that over the entire range of densities considered (except at $r_s = 2$), the VBT results lie considerably below those of the LDA. Although both formalisms have their origin in the energy functional theorem of Hohenberg and Kohn (11), the VBT invokes no approximation except that it requires the electrostatic potential to approach its asymptotic value inside the system faster than x^{-1}, a condition which is satisfied for this model calculation (see Appendix C). Thus the VBT results are exact for all densities and we do not expect these results to differ significantly for any other choice of criterion employed for the determination of the constant of integration.

On the other hand, it has been shown (67,73) that for the infinite potential barrier the sum of the exchange and

TABLE IV

Results for metallic and lower density (r_s=2-14) surface energies E_s as obtained by application of the Vannimenus-Budd theorem (VBT) and within the local density approximation (LDA). The parameters of the model system are determined by the constraints set by the BVT, self-consistency of the surface dipole barrier and charge neutrality, and are the same for both sets of calculations. The Wigner expression for the correlation energy is used.

r_s	dE_s/dr_s	Surface Energies (erg/cm^2)	
		VBT	LDA
2.0	3356	-950	-950
2.5	666	-113	42
3.0	117	53	202
3.5	-9.8	72	203
4.0	-37	59	183
4.5	-26	43	141
5.0	-18	33	109
5.5	-13	25	85
6.0	-9.2	20	67
7.0	-5.2	13	44
8.0	-3.1	8.7	31
10.0	-1.3	4.5	16
12.0	-0.65	2.7	10
14.0	-0.35	1.7	6.2

correlation contributions to the surface energy for r_s=2-6 as obtained within the random phase approximation (RPA) is about 10% larger than that obtained in the LDA even though the results for the exchange and correlation energies taken separately are significantly different. The RPA is, however, less accurate at lower densities. Furthermore, in comparison with the wavevector decomposition-interpolation scheme (72,73) for the exchange-correlation energy of an inhomogeneous electron gas, the LDA results for r_s=6 for a self-consistent calculation are again observed to be 10% too small although they improve slightly for higher densities. These results imply that any more accurate calculation of the exchange-correlation contribution would lead to larger values for the total surface energy since the parameters of the present model potential remain fixed having been determined by criteria independent of this property. Thus, for metallic densities, the difference in the VBT and LDA results are particularly surprising. The discrepancy for lower densities can certainly be attributed to the lack of validity of the LDA since the approximation is correct to terms of order of the square of the gradients of the electron density (12). It is interesting to note that even for r_s=4, in the work of Lang and Kohn (13), the density changes by a factor of a 1000 over a distance of a Fermi wavelength about the surface, changing even more rapidly for larger r_s. However, one way to arrive at more definitive conclusions regarding the accuracy of the various results is to perform

calculations for the exchange and correlation energy for potentials more realistic than the infinite barrier, such as the linear potential or FLP models which enable a study over a wide range of density profiles. Such a calculation for the surface exchange energy is presented in Chap. VI.

In conclusion we note that the use of model potentials together with certain theoretical constraints provides an accurate means of studying the inhomogeneous electron gas system. It not only obviates the necessity of self-consistent numerical solutions of the Schrodinger equation for each particle, but also enables calculations for most properties to be primarily analytic. Yet another advantage of such model potential calculations is that the choice of constraints can be tailored to the specific property of interest. The various properties of the inhomogeneous system determined are the surface dipole barrier, work function and surface energy, the last quantity being obtained both within the LDA and via the VBT. The results of these calculations indicate that although the work function decreases with increasing density it does not saturate at some finite value in the high density limit but rather vanishes at a density corresponding to approximately $r_s=0.4$. Furthermore, the use of the Gell Mann-Brueckner and Wigner expressions for the correlation energy lead to insignificant differences in the values of the high density work functions. For metallic densities, the results for the surface dipole

barrier and work function determined are within 0.3 eV of those of the fully self-consistent calculations of Lang and Kohn. The upper bounds obtained for metal surface energies in the LDA lie within 5 ergs/cm^2 of the LK results for $r_s \geq 2.5$ and differ by less than 3% for $r_s=2$. Finally, surface energies for metallic and lower densities have been calculated by application of the VBT. For the same choice of single-particle Hamiltonian, these results lie significantly below those of a LDA calculation over the entire range of densities considered. Due to the substantial variation in the density profiles that can be achieved, such model potentials also provide a means by which to study the convergence properties of various exchange-correlation (68,75,79) and kinetic energy (40-43,48) density gradient expansions. The single-particle wave functions generated can furthermore be employed in variational calculations involving more realistic surface energy functionals which include the effects of the periodic lattice. We note, however, that the constraint of the BVT and the sum rule for the surface energy as given by the VBT are valid only within the jellium approximation. The generalization of these theorems to include band structure effects and the periodic potential of the lattice would thus enable a study of those solids for which the free electron approximation is not valid, such as insulators, semiconductors, semimetals, and some metals.

IV. STUDY OF THE DENSITY GRADIENT EXPANSION FOR THE KINETIC ENERGY AS APPLIED TO SURFACE PHYSICS

According to the variational formalisms for single-particle expectation values to be discussed in Chap. V, the density of an inhomogeneous interacting electron gas may be obtained accurately without having to resort to the solution of the Schrodinger-like Kohn-Sham equations. Employing only crude approximations to the exact wave function, these variational principles lead to results for the density correct to second order as is the case for the energy on application of the Rayleigh-Ritz variational principle. Thus within such a formalism one obtains directly the density rather than single-particle wave functions from which the density is obtained. In order to determine the surface kinetic energy of the interacting system one therefore has to resort to the density gradient expansion formalism for this property. This expansion is also a key ingredient of all statistical calculations on surfaces (94,23,24). The convergence properties of such an expansion are thus of considerable importance. In this chapter we present a study of the kinetic energy density gradient expansion as applied to surfaces and arrived at important conclusions with regard to its accuracy for the metal surface problem. In studying the convergence properties of this expansion we therefore restrict ourselves to density profiles of the form that exist at surfaces, but

which can be made to vary either rapidly (corresponding to low bulk densities) or very slowly (corresponding to high bulk densities) in comparison with the local Fermi wavelength and screening length, with the intermediate densities corresponding to those existing at metallic surfaces.

The density gradient expansion for the kinetic energy contribution to the surface energy of an inhomogeneous electron gas may be obtained from Eqs. 2.11-2.14 with the appropriate subtraction of a bulk term from Eq. 2.12. With the total kinetic energy density functional written as the sum of only the TF plus the first gradient correction, the corresponding Euler equation for the density as defined from Eq. 2.2 is

$$\frac{3\pi^2}{2}\rho(\vec{r})^{2/3} + \frac{\lambda}{8}\left(\frac{\vec{\nabla}\rho(\vec{r})}{\rho(\vec{r})}\right)^2 - \frac{\lambda}{4}\frac{\nabla^2\rho(\vec{r})}{\rho(\vec{r})} + V(\vec{r}) = E \qquad (4.1)$$

where $V(\vec{r})$ is the potential in which the non-interacting particles move and E the Langrange multiplier ensuring the conservation of the total number of particles. For the example of a weakly perturbed uniform system of non-interacting fermions it has been shown (95,96) from the above equation that the original von Weisacker coefficient gives asymptotically exact results for short wavelength perturbations corresponding to rapidly varying densities, whereas $\lambda = 1/9$ gives asymptotically exact results for the

case of slowly varying densities. The von Weisacker density does, however, lead to an upper bound for the energy (97). For atomic systems (98) the von Weisacker coefficient leads to good densities for the outer part of atoms as compared to those obtained quantum mechanically whereas a coefficient of $\lambda=1/5$ appears to be appropriate for interior densities.

The model effective potential we use for the study of the kinetic energy density gradient expansion is the linear potential model (36,37) which has also recently been employed (79,80) to study the gradient expansion for the exchange-correlation energy of the inhomogeneous electron gas. The electron density is thus a function only of the co-ordinates of the direction of the inhomogeneity. This potential is similar to the FLP model of Chap. III except that the potential is no longer a constant beyond a specific point in space. The semi-analytic expressions of all the surface properties for this model are given in Ref. 36. They may also be obtained from the expressions of the FLP model by letting the barrier height tend to infinity. This is a much simpler model potential since it involves only one variable parameter. Furthermore, the requirement of self-consistency of the surface dipole barrier does not have to be satisfied. As with the FLP model, the primary advantage of this model potential is that by adjusting the field strength it is possible to change the density from one which is extremely rapidly varying to one which is very slowly varying, so that the gradient of the density can be physi-

cally changed for each point in space. This model potential also leads to electronic densities in the metallic range (and hence to all metal surface properties) which very closely approximate (36,37) the self-consistently obtained values of Lang and Kohn (13), particularly for medium and high density metals. Thus meaningful conclusions regarding the density gradient expansion for the kinetic energy can be arrived at for the metal surface problem. A calculation employing the step potential model has recently been performed (99) but due to the limitations of this model (34,35) only trends with respect to the convergence of the gradient expansion can be observed. In addition this representation of the effective potential at a metal surface does not lead to accurate densities.

The potential which gives rise to the inhomogeneous density profile is assumed to be

$$V(x) = Fx\Theta(x), \tag{4.2}$$

where F is the field strength defined in terms of the slope parameter x_F as $F=E_F/x_F$, E_F is the Fermi energy, and θ is the step function. The solution of the Schrodinger equation for this potential is

$$\psi_k(x) = \begin{cases} B \sin[kx+\delta(k)] & \text{for} \quad x \leq 0 \\ C_k Ai(\zeta) & \text{for} \quad x \geq 0 \end{cases} \tag{4.3}$$

where

$$B = -(2/L)^{1/2}$$

$$C_k = B \sin\delta(k)/Ai(-\zeta_o)$$

and

$$\delta(k) = \cot^{-1}[\zeta_o^{-1/2} Ai'(-\zeta_o)/Ai(-\zeta_o)].$$

In the above equations the arguments ζ and ζ_o of the Airy function Ai and its derivative Ai' are defined as in Chap. III. With a change of variables to $y=xk_F$ and $q=k/k_F$, the density and its first and second derivatives normalized with respect to the bulk density are

$$n(y) = \begin{cases} 1 - \frac{3}{2}\int_0^1 dq\,(1-q^2)\cos 2(qy+\delta) & y \le 0 \\ 3\int_0^1 dq\,(1-q^2)\frac{\beta_o}{\Lambda(-\beta_o)} A_i^2(\beta) & y \ge 0 \end{cases} \tag{4.4}$$

$$\frac{dn(y)}{dy} = \begin{cases} 3\int_0^1 dq\,(1-q^2)\,q\sin 2(qy+\delta) & y \le 0 \\ 6\,y_F^{-1/3}\int_0^1 dq\,(1-q^2)\frac{\beta_o}{\Lambda(-\beta_o)} A_i(\beta)A_i'(\beta) & y \ge 0 \end{cases} \tag{4.5}$$

$$\frac{d^2n(y)}{dy^2} = \begin{cases} 6\int_0^1 dq\,(1-q^2)\,q^2\cos 2(qy+\delta) & y\le 0 \\ 6y_F^{-2/3}\int_0^1 dq\,(1-q^2)\,\frac{\zeta_0}{\Lambda(-\zeta_0)}\left[Ai'^2(\zeta)+\zeta Ai^2(\zeta)\right] & y\ge 0 \end{cases} \tag{4.6}$$

where the slope parameter $y_F = x_F k_F$ and

$$\Lambda(-\zeta_0) = Ai'^2(-\zeta_0) + \zeta_0 Ai^2(-\zeta_0). \tag{4.7}$$

Note that the density and its derivatives as written in Eqs. 4.4-4.6 are universal functions of the slope parameter y_F. Large values of the slope parameter correspond to slowly varying densities whereas the $y_F=0$ limit represents the infinite potential barrier model corresponding to a very rapidly varying density. With these expressions for the density and its derivatives, we then obtain the various components of the density gradient expansion E_k^{GE} for the kinetic energy as discussed above. For particles moving in the linear potential V(x) of Eq. 4.2, the expressions (Eq. 2.27) for the exact kinetic energy contribution to the surface energy may be simplified by exploiting the equality of the phase shift rule of Sugiyama (5,85) to the charge neutrality condition. This relation can also be obtained from Eq. B.4 in the limit that the barrier height goes to infinity. Thus the exact surface kinetic energy as a universal function of the slope parameter may be written as

$$\frac{160\pi}{k_F^4} E_k = 1 - \frac{64 y_F}{35\pi} + \frac{4 y_F^{1/3}}{3\pi} \int_0^1 dq (1-q^2)(3+5q^2) \frac{A_i(-s_0) A_i'(-s_0)}{A(-s_0)} \quad (4.8)$$

In Fig. 13 we plot the variation of the universal functions of the exact kinetic energy E_k/k_F^4 together with those of the Thomas-Fermi (TF) term $E_s^{(1)}$ and the sum of $E_k^{(1)}$ plus the first gradient correction $E_k^{(2)}$ for both $\lambda=1$ and $\lambda=1/9$ as a function of the slope parameter y_F. We also plot the universal function of the sum of all three terms of the gradient expansion E_k^{GE} with $\lambda=1/9$ and $\gamma=1$. Note that the origin of the abscissa in the figure is at $y_F=0.5$. The graph demonstrates definitively the convergence of the gradient expansion E_k^{GE} as the density becomes more slowly varying. The percentage errors in the results for the TF, TF plus first gradient correction and TF plus first and second gradient corrections over this range of slope parameter are listed in Table V. Over the entire range of slope parameter considered, the Thomas-Fermi term may be observed to be a very poor approximation to the exact result even for slowly varying densities. At $y_F=6$, this error is still 4% whereas E_k^{GE} has converged to within 0.2% of the exact result. For rapidly varying densities, TF fails as anticipated being in error by 273% at $y_F=0.5$. The addition of the first density gradient correction improves results considerably becoming a better and better approximation as the density becomes more slowly varying. For example at $y_F=1$, the addition of

TABLE V

Percentage errors in (i) the Thomas-Fermi (TF) contribution $E_k^{(1)}$ to the surface kinetic energy, (ii) the sum of TF and first gradient correction $E_k^{(1)} + E_k^{(2)}$, and (iii) in the sum of TF and first and second gradient corrections $E_k^{GE} = E_k^{(1)} + E_k^{(2)} + E_k^{(3)}$.

SLOPE PARAMETER y_F	$E_k^{(1)}$ (THOMAS-FERMI)	$E_k^{(1)} + E_k^{(2)}$ (λ=1/9)	E_k^{GE} (λ=1/9; γ =1)	E_k^{GE} (λ=1/9; γ =1.336)
0.5	273	161	41	0
1.0	86	44	16	6
1.5	46	20	7	3
2.0	30	11	4	1
3.0	15	4	1	0.1
4.0	9	2	0.4	0.2
5.0	6	1	0.3	0.05
6.0	4	0.8	0.2	0.01

$E_k^{(2)}$ reduces an error of 86% in the TF results to 44%, and at $y_F=6$ gives rise to a result within 0.8% of the exact value. As may be observed from column 4 of Table V, the inclusion of the second density gradient term to the series removes practically all error for $y_F \geq 2.0$. However, even for rapidly varying densities, this form of the second gradient term gives rise to substantial corrections in the appropriate direction. At $y_F=1$, E_k^{GE} is in error by only 16%.

Having demonstrated the convergence of the density gradient expansion for the kinetic energy, we next wish to understand how meaningful the application of such an expansion is for the metal surface problem. In order to do this we must develop a correspondence between a given bulk density and a specific density profile at the surface as produced by this model calculation. In other words, we must relate the slope parameter y_F which determines the density variation at the surface to the bulk density or equivalently the Wigner-Seitz radius r_s. As in Chap. III one criterion we use is the BVT. A plot of this correspondence between y_F and r_s for the LP model is given in Fig. 14. Another method by which we may relate the bulk density to the slope parameter is by application of the variational principle for the energy. We write the surface energy as the sum of the kinetic, electrostatic and the exchange-correlation energy as determined in the LDA, and minimize the energy with respect to the slope parameter for a specific value of r_s. The results (37) of the application of this criterion for

the correspondence between r_s and y_F are also plotted in Fig. 14. Note that in either case the surface density of metals (for which $2 \leq r_s \leq 6$) may be represented by values of the slope parameter in the range $0 \leq r_s \leq 4$. A study of both Figs. 13 and 14 thus indicates that the density gradient series for the kinetic energy (with $\lambda = 1/9$ and $\gamma = 1$) is an excellent approximation for high density metals, reasonably good for medium densities and poor for low density metals. On the other hand, the sum of the TF plus first gradient correction with $\lambda = 1/9$ leads to poor results over the entire metallic range being consistently well below the exact results. It is thus possible to understand why the surface energy values of the statistical calculations of both Smith (23) and Paasch and Heitschold (24) lie considerably below those of the self-consistent calculations of Lang and Kohn (13). These author's employed parametrized analytic forms for the density but included only the first density gradient correction for the kinetic energy. They thus underestimated the kinetic energy considerably which in turn led to a lower value for the total surface energy. Thus if the statistical approach is to be employed for metal surface calculations it is imperative that the second density gradient correction as given by Eq. 2.14 be included. Recently we have calculated the surface energies by using Smith's density with the inclusion of the second density gradient correction of Eq. 2.14 in the kinetic energy term. It is shown (49) that, with the correct energy functional, variational minimization

of the energy gives rise to nearly exact results for the surface energies when compared with those of LK.

We have also plotted in Fig. 13 the variation of $E_k^{(1)}+E_k^{(2)}$ for the original von Weisacker coefficient $\lambda=1$. It is evident that the use of this coefficient leads to results for the kinetic energy which are in substantial error over the entire range of slope parameter considered in the figure, even having the wrong sign for $y_F<2.5$. However, based on the work of Jones (96) as discussed earlier, it is expected that the von Weisacker coefficient should lead to convergence for the very rapidly varying limit. In order to see whether this is the case, we have extended our calculations to accurately determine the various components of the density gradient expansion in the range $0\leq y_F\leq 0.5$ and the results are plotted in Fig. 15. Note that $y_F=0$ corresponds to the infinite barrier potential for which the density is most rapidly varying. A study of the figure indicates that even for rapidly varying densities the use of the von Weisacker coefficient still leads to substantial errors and that even in the infinite barrier limit there is no indication of convergence. It does however have the right sign for $y_F<0.25$. On the other hand, the use of $\lambda=1/9$ is still a better approximation for $y_F>0.25$ and the addition of the second density gradient correction improves matters still further. Of course, for $y_F=0$, $E_k^{(3)}$ diverges. It thus appears that for physical density profiles which are rapidly varying, the coefficient $\lambda=1/9$ is still the correct one

although one must add in the correction due to the second density gradient term.

An interesting question which thus arises is what value of λ would lead to the exact kinetic energy if only the TF plus first density gradient correction of the expansion were to be employed in the calculation. This is important since Eq. 4.1 has been solved in many applications in atomic and molecular physics and for the metal surface problem (94) (with $\lambda=1/9$). We have therefore plotted in Fig. 16 the variation of $\lambda=(E_k-E_k^{(1)})/E_k^{(2)}$ as a function of the slope parameter. The fact that there is a substantial variation in the value of λ thus obtained indicates that no one value of the coefficient will suffice over the entire range of densities considered. However, for a specific metal the correct value of λ to be used in Eq. 4.1 or in any parametrized density calculation can be obtained from this graph since there exist reliable criteria for the correspondence between the slope parameter and the Wigner-Seitz radius. An alternative approach would be to solve the Euler equation (Eq. 4.1) in conjunction with the constraint of the BVT.

Finally we note that although the results of the density gradient with $\lambda=1/9$ and $\gamma=1$ are very accurate in the range of both metallic and higher densities, they still lie a few percent below the exact values. Thus to improve matters further, we propose the following semi-emperical method for the determination of the coefficient γ of the

second density gradient correction. We adjust the coefficient such that the results of the gradient expansion agree with the exact result at $y_F=0.5$. This value of y_F corresponds to a very rapidly varying density for which there is a substantial error between the exact result and that of the original gradient expansion (see Table V). The value of γ thus obtained is 1.336. The results of using this coefficient for the second gradient correction are shown in Fig. 17, and the percentage errors are given in the last column of Table V. Note that the energy scale has been considerably expanded in this diagram. As may be observed, the improvement in the results over those shown in Fig. 13 are substantial for all densities being in error by less than 3% for $y_F \geq 1.5$ and within 0.01% of the exact result at $y_F=6$.

In conclusion we note that we have demonstrated the convergence of the density gradient expansion for the kinetic energy for a semi-infinite system of non-interacting fermions confined at its surface by a linear potential. The value of 1/9 for the coefficient of the first density gradient expansion term is the appropriate choice for slowly varying densities in agreement with theoretical predictions, and should also be employed for rapidly varying densities such as those existing at metal surfaces provided the second gradient correction is included. The choice of the original von Weisacker coefficient, however, leads to results which are consistently in error for both rapidly and slowly vary-

ing densities. A semi-emperically determined value of 1.336 for the coefficient of the second density gradient term leads to results which are essentially exact over a very wide range of density profiles. Obviously, as shown above, the addition of this second density gradient contribution with its non-linear response terms is an important factor for convergence and particularly so for metal surface calculations (49). In Ref. 79 evidence was presented that indicated that the first density gradient correction for the exchange-correlation energy was inappropriate for jellium metal surface densities. Thus together with the conclusion of this work we expect the second density gradient correction including its non-linear response terms to be necessary components of any gradient expansion calculation of the exchange-correlation energy of metal surfaces.

V. APPLICATION OF VARIATIONAL PRINCIPLES FOR SINGLE-PARTICLE EXPECTATION VALUES TO THE METAL SURFACE PROBLEM

An accurate knowledge of the particle density is intrinsic to the determination of all single-particle properties of a quantum mechanical system. For systems containing relatively few particles the most important technique for the determination of the density is the Rayleigh-Ritz (33) variational principle (VP) for the energy. The application of this principle yields an upper bound to the ground state energy in error by $O(\delta^2)$ if the trial wave function is in error by $O(\delta)$. However, if the resulting wave function is employed to determine other properties, such as the density, which are not represented by operators in the Hamiltonian, the results have in general an error of $O(\delta)$ of unknown sign unless the trial wave function is the solution of the Hartree-Fock equations, including non-local exchange, in which case the error is of $O(\delta^2)$ (100). However, variational formalisms for the determination of single-particle expectation values and hence the density exist. The density of an interacting N-particle system is simply the expectation value of the single-particle operator

$$W = \sum_{i=1}^{N} \delta(\vec{r}_i - \vec{r}). \tag{5.1}$$

Although a complete exposition of this variational method has been given in published papers (51-55), solid state physicists are generally not familiar with these techniques since thus far they have been applied only to few particle atomic systems.

In this chapter we wish to demonstrate the applicability of this variational method to the many-body problem by determining the density variation of the inhomogeneous electron gas at jellium surfaces. The extension of this formalism to incorporate the discrete ionic lattice is discussed in a latter section. This thus constitutes yet another accurate method for the study of surfaces not requiring the heavy numerical computations involved in fully self-consistent or nearly fully self-consistent calculations. Prior to proceeding with this application of the variational formalism to the metal surface problem we give in the next section a brief description of the general theory involved, and introduce and discuss simplifications (based on the Kohn-Sham density functional formalism) which are particularly meaningful for the easy solution of the many-body problem.

A. Variational Principle

The variational principle (VP) which yields results correct to second order for the expectation value of an arbitrary Hermitian operator W is that due to Delves (101) and Schwartz (102). The variational approximation <W> to the exact expectation value using the Delves-Schwartz formalism is given as

$$\langle W \rangle = \overline{W} + 2\mathrm{Re}\langle \psi_{1T} | H-E | \psi_{0T} \rangle, \tag{5.2}$$

$$\overline{W} = \langle \psi_{0T} | W | \psi_{0T} \rangle, \tag{5.3}$$

where ψ_{0T} is the system trial wave function, ψ_{1T} is an auxiliary function and where H and E are the exact Hamiltonian and eigenenergy of the system, i.e.

$$H\psi_0 = E\psi_0. \tag{5.4}$$

The equation satisfied by the auxiliary function is

$$(H-E)\psi_1 = (\overline{W}_E - W)\psi_0, \tag{5.5}$$

where $\overline{W}_E$ is the exact expectation value of the operator W. The above equation is analogous to the expression in perturbation theory for the energy correct to first order and we may thus interpret ψ_1 as being a perturbational correction

to ψ_0 due to the perturbation W (60). Delves (101) has shown that if ψ_{0T} differs from ψ_0 by $O(\delta)$ and ψ_{1T} differs from ψ_1 by $O(\delta_1)$, then employing the Hermiticity of H, $\langle W \rangle$ differs from $\overline{W}_E$ by $O(\delta^2, \delta\delta_1)$, whereas $\overline{W}$ differs from $\overline{W}_E$ by $O(\delta)$.

In the application of Eq. 5.2 to any system, the unknown value of the exact energy E may be eliminated provided the auxiliary function can be orthogonalized to the trial wave function. The parameters in a ψ_{0T} of a given form can be determined by minimizing the energy but it is generally not possible to determine the parameters in a ψ_{1T} of a given form numerically by making the variational estimate of the expectation value stationary with respect to their variations. This is due to the property that the estimate $\langle W \rangle$ does not provide a bound and hence its extremum is generally a saddle point which is difficult to find numerically. Moreover, there may exist several such extrema and it may not be clear which one is physically significant. This problem has been circumvented by constructing a subsidiary functional (103,104) M involving the trial wave function ψ_{0T}, the auxiliary function ψ_{1T}, the Hamiltonian H and the operator W representing the observable in question, which when minimized leads to the best estimate of ψ_{1T} for a given ψ_{0T}. It is to be emphasized that this subsidiary variational principle is a minimum principle. The functional M is given as

$$M[\psi_{0T},\psi_{1T},H,W] = \langle\psi_{1T}|H-E_0|\psi_{1T}\rangle + \langle\psi_{1T}|W|\psi_{0T}\rangle$$

$$+ \langle\psi_{0T}|W|\psi_{1T}\rangle, \qquad (5.6)$$

subject to the orthogonality constraint

$$\langle\psi_{1T}|\psi_{0T}\rangle = 0, \qquad (5.7)$$

and where E_0 is the eigenvalue of the approximate Hamiltonian H_0 with eigenfunction ψ_{0T} i.e. $H_0\psi_{0T}=E_0\psi_{0T}$. However, the choice for the auxiliary function is still strictly arbitrary and there is no systematic method to determine ψ_{1T} once the trial wave function ψ_{0T} for a given system has been chosen.

Such a systematic procedure for the determination of the auxiliary function ψ_{1T} for single-particle operators of the form

$$W = \sum_i W(\vec{r}_i), \qquad (5.8)$$

has been derived by Sahni and Krieger (52,55) by variational minimization of the functional $M[\psi_{0T},\psi_{1T},H,W]$, with respect to arbitrary variations in the auxiliary function, having assumed ψ_{0T} to be either a Hartree-product or Slater-determinant type trial wave function. By this method ψ_{1T} is found to be dependent on the operator whose expectation

value is being determined and independent of any further parameters other than those involved in the initial choice for the trial wave function ψ_{0T} as discussed below. In the Hartree case for which the trial wave function ψ_{0T} is a product of the single-particle states $\psi_i(\vec{r})$:

$$\psi_{0T} = \Pi_i \psi_i(\vec{r}_i), \tag{5.9}$$

with

$$\langle \psi_i | \psi_j \rangle = \delta_{ij},$$

it can be seen (60) from the perturbational interpretation of Eq. 5.5, that the only states coupled to ψ_{0T} by the single particle operator $W=\sum_i W(\vec{r}_i)$ are those states with only one single particle wave function different from those in ψ_{0T}. Hence the auxiliary function was chosen (105,51) to be of the form

$$\psi_{1T} = \sum_i f_i(\vec{r}_i)\psi_{0T}. \tag{5.10}$$

For a given trial wave function ψ_{0T}, and a non-relativistic N-particle Hamiltonian of the form

$$H = -\sum_{i=1}^{N} \nabla_i^2 + V(\vec{r}_1,\ldots,\vec{r}_N), \tag{5.11}$$

variational minimization (52) of the functional M with respect to ψ_{1T}, subject to the orthogonality constraint of Eq. 5.7 leads to a set of coupled integral-differential equations for the components $f_i(\vec{r}_i)$ of the auxiliary function. The resulting equations can be uncoupled in different approximations (52). In the limit of large N, all decoupling approximations lead to the following second order differential equation for the components $f_i(\vec{r}_i)$ of the auxiliary function

$$\nabla_i^2 f_i(\vec{r}_i) + \frac{2}{\psi_i(\vec{r}_i)} \vec{\nabla}_i f_i(\vec{r}_i) \cdot \vec{\nabla}_i \psi_i(\vec{r}_i) = \frac{1}{\psi_i(\vec{r}_i)} \left[W(\vec{r}_i) - \bar{W}_i \right] \psi_i(\vec{r}_i) \tag{5.12}$$

with

$$W_i = \langle \psi_i(\vec{r}) | W(\vec{r}) | \psi_i(\vec{r}) \rangle,$$

which includes the case where $W(\vec{r}_i)$ may be a differential operator. With the auxiliary function determined by solution of the above differential equation, the expectation value of the operator W can then be obtained correct to second order by substitution into Eq. 5.2. We emphasize that within the Sahni-Krieger formalism the auxiliary function is fully determined once the specific choice of the

trial single-particle wave functions is made. Furthermore, due to the fact that it is possible to satisfy the orthogonality constraint of Eq. 5.7 (say by an appropriate choice of constant in the solution of Eq. 5.12), a knowledge of the ground state energy of the system is not necessary. Thus replacing E by E_0 in Eq. 5.2 we have

$$\langle W \rangle = \overline{W} + 2\mathrm{Re}\langle \psi_{1T} | \delta V | \psi_{0T} \rangle, \tag{5.13}$$

where

$$\delta V = H - H_0.$$

It is, however, possible to rewrite Eq. 5.13 in such a manner that one may employ instead a function $\psi'_{1T} = \sum_i f'_i(\vec{r}_i)\psi_{0T}$ (where the $f'_i(\vec{r}_i)$ are solutions of the differential Eq. 5.12) for which the orthogonality constraint of Eq. 5.7 is not satisfied, i.e.

$$\langle \psi'_{1T} | \psi_{0T} \rangle \neq 0.$$

To derive this alternate expression for $\langle W \rangle$ consider the orthogonalized auxiliary function ψ_{1T} to be of the form

$$\psi_{1T} = \psi'_{1T} - \eta\, \psi_{0T},$$

where η is an arbitrary constant ensuring the orthogonality constraint of Eq. 5.7. With the expectation δV defined as

$$\overline{\delta V} = \langle \psi_{0T} | \delta V | \psi_{0T} \rangle,$$

the expression for the variational estimate $\langle W \rangle$ may then be written as

$$\langle W \rangle = \overline{W} + 2\mathrm{Re}\langle \psi'_{1T} - \eta \psi_{0T} | \delta V - \overline{\delta V} | \psi_{0T} \rangle$$

$$= \overline{W} + 2\mathrm{Re}\langle \psi'_{1T} | \delta V - \overline{\delta V} | \psi_{0T} \rangle, \qquad (5.14)$$

where now in Eq. 5.14 only the non-orthogonalized auxiliary function ψ'_{1T} appears.

In the above discussed variational formalism for the expectation $\langle W \rangle$, the exact non-relativistic Hamiltonian is assumed employed in the determination of the correction term to $\overline{W}$. Thus the many-body system being studied is represented exactly. This is in contrast to the density functional formalism of Kohn and Sham in which although the density is obtained self-consistently, the exchange-correlation energy functional must be approximated as its exact form is as yet unknown. Thus, for example, the Lang-Kohn (13) density is exact, but only within the local density approximation. No such local approximations are involved in the variational

formalism since the Hamiltonian employed incorporates all Coulomb interactions explicitly.

It is, however, possible to further simplify this variational procedure by incorporating the basic idea of the Kohn-Sham theory (12) into the formalism. This can be achieved by replacing the potential $V(\vec{r}_1,\ldots,\vec{r}_N)$ of Eq. 5.11 (which usually contains both single and two-particle operators) by a sum of single-particle effective potentials. That such an effective potential exists for an interacting inhomogeneous electron gas system has, of course, been shown rigorously to be the case by Kohn and Sham. With this choice of single-particle type Hamiltonian, the expectation <W> may now be written as

$$\langle W\rangle = \sum_{i=1}^{N} \left\{ \int \psi_i^*(\vec{r}_i)\, W(\vec{r}_i)\, \psi_i(\vec{r}_i)\, d\vec{r}_i \right. \tag{5.15}$$

$$\left. + 2\,\mathrm{Re} \int f_i^*(\vec{r}_i)\, \psi_i^*(\vec{r}_i) \left[\delta V(\vec{r}_i) - \overline{\delta V}_i\right] \psi_i(\vec{r}_i)\, d\vec{r}_i \right\}$$

where $\delta V(\vec{r}_i)$ is the difference between the assumed single-particle Hamiltonian and that of the trial system H_0, and

$$\overline{\delta V}_i = \langle \psi_i | \delta V(\vec{r}_i) | \psi_i \rangle .$$

Thus, in this form, the expectation <W> is determined by first calculating the contribution of each particle (which now depends only on the position of that particle) and then

summing over all the particles. However, as in the Kohn-Sham theory, the many-body complexity (and any approximations) are now incorporated into the choice of the effective potential.

The variational principle as written in Eq. 5.15 can be employed in many different ways. For example, it can be most effective in providing rapidly convergent results for the density provided the effective potential is a function of the density. This can be seen as follows: If $\rho_0(\vec{r})$ is the electron density of the trial system (corresponding to $\overline{W}$ in Eq. 5.15), the density $\rho(\vec{r})=\langle W\rangle$ can be obtained by iterating this equation, i.e. first use $\rho(\vec{r})$ to determine δV and calculate a $\rho(\vec{r})$, then substitute this $\rho(\vec{r})$ in δV and calculate a new $\rho(\vec{r})$ until self-consistency is achieved i.e. until the value of a property determined by this density such as the surface dipole barrier is unchanged by further iteration. The advantage of this procedure is its rapid convergence, i.e., an error in the single-particle state $\psi_i(\vec{r})$ of $O(\delta)$ gives a density correct to $O(\delta^2)$ whereas if we numerically integrated the Schrodinger equation and iterated to obtain the density at each stage, an error in $\psi_i(\vec{r})$ of $O(\delta)$ would give a density correct only to $O(\delta)$.

A second way in which this variational principle may be used to determine the density or any other single-particle property is to employ a parametrized model effective potential in the correction term. The density obtained correct to second order may then be varied to determine either the

stationary value of any property of interest, or adjusted to satisfy certain theoretical and physical constraints. The idea of the use of model potentials in conjunction with constraints has already been shown in Chap. III to lead to very accurate results, and is sufficient justification for the adoption of the same procedure within this formalism. Yet another approximation would be to determine the effective potential (which is a sum of the electrostatic and exchange-correlation contributions) within the LDA or LDA with gradient corrections using ρ_0 as the input density. The only parameters in the problem in this case are those that appear in the trial density ρ_0 and these could then be adjusted to satisfy the various constraints. However, it is to be emphasized, that the variational principle in its more general form Eq. 5.13 in which the exact Hamiltonian is employed may also be used to determine the density in this manner, in which case no approximation except that in the choice of trial wave function is made.

In order to demonstrate the applicability of the above variational formalism to the inhomogeneous many-particle system, we apply, in the following section, the single-particle-effective-potential version of the formalism with a model effective potential to determine the density at a jellium surface and from it other properties such as the work function and surface energy.

B. Application to Jellium Surfaces

We determine the surface density $\rho(x)$ of jellium metal, correct to second order, by application of the above variational formalism for single-particle expectation values to the operator

$$W = \sum_i \delta(x_i - x). \tag{5.16}$$

As in all our previous work we will consider the crystal to be semi-infinite. Due to the translational invariance in the plane parallel to the surface in the jellium approximation, we choose our trial wave function to be of the form

$$\psi_{0T} = \prod_i \psi_k(x_i) \exp[i(k_y y_i + k_z z_i)], \tag{5.17}$$

where $k \equiv k_x$, k_y, and k_z are the components of the electron momentum $\vec{k}$. For the semi-infinite crystal and arbitrary effective potential at the surface, Eq. 5.15 for the density may be written as

$$\rho(x) = \rho_0(x) + \rho_1(x) \tag{5.18}$$

with

$$\rho_0(x) = 1/(2\pi) \sum_{k \leq k_F} (k_F^2 - k^2) |\psi_k(x)|^2 , \tag{5.19}$$

$$\rho_1(x) = 2\,\mathrm{Re} \sum_{k \le k_F} (k_F^2 - k^2) \int f_k^*(x_i, x)\, \psi_k^*(x_i)\, \delta V(x_i)\, \psi_k(x_i)\, dx_i \qquad (5.20)$$

where $\rho_0(x)$ is the density corresponding to the trial set $\psi_k(x_i)$ and $\rho_1(x)$ is the correction term. Note that in the above expression for $\rho_1(x)$, the $\overline{\delta V}_i$ term is absent since its contribution vanishes as x^{-1} in the limit as the crystal is made semi-infinite. Similarly, the $\overline{W}_i$ term in the differential equation for the components of the auxiliary function may also be eliminated since it too vanishes as x^{-1} in the limit as x goes to $-\infty$. The differential equation for the $f_i(x_i)$ corresponding to the density operator is then

$$\frac{d^2 f_k(x_i)}{dx_i^2} + \frac{2}{\psi_k} \frac{d\psi_k(x_i)}{dx_i} \cdot \frac{d f_k(x_i)}{dx_i} = \delta(x_i - x) \qquad (5.21)$$

As our trial wave function we choose those generated by the linear potential model (36) for which $V_{\mathrm{eff}}^{\mathrm{trial}}(x) = F\Theta(x)$, where F is the field strength and the step function. These wave functions are no more complex to work with than those of the step model but far superior (36,37). Thus

$$\psi_k(x_i) = B\{\sin\delta(k)\,\mathrm{Ai}(\zeta_i)/\mathrm{Ai}(-\zeta_o)\;\Theta(-x_i)$$

$$+ \sin[kx_i + \delta(k)]\;\Theta(x_i)\}, \qquad (5.22)$$

where B is the normalization constant, $\delta(k)$ the phase shift

and $Ai(\zeta_i)$ is the Airy function. Expressions for the phase shift and the normalization constant are given in Chap. IV. Employing this trial wave function and appropriate boundary conditions the differential Eq. 5.21 for the components of the auxiliary function can be solved analytically even though one is here dealing with Airy functions. The details of this solution together with a discussion of the boundary conditions employed are given in Appendix E. The analytic solution is given below:

For $x_i \geq 0$ (5.23)

$$f_i(x_i,x) = \frac{\pi}{k_F} y_F^{1/3} A_i^2(\beta) \left\{ \frac{B_i(-\beta_0)}{A_i(-\beta_0)} \theta(\beta+\beta_0) - \frac{B_i(\beta_i)}{A_i(\beta_i)} \theta(\beta-\beta_i) + \frac{B_i(\beta)}{A_i(\beta)} \left[\theta(-\beta_0-\beta) - \theta(\beta_i-\beta) \right] \right\}$$

$$+ \frac{1}{2k} \sin 2(kx+\delta)\, \theta(-x) + \frac{1}{2k} \sin 2\delta \frac{A_i^2(\beta)}{A_i^2(-\beta_0)} \theta(\beta+\beta_0)$$

For $x_i \leq 0$

$$f_i(x_i,x) = \frac{1}{k} \sin^2(kx+\delta) \cot(kx_i+\delta) \left[\theta(x-x_i) - \theta(x) \right]$$

$$+ \frac{1}{k} \sin^2\delta \cot(kx_i+\delta) \frac{A_i^2(\beta)}{A_i^2(-\beta_0)} \theta(\beta+\beta_0)$$

$$+ \frac{1}{2k} \sin 2(kx+\delta)\, \theta(x_i-x)$$

We next have to make an assumption as to the effective potential at the surface. For purposes of the present demonstration of the applicability of this formalism to the many-body problem we choose our effective potential to be that of the finite linear potential model (Eq. 3.1) discussed in Chap. III. Thus

$$V_{eff}(x) = Fx[\Theta(x)-\Theta(x-b)] + V\Theta(x-b),$$

where F is the field strength and V the barrier height. These latter quantities are described in terms of the parameters b and x_F respectively, defined by the relation $F=V/b=E_F/x_F$, where E_F is the Fermi energy. The principle advantage of employing the FLP model in this case is that it leads to a certain degree of analytical simplicity in our calculations, in addition to the fact that the model potential itself can be solved exactly and gives rise to accurate results. The electronic density of the system can thus be obtained, correct to second order, by substitution of the above determined function $f_k(x_i)$ into Eq. 5.20. Furthermore, employing expressions for indefinite integrals of Airy functions derived in Appendix A, the spatial integral in Eq. 5.20 for $\rho_1(x)$ as well as those for all the other surface properties can be solved analytically.

With a change of variables to $y=xk_F$, $y_i=x_ik_F$ and $q=k/k_F$, the expression for the normalized charge density ($n(y)=\rho(y)/\bar{\rho}$, where $\bar{\rho}=k_F^3/3\pi^2$), as well as for all the sur-

face properties obtained by using this corrected density can again be described in terms of universal functions of the slope and barrier height parameters $y_F = x_F k_F$ and $y_b = b k_F$. The results are given below:

Electronic Density

$$n(y) = n_0(y) + n_1(y) \tag{5.24}$$

$$n_0(y) = 3\int_0^1 dq\,(1-q^2)\frac{\sin^2\delta}{A_i^2(-\beta_0)}\,A_i^2(\beta) \qquad y \geq 0$$

$$= 3\int_0^1 dq\,(1-q^2)\sin^2(qy+\delta) \qquad y \leq 0 \tag{5.25}$$

$$n_1(y) = \int_0^1 dq\,(1-q^2)\frac{\sin^2\delta}{A_i^2(-\beta_0)}\left\{A_i^2(\beta)\left[H(\beta_b)Q(-\beta_0) - 2\pi G(\beta_b)\right]\right.$$
$$\left. - (\beta - 3\beta_b)\,A_i(\beta)\,A_i'(\beta)\right\} \qquad y \geq y_b \tag{5.26}$$

$$= \int_0^1 dq\,(1-q^2)\frac{\sin^2\delta}{A_i^2(-\beta_0)}\,H(\beta_b)\left\{A_i^2(\beta)\,Q(-\beta_0) - 2\pi A_i(\beta)\,B_i(\beta)\right\}$$

$$y_b \geq y \geq 0$$

$$= \int_0^1 dq\,(1-q^2)\frac{\sin^2\delta}{A_i^2(-\beta_0)}\frac{1}{\sqrt{\beta_0}}\,H(\beta_b)\sin 2(qy+\delta)$$

$$y \leq 0$$

where

$$Q(-\zeta_o) = \frac{\sin 2\delta}{\sqrt{\zeta_o}} \frac{1}{A_i^2(-\zeta_o)} + 2\pi \frac{B_i(-\zeta_o)}{A_i(-\zeta_o)}$$

$$H(\zeta_b) = \zeta_b \Lambda(\zeta_b) + \frac{1}{2} A_i(\zeta_b) A_i'(\zeta_b)$$

$$G(\zeta_b) = \zeta_b \left[A_i'(\zeta_b) B_i'(\zeta_b) - \zeta_b A_i(\zeta_b) B_i(\zeta_b) \right] + \frac{1}{2} A_i'(\zeta_b) B_i(\zeta_b)$$

$$\Lambda(\zeta_b) = A_i'^2(\zeta_b) - \zeta_b A_i^2(\zeta_b)$$

in which ζ_o and ζ_b are defined as in Chap. III.

Jellium Edge Position

The jellium edge or metal surface position y_c is obtained from the charge neutrality condition as

$$y_c = y_a - \int_{-\infty}^{+\infty} n_1(y)\, dy \qquad (5.27)$$

$$y_c = y_a - \int_{-\infty}^{} n_1(y)\, dy \qquad (5.27)$$

where $y_c = y_a + \frac{y_F^{1/3}}{2} \int_0^1 dq\,(1-q^2) \frac{\sin^2\delta}{A_i^2(-\zeta_o)} \left[3\Lambda(\zeta_b) - \frac{1}{\zeta_o} H(\zeta_b) \cot 2\delta \right]$ h

the trial system is charge neutral, i.e.

$$y_a = -\frac{3\pi}{8} + \frac{2}{5} y_F - \frac{3}{4} \int_0^1 dq\,(1-q^2) \frac{1}{q} \sin 2\delta \qquad (5.28)$$

Surface Dipole Barrier

For the electronic density n(y) of Eq. 5.24, the surface dipole barrier is defined as

$$\Delta\phi = 4k_F/(3\pi) \int_{-\infty}^{+\infty} y n_T(y) dy, \qquad (5.29)$$

where $n_T(y)=n(y)-\Theta(y_c-y)$ is the total charge density satisfying Poisson's equation. By performing the spatial integral in the above equation the surface dipole barrier may be written as

$$\Delta\phi = (\Delta\phi)_0 + (\Delta\phi)_1, \qquad (5.30)$$

where $(\Delta\phi)_0$ is the dipole barrier obtained from the total charge density of the trial system, and $(\Delta\phi)_1$ is the correction term which includes the contribution both due to the corrected electronic density and to the appropriate shift of the jellium background necessary to maintain overall charge neutrality. The expressions for $(\Delta\phi)_0$ and $(\Delta\phi)_1$ respectively are

$$\frac{(\Delta\phi)_0}{k_F} = \frac{1}{\pi} + \frac{1}{2}K(0) + \frac{16}{105}\frac{y_F^2}{\pi} - \frac{2}{3}\frac{y_a^2}{\pi} + \frac{1}{\pi}\int_0^1 dq\,(1-q^2)\frac{\sin^2\delta}{q^2} \qquad (5.31)$$

$$-\frac{2}{3\pi} y_F \int_0^1 dq\,(1-q^2)\,q \sin 2\delta$$

where

$K(0)=y_F^{1/3}Ai(0)/Ai'(0)$, and

$$\frac{(\Delta\phi)_1}{k_F} = \frac{1}{6}\frac{y_F^{1/3}}{A_i'^2(0)} H(y_b y_F^{-1/3}) - \frac{2}{3\pi}(y_c^2 - y_a^2) \tag{5.32}$$

$$+ \frac{y_F^{2/3}}{3\pi}\int_0^1 dq\,(1-q^2)\frac{\sin^2\delta}{A_i^2(-\xi_0)}\left\{H(\xi_b)\left[\frac{1}{\xi_0^{3/2}}\sin 2\delta - \frac{4}{3}\cos 2\delta\right]\right.$$

$$\left. + 2\Lambda(\xi_b)(3\xi_0 - \xi_b) - 2A_i(\xi_b)A_i'(\xi_b)\right\}$$

Electrostatic Potential

The electrostatic potential V_{es} defined in Eq. 2.22 may be written as

$$V_{es}(y) = V_{es}^{(0)}(y) + V_{es}^{(1)}(y), \tag{5.33}$$

where $V_{es}^{(0)}(y)$ is due to the total charge density of the trial system and $V_{es}^{(1)}(y)$ due to the correction charge distribution and shift of the jellium background.

For $y \geq 0$

$$\frac{V_{es}^{(0)}(y)}{k_F} = \frac{(\Delta\phi)_0}{k_F} + \frac{2}{3\pi}(y - y_a)^2\,\theta(y_a - y) \tag{5.34}$$

$$+ \frac{4}{3\pi}y_F^{2/3}\int_0^1 dq\,(1-q^2)\frac{\sin^2\delta}{A_i^2(-\xi_0)}\left[2\xi\Lambda(\xi) + A_i(\xi)A_i'(\xi)\right]$$

For $y \leq 0$

$$\frac{V_{es}^{(0)}(y)}{k_F} = \frac{1}{\pi} + \frac{1}{2}K(0) + \frac{1}{2}y - \frac{2}{3\pi}(y-y_a)^2\,\theta(y-y_a) \qquad (5.35)$$

$$+ \frac{1}{\pi}\int_0^1 dq\,(1-q^2)\frac{1}{q^2}\sin^2(qy+\delta)$$

For $y \geq y_b \geq 0$

$$\frac{V_{es}^{(1)}(y)}{k_F} = \frac{(\Delta\phi)_1}{k_F} + \frac{2}{3\pi}(y-y_c)^2\,\theta(y_c-y) - \frac{2}{3\pi}(y-y_a)^2\,\theta(y_a-y) \qquad (5.36)$$

$$+ \frac{2}{q\pi}y_F^{2/3}\int_0^1 dq\,(1-q^2)\frac{\sin^2\delta}{A_i^2(-s_0)}\Big\{2\Big[H(s_b)Q(-s_0) - 2\pi G(s_b)\Big]$$

$$- \Big[2s\Lambda(s) + A_i(s)A_i'(s)\Big] + 2A_i(s)A_i'(s) + (s+qs_b)\Lambda(s)\Big\}$$

For $0 \leq y \leq y_b$

$$\frac{V_{es}^{(1)}(y)}{k_F} = \frac{(\Delta\phi)_1}{k_F} + \frac{2}{3\pi}(y-y_c)^2\,\theta(y_c-y) - \frac{2}{3\pi}(y-y_a)^2\,\theta(y_a-y) \qquad (5.37)$$

$$+ \frac{2}{q\pi}y_F^{2/3}\int_0^1 dq\,(1-q^2)\frac{\sin^2\delta}{A_i^2(-s_0)}\Big\{2H(s_b)Q(-s_0)\Big[2s\Lambda(s) + A_i(s)A_i'(s)\Big]$$

$$- 4\pi H(s_b)\Big[2sA_i'(s)B_i'(s) - 2s^2A_i(s)B_i(s) + \frac{1}{2}A_i(s)B_i'(s)$$

$$+ \frac{1}{2}A_i'(s)B_i(s)\Big] + 3A_i(s_b)A_i'(s_b) + 3(s_b+3s)\Lambda(s_b)\Big\}$$

For $y \leq 0$

$$\frac{V_{es}^{(1)}(y)}{k_F} = \frac{y_F^{1/3}}{6}\frac{H(y_b y_F^{1/3})}{A_i'^2(0)} + \frac{2}{3\pi}(y_c - y_a)\left[2y - (y_c + y_a)\right] \qquad (5.38)$$

$$+ \frac{2}{3\pi}\left[(y-y_c)^2\,\theta(y_c-y) - (y-y_a)^2\,\theta(y_a-y)\right]$$

$$+ \frac{y_F^{2/3}}{3\pi}\int_0^1 dq\,(1-q^2)\frac{1}{\xi_0^{3/2}}\frac{\sin^2\delta}{A_i^2(-\xi_0)}H(\xi_b)\sin 2(qy+\delta)$$

In the above equations $\Lambda(\zeta)=Ai'^2(\zeta)-\zeta Ai^2(\zeta)$.

Electrostatic Energy

The universal function for the electrostatic energy may be written as

$$E_{es}/k_F^3 = 1/(6\pi^2)\{\int_{-\infty}^{+\infty} dy\,n(y)V_{es}(y)/k_F - T(y_F,y_b)\}. \qquad (5.39)$$

For $y_c \geq 0$

$$T(y_F,y_b) = \frac{1}{8} + \frac{1}{2}K(0)\left[\frac{1}{\pi}+\frac{1}{2}K(0)\right] + \frac{1}{2}J(0)\left[\frac{1}{\pi}+\frac{1}{2}K(0)\right]$$

$$+ \frac{1}{2\pi}\int_0^1 dq\,\frac{1}{q^2}\left\{K(0)+J(0)-(1-q^2)\left[\frac{\sin 2\delta}{2q}+J(q)\cos 2\delta\right]\right\}$$

$$+ \int_0^{y_c} dy\,\frac{V_{es}(y)}{k_F}$$

For $y_c \leq 0$

$$T(y_F, y_b) = \frac{1}{8} + y_c\left(\frac{1}{\pi} + \frac{1}{4}y_c\right) + \frac{1}{2}K(0)\left[\frac{1}{\pi} + \frac{1}{2}K(0) + y_c\right]$$

$$+ \frac{1}{2}J(0)\left[y_c + \frac{1}{\pi} + \frac{1}{2}K(0)\right]$$

$$+ \frac{1}{2\pi}\int_0^1 dq \frac{1}{q^2}\left\{K(0) + (1-q^2)\left[y_c - \frac{1}{2q}\sin 2(q y_c + \delta)\right]\right\}$$

$$+ \frac{1}{2\pi}\int_0^1 dq \frac{1}{q^2}\left\{J(0) - (1-q^2)J(q)\cos 2(q y_c + \delta)\right\}$$

and

$$J(q) = y_F^{1/3}\frac{H(\beta_b)}{3\Lambda(-\beta_0)} \quad , \quad J(0) = y_F^{1/3}\frac{H(y_b y_F^{-1/3})}{3A_i'^2(0)}$$

Kinetic Energy

The use of this variational formalism determines the density directly instead of the single-particle wave functions. It is thus not possible to obtain the kinetic energy contribution to the surface energy exactly as given in the Kohn-Sham scheme, since that requires knowledge of the single-particle wave function and its asymptotic phase shift. In order to determine the surface energy one therefore must resort to the density gradient expansion formalism and include terms of $O(\nabla^4)$ as discussed in Chap. IV. The surface kinetic energy in its gradient expansion form can be expressed as

$$E_k^{GE}[n] = E_k^{(1)} + E_k^{(2)} + E_k^{(3)}, \qquad (5.40)$$

where $E_k^{(1)}$, $E_k^{(2)}$ and $E_k^{(3)}$ are the components of the gradient expansion as defined in Eqs. 2.12-2.14. For the coefficients λ and γ of Eqs. 2.13 and 2.14 we employ $\lambda=1/9$ and $\gamma=1.336$ as discussed in Chap. IV.

C. Demonstration of Stationary Property of Variational Formalism

Prior to discussing any results, we wish to demonstrate in this section the mechanics of the variational formalism as applied to the many-body problem by which a property of interest is made insensitive to variations about its saddle point (and in fact that such a saddle point exists), and the corresponding changes that occur in the correction density in order to achieve this insensitivity. We restrict ourselves to a one-dimensional variation by plotting in Fig. 18 the surface dipole barrier $\Delta\phi$ as obtained by employing the density determined correct to second order, as a function of the barrier height parameter. The field strength and jellium edge parameters are adjusted so as to satisfy the constraints set by the BVT and charge neutrality respectively. The corresponding variation of $(\Delta\phi)_0$ is also plotted together with the value obtained by Lang and Kohn (14). Note how the variational principle corrects an approximately linear variation of $(\Delta\phi)_0$ to one in which $\Delta\phi$ is essentially horizontal about the correct answer. Thus for any choice of the variational parameter in the substantial range shown in the figure, the result obtained is nearly exact. An obvious choice of the parameter is that which extremizes the result. Another choice, as discussed in Chap. III, is that for which the barrier height is obtained self-consistently. Although the value of the parameter obtained by application of the two constraints are different, the results for the surface

dipole barrier are nearly the same, the extremum value of $\Delta\phi$ being 3.92eV whereas the self-consistent value is 3.82eV. In order to see how the correction term of the charge density $n_1(y)$ changes as one varies the variational parameter y_b, we plot $n_1(y)$ in Fig. 19 for two values of y_b in Fig. 18. One (y_b=1.20) corresponds to a value for which there is a large correction $(\Delta\phi)_1$ to $(\Delta\phi)_0$ and the other (y_b=1.82) for which the total surface dipole barrier is an extremum. As may be observed from the figure, the amplitude variation of $n_1(y)$ is considerably different for the two values of the parameters employed thus demonstrating how the correction to the trial density changes in order to eliminate practically all error in the result for the dipole barrier over the very substantial range of variational parameter considered.

Although the value of barrier height parameter for which the surface dipole barrier is an extremum leads to an accurate result, such a choice would be even more meaningful if in fact we had employed the exact Hamiltonian in our calculations. In the application of this variational formalism to atomic systems (51-57), the exact non-relativistic Hamiltonian has always been used to determine the correction term. The extremum value of a specific property thus obtained has always proved to be more accurate than that obtained by employing a predetermined value of the variational parameter. However, since in our work we have employed a model-potential single-particle type Hamiltonian it is more

appropriate to determine the parameters in the density by ensuring that they all satisfy various theoretical and physical constraints. Of course, it is to be emphasized that either choice should lead to meaningful results since the property of interest is considerably insensitive to variations near and about its extremum value.

D. Results and Discussion

In this section we present results for metallic surface dipole barriers, work functions, and surface energies by employing the parametrized density determined correct to second order with the parameters adjusted so as to satisfy appropriate constraints tailored to specific properties of interest. In the calculations for both the work function and surface energy, the jellium edge parameter y_c is fixed to ensure overall charge neutrality and the barrier height parameter y_b by the requirement of self-consistency of the dipole barrier. For the determination of surface dipole barriers and work functions, the field strength parameter y_F is adjusted as in Chap. III to satisfy the constraint set on the electrostatic potential by the BVT. This condition can be satisfied exactly only for $r_s<4.3$. For the surface energy, the parameter y_F is varied till the energy is a minimum. All the parameters in the expression for the density are thus fully determined. It is, however, possible to improve the accuracy of the density still further in this jellium model problem by incorporating the integral sum rule of the Mahan-Schaich theorem (MST) (see Eq. 2.33). Note that the MST is satisfied for arbitrary effective potential. The electronic density n(y) can thus be improved by introducing a parameter α such that

$$n(y) = n_0(y) + \alpha n_1(y),$$

and by adjusting α till n(y) satisfies the integral relationship of the MST. This procedure in effect corresponds to incorporating the contribution of the higher order terms in the series for the density, thus improving it. It turns out that the iteration procedure for the determination of a unique value of α for each density converges quite satisfactorily, the values for α ranging from 2.55 for r_s=2.5 to 3.10 at r_s=4.0.

In Table VI we present the results for the surface dipole barrier and work function in the density range r_s=1.0-4.0. For the results in parenthesis all constraints except the MST are satisfied. Since the exact solution of the assumed Hamiltonian employing the same constraints is known (see Chap. III), a comparison between the variational and exact results is meaningful and we include the latter results in the table. Note that for $r_s \geq 1.5$, the results obtained by the variational fromalism are essentially the same as the exact values, differing by at most 0.04eV. The results for which the MST is not satisfied are only slightly less accurate although for $r_s \geq 2$ they are still within 0.04eV of the exact result.

As discussed earlier the kinetic energy contribution to the surface energy must be obtained by its density gradient expansion, since within this formalism it is the density rather than the single-particle wave function that is being determined. With the exchange-correlation contribution

TABLE VI

Results for the surface dipole barrier $\Delta\phi$ and work function Φ by employing densities determined via the variational principle (VP) for the density. The slope, barrier height, and jellium edge parameters y_F, y_b, and y_c quoted are determined by application of the BVT, self-consistency of $\Delta\phi$ and charge neutrality respectively, employing the Wigner function for the correlation energy. The integral constraint of the Mahan-Schaich theorem (MST) is also satisfied by these densities. The results in parenthesis are determined by densities which do not satisfy the additional constraint of the MST.

r_s	y_F	y_b	y_c	Dipole Barrier $\Delta\phi$(eV)		Work Function Φ(eV)	
				VP	Exact[a]	VP	Exact[a]
1.0	6.60	7.30	2.64	37.36 (37.05)	37.51	5.28 (4.97)	5.43
1.5	4.91	5.97	1.95	14.62 (14.53)	14.66	4.78 (4.69)	4.82
2.0	3.74	4.99	1.48	7.09 (7.06)	7.10	4.17 (4.14)	4.18
2.5	2.79	4.07	1.10	3.82 (3.81)	3.82	3.70 (3.69)	3.70
3.0	1.94	3.11	0.76	2.16 (2.14)	2.16	3.34 (3.32)	3.34
3.5	1.16	2.03	0.39	1.20) (1.19)	1.21	3.03 (3.02)	3.04
4.0	0.36	0.67	-0.11	0.60 (0.60)	0.64	2.75 (2.75)	2.79

a. see Chap. III.

treated within the LDA, the total surface energy functional E_s is

$$E_s[n] = E_{es}[n] + E_k^{GE}[n] + E_{xc}^{LDA}[n], \tag{5.41}$$

where the electrostatic E_{es} and kinetic E_k^{GE} energy contributions are given Eqs. 5.39 and 5.40. With the density satisfying the MST, and the jellium edge and barrier height parameters determined by charge neutrality and self-consistency of the dipole barrier respectively, the surface energy functional $E_s[n]$ is then minimized with respect to the field strength parameter. The results over the metallic density range of this variational self-consistent calculations are given in Table VII. For purposes of comparison of two distinctly different methods for determining the density, we also include the results of Lang and Kohn in the table. Note that for r_s=2.5-6.0 our results and those of LK are within 8 ergs/cm^2 of each other and differ in many cases by only 1 erg/cm^2. For r_s=2.0, the result differs by less than 4%. The accuracy of our results arise in part due to our use of the VP for the energy. However, these results are also indicative not only of the accuracy of the density determined but also of the energy functional employed. The latter conclusion reiterates our earlier contention of the importance of including the second density gradient correction in the gradient expansion for the kinetic energy functional.

TABLE VII

Results for metallic density surface energies E_s by application of the Rayleigh-Ritz variational principle (VP) for the energy. The barrier height and jellium edge parameters y_b and y_c quoted are determined by the self-consistency of the surface dipole barrier and the requirement of charged neutrality respectively, whereas the slope parameter y_F is fixed by variational minimization of the total LDA surface energy functional. The Wigner expression for the correlation energy per particle is employed. The parametrized densities employed are those obtained by the VP for the density.

r_s	y_F	y_b	y_c	Surface Energies (ergs/cm^2)		$\lvert E_{s(LK)}-E_s \rvert$ (ergs/cm^2)
				VP	Lang-Kohn[a]	
2.0	3.40	4.28	1.35	-971	-1008	37
2.5	2.60	3.70	1.03	35	36	1
3.0	1.98	3.18	0.77	192	199	7
3.5	1.53	2.76	0.57	186	194	8
4.0	1.21	2.44	0.41	154	158	4
4.5	1.02	2.31	0.31	123	124	1
5.0	0.85	2.13	0.21	97	98	1
5.5	0.75	2.08	0.14	78	77	1
6.0	0.70	2.13	0.11	63	60	3

a. see Ref. 13.

In concluding this section, we note that we have demonstrated the utility and accuracy of the variational formalism for the density to the case of the inhomogeneous electron gas system at a surface. The results for the surface dipole barrier and work function are observed to be as accurate as those of an exact calculation. The surface energies obtained by these variational densities are essentially equivalent to those determined by a fully self-consistent calculation of the density. We believe that the above application to the jellium case is an important step in demonstrating the power and usefulness of this variational technique, since it is imperative that any new formalism be first proved accurate with regard to simple and ideal systems for which a few answers exist, prior to its use for more complex systems. Further work is required not only in developing formal connections between this variational formalism and the density functional theory, but also in completing calculations in which a more realistic Hamiltonian is employed. We conclude this chapter by indicating in the following section how the crystal lattice may be incorporated into the variational scheme in order to determine accurately the electronic density variation at a real metal surface.

E. Inclusion of Ionic pseudopotentials

The above procedure for the determination of the density correct to second order can be extended to a more realistic metal surface system by adding a local ionic pseudopotential $v_{ps}(r)$ to the Hamiltonian. This local pseudopotential treatment is appropriate for metals with s- and p-band electrons. It must be modified for noble and transition metals where d-band electrons are important (106-108). It can easily be shown that the inclusion of a local ionic pseudopotential to the Hamiltonian is equivalent to adding a term $\delta v_{ps}(x)$ to the $V_{eff}(x)$ of the jellium model approximation, where

$$\delta v_{ps}(x) = v_{ps}(x) + \int \frac{\rho_+(x')}{|x-x'|}\, dx' \tag{5.42}$$

is the difference between the ionic pseudopotential averaged over the plane parallel to the metal surface and the electrostatic potential of the positive jellium background $\rho_+(x)=\bar{\rho}\Theta(-x)$.

Thus within our variational formalism the density may be written as

$$\rho(x) = \rho_0(x) + \rho_1(x) + 2\,\mathrm{Re} \sum_{k\le k_F} (k_F^2 - k^2) \cdot \int f_k^*(x_i, x)\, \psi_k^*(x_i)\, \delta v_{ps}(x_i)\, \psi_k(x_i)\, dx_i \tag{5.43}$$

where $\rho_0(x)$ and $\rho_1(x)$ are defined in Eqs. 5.19 and 5.20 respectively and where the last term corresponds to the contribution to the density variation at the surface due to the presence of the ionic lattice. Note that the above expression for the density is now dependent on the specific crystal face of interest. In our calculation we propose to employ the Ashcroft pseudopotential (109) for which

$$V_{ps}(r) = -z/r + z/r\ \Theta(r_c - r), \tag{5.44}$$

where r_c is the Ashcroft core radius. The values for r_c for various metals (Al, Pb, Zn, Mg, Li, Na, K, Rb, Cs) are given in the work of Lang and Kohn (13) and for Ca, Sr, and Ba by Paasch and Heitschold (24). For all metals with the exception of Li, Zn, and Ba, the use of this pseudopotential leads to theoretical binding energies which agree well with experimental values (110,80). For Ca and Sr the magnitude of this difference is 0.5 and 0.6 eV respectively (80), the difference for the remaining metals (110) being less than 0.4 eV. This is particularly important since the first order pseudopotential energy, which as shown by Monnier and Perdew (110) and Sahni and Gruenebaum (80) is a term contributing to the work function, is then in error by at most 0.6 eV for all metals except Li, Zn, and Ba. The use of these pseudopotentials is thus most appropriate.

Since our choice of trial wave function of Section C is good and the corresponding auxiliary function analytically

well-defined, it is possible and meaningful to employ these functions in Eq. 5.43 in order to determine the density accurately. For the work function the parameters can again be obtained by various constraints such as the self-consistency of the surface dipole barrier, or by the determination of its stationary value.

The inclusion of the ionic pseudopotential leads, as described by LK, to the classical cleavage $E_{cl}[\rho]$ and pseudopotential $E_{ps}[\rho]$ energy contributions to the surface energy functional. The expressions for these terms are respectively

$$E_{cl}[\rho] = \beta Z \bar{\rho} \tag{5.45}$$

and

$$E_{ps}[\rho] = \int_{-\infty}^{+\infty} \delta v_{ps}(x)[\rho(x)-\bar{\rho}\Theta(-x)]dx, \tag{5.46}$$

where β is the cleavage energy constant (111,13) and Z the ionic charge. Employing these crystal face dependent densities (which are correct to second order), the surface energy can then be determined by variational minimization of the total surface energy functional

$$E_s[\rho] = E_k^{GE}[\rho]+E_{es}[\rho]+E_{xc}^{LDA}[\rho]+E_{cl}[\rho]+E_{ps}[\rho]. \tag{5.47}$$

We can also easily include, in the above energy functional, a correction to the LDA exchange-correlation contribution as determined either by the wave-vector analysis (72,73,79) or gradient expansion (80) methods.

With the inclusion of the ionic pseudopotential the expression for the work function is given as (80)

$$\Phi = (\Delta\phi)_r - \bar{\mu} - \langle\delta v\rangle, \tag{5.48}$$

where $(\Delta\phi)_r$ is the electronic relaxation dipole barrier evaluated using the variational density and is defined as

$$(\Delta\phi)_r = V_{es}(\infty) - V_{es}(-\infty) = 4\pi \int_{-\infty}^{+\infty} x[\rho(x) - \bar{\rho}\Theta(-x)]dx,$$

and where $\langle\delta v\rangle$ is the average value of $\delta v_{ps}(r)$ over the volume of the semi-infinite crystal.

Finally, as we mentioned in the introduction, non-fully self-consistent three dimensional calculations do exist for a few metals and for a few crystal faces (see Refs. 15-22). They do, however, require heavy numerical computations. The principle additional approximation beyond the LDA in the majority of these calculations is a variational restriction on the number density arising from the use of a finite wave function basis. The above described variational formalism not only obviates the necessity of heavy numerical computations, but also offers an accurate and easy method for the

determination of the crystal face dependence of the surface energy and work function. A further advantage of the variational method over the fully self-consistent method is that the former may be employed with any explicit density functional for the energy including non-local treatments of exchange and correlation whereas the latter usually requires a local approximation. The determination of crystal face dependent work functions and surface energies of twelve simple metals is presently in progress.

VI. STUDY OF THE INHOMOGENEOUS HARTREE-FOCK GAS AT SURFACES

In this last chapter we study the surface properties of an inhomogeneous Hartree-Fock (HF) gas interacting only via Pauli correlation. It is interesting to note that although there is such substantial interest in surface physics, a fully self-consistent calculation (including non-local exchange) of the surface properties of an inhomogeneous HF gas does not exist. Such a self-consistent calculation was originally considered by Bardeen (2). However, due to the computational difficulties at that time, some of which still exist today, he was unable to solve the HF equation self-consistently. Instead, the exchange potentials were obtained by evaluating them at two points in space, one using the step-model wave function and the other using the infinite barrier model (IBM) wave function, and then drawing smooth curves through these points. These potentials were then held fixed throughout the calculation, and it was only the electrostatic potential which was obtained self-consistently. Bardeen also made yet another approximation. In calculating the exchange potential he set the components of the electron momentum parallel to the surface to zero and then replaced the momentum in the perpendicular direction in the final result by the magnitude of the total momentum. Such a procedure is entirely valid for the homogeneous case (112) but its validity for the inhomogeneous case is un-

clear. We, however, adopt a different approach in order to solve this problem and determine the total non-local and hence the non-local surface exchange energy contribution by employing accurate wave functions in conjunction with the Rayleigh-Ritz variational principle for the energy.

The total exchange energy of an interacting system of particles is defined in terms of the single-particle density matrix $\rho(\vec{r},\vec{r}')$ as

$$E_x = -\frac{1}{4}\int d\vec{r}\int d\vec{r}' \frac{|\rho(\vec{r},\vec{r}')|^2}{|\vec{r}-\vec{r}'|} \tag{6.1}$$

where

$$\rho(\vec{r},\vec{r}') = 2\sum_{\vec{k}} \psi_{\vec{k}}(\vec{r})\psi^*_{\vec{k}}(\vec{r}'),$$

and where $\psi_k(\vec{r})$ is the electronic wave function. It can be shown (see Appendix F) that the above expression for the exchange energy may be written as

$$E_x = -\frac{2\pi}{A}\sum_{\vec{k}}\sum_{\vec{k}'}\frac{1}{P}\iint d\vec{r}\, d\vec{r}'\, e^{-P|x-x'|}\, \psi^*_{\vec{k}}(x)\psi^*_{\vec{k}'}(x)\cdot \psi_{\vec{k}}(x')\psi_{\vec{k}'}(x') \tag{6.2}$$

where $\psi_k(x)$ is the component of the wave function in the direction of the inhomogeneity and $P^2=[(k_y-k_y')^2+(k_z-k_z')^2]$. The surface contribution to the exchange energy can then be determined following the method of Harris and Jones (66).

The exact total surface energy functional of the density $E_s[\rho]$ for this inhomogeneous HF gas within the Kohn-Sham scheme can be written as

$$E_s[\rho] = E_k[\rho] + E_{es}[\rho] + E_x[\rho], \qquad (6.3)$$

which is a sum of the kinetic E_k, electrostatic E_{es}, and exchange E_x energy components respectively. Since each of these energy functionals is known exactly, rigorous upper bounds for the surface energy can be obtained on application of the Rayleigh-Ritz variational principle provided the variational wave function is a plane wave in the bulk.

Two exact calculations of the surface exchange energy have been performed recently, one for the IBM (66,67) and the other for the step model by Mahan (113). For the IBM case the correlation energy contribution to the surface energy has also been determined exactly within the RPA (67). The results indicate that for any density, the exchange and correlation contributions are approximately the same. Furthermore, the use of these densities leads to the conclusion that the error between the exact and the local density approximation (LDA) calculations for exchange remains precisely the same as the density is made more slowly varying by changing the value of the Wigner-Seitz radius. As a consequence, the percent error between the 'exact' RPA (67) and the local values of the correlation energy increases with increasing density. These conclusions are obviously

unphysical since the LDA value of a property should approach the exact value as the density becomes more slowly varying. Although the step model wave functions are an improvement over those of the IBM, they are still poor representations (34,35) of the wave functions that exist at surfaces. For example, the use of the step model led Mahan to the conclusion that the universal functions of both the surface electrostatic and exchange energies remain essentially the same as the density is made more slowly varying. The use of the far superior and more realistic LP and FLP models indicate this not to be the case (see Chap. III and Ref. 36) for the electrostatic energy and, as will be shown in Section A below), neither to be the case for the surface exchange energy. The accurate determination of the exchange energy is also very important for the determination of the correlation energy since this latter quantity is usually obtained by subtracting the exchange energy from the exchange-correlation energy which is usually obtained within various formalism such as the RPA (67), the wave-vector analysis (72,73,79), and gradient expansion (80) methods. In order to determine the surface exchange energy accurately we employ the realistic and physically meaningful wave functions generated by the linear potential model for which the effective potential is assumed to be

$$V_{eff}(x) = F\Theta(x), \tag{6.4}$$

where F the field strength is defined in terms of the slope parameter x_F and the Fermi energy E_F as $F=E_F/x_F$. The solution of the Schrodinger equation for this potential is

$$\psi_k(x) = B\{\sin\delta(k)\,Ai(\zeta)/Ai(-\zeta_o)\;\theta(-x) + \sin[kx+\delta(k)]\;\theta(x)\}, \qquad (6.5)$$

where B is the normalization constant, $\delta(k)$ the phase shift, $Ai(\zeta)$ the Airy function, and where $\zeta_o=(k_F x_F)^{2/3}k^2/k_F^2$, $\zeta=x(2F)^{1/3}-\zeta_o$. The expressions for the phase shift and normalization constant are given in Chap. IV, Eq. 4.3. As mentioned in Chap. IV, all surface properties within this model potential can be written in terms of universal functions of the slope parameter (36). This is also the case for surface exchange energy. For the HF gas, the Wigner-Seitz radius r_s may again be related to the field strength parameter via either the Budd-Vannimenus theorem (32) constraint or that set by the variational minimization of the energy.

With a change of variables to $y=xk_F$, $q=k/k_F$, $q'=k'/k_F$, and $p=P/k_F$, where k_F is the Fermi momentum, the expressions for the electronic density (normalized with respect to its bulk value) $n(y)$, metal surface position y_a, surface dipole barrier $\Delta\phi$ and electrostatic potential $V_{es}(y)$ within this LP model effective potential as a universal function of the slope parameter $y_F=x_Fk_F$ are given in Eqs. 5.25, 5.28, 5.31,

and 5.34-35 respectively (see also Ref. 36). The results for various components of the surface energy, which may also be written in terms of universal functions of y_F, are given below.

Exchange Energy

We have derived the surface contribution to the exchange energy following the method of Harris and Jones (66) and Mahan (113). However, in our calculations, we have considered a semi-infinite lattice and not a finite box as have these other authors (66,113). The expression for the universal function E_x/k_F^3 is given below. A detailed derivation of this result is given in Appendix F.

(6.6)

$$\frac{E_x}{k_F^3} = \frac{y_a}{4\pi^3} + \frac{1}{8\pi^3}\int_0^2 dp \int_0^1 dq\, p \left\{ \frac{H(p,0,q)+H(p,q,0)}{p^2+q^2} - \frac{H(p,q,q)}{p^2} \right\}$$

$$- \frac{1}{4\pi^4}\int_0^2 dp \int_0^1 dq \int_0^1 dq'\, p\, H(p,q,q') \left\{ \frac{1}{p^2+q_-^2}\left(\frac{\sin 2\delta_-}{2q_-} - \frac{\sin 2\delta}{2q} - \frac{\sin 2\delta'}{2q'}\right) \right.$$

$$+ \frac{1}{p^2+q_+^2}\left(\frac{\sin 2\delta_+}{2q_+} - \frac{\sin 2\delta}{2q} - \frac{\sin 2\delta'}{2q'}\right) + \frac{1}{p}\left(\frac{q_-\sin 2\delta_-}{p^2+q_-^2} - \frac{q_+\sin 2\delta_+}{p^2+q_+^2}\right)^2$$

$$\left. - p\left(\frac{\cos\delta_-}{p^2+q_-^2} - \frac{\cos\delta_+}{p^2+q_+^2}\right)^2 \right\} - \frac{1}{\pi^4}\int_0^2 dp \int_0^1 dq \int_0^1 dq' \frac{\sin\delta}{A_i(-s_0)} \frac{\sin\delta'}{A_i(-s_0')} H(p,q,q')$$

$$\cdot\left\{p\frac{\cos\delta_-}{p^2+q_-^2}-p\frac{\cos\delta_+}{p^2+q_+^2}+q_-\frac{\sin\delta_-}{p^2+q_-^2}-q_+\frac{\sin\delta_+}{p^2+q_+^2}\right\}\int_0^\infty dy\, e^{-py}A_i(y,q)A_i(y,q')$$

$$-\frac{1}{\pi^4}\int_0^2 dp\int_0^1 dy\int_0^1 dy'\,\frac{\sin^2\delta}{A_i^2(-\xi_0)}\frac{\sin^2\delta'}{A_i^2(-\xi_0')}H(p,q,q')\int_0^\infty dy\int_0^\infty dy'\, e^{-p|y-y'|}\cdot$$

$$\cdot A_i(y,q)A_i(y,q')A_i(y',q)A_i(y',q')$$

where $q_+=q+q'$, $q_-=q-q'$, $\delta=\delta(q)$, $\delta'=\delta(q')$, $\delta_+=\delta+\delta'$, $\delta_-=\delta-\delta'$, and where

$$H(p,q,q')=\begin{cases}\pi(q'^2-q^2) & \text{for } \xi^2\geq 1-q'^2 \text{ and } \xi>0\\ \pi\left[(1-q'^2)+(1-q^2)\right] & \text{for } \xi^2\geq 1-q'^2 \text{ and } \xi<0\\ \pi(1-q^2)-2\left[(1-q'^2)\sin^{-1}\dfrac{\xi}{\sqrt{1-q'^2}}+\xi\sqrt{1-q'^2-\xi^2}\right] & \text{for } \xi^2<1-q'^2\end{cases}$$

$$\xi=\frac{1}{2p}(p^2+q^2-q'^2)$$

Kinetic Energy

$$\frac{160\pi}{k_F^4}E_k=1-\frac{64y_F}{35\pi}+\frac{4y_F^{1/3}}{3\pi}\int_0^1 dq\,(1-q^2)(3+5q^2)\frac{A_i(-\xi_0)A_i'(-\xi_0)}{\Lambda(-\xi_0)}$$

(6.7)

where $\zeta_o = q^2 y_F^{2/3}$, and $\Lambda(-\zeta_o) = Ai'^2(-\zeta_o) + \zeta_o Ai^2(-\zeta_o)$.

Electrostatic Energy

$$\frac{4\pi^2}{k_F^3} E_{es} = -\frac{1}{12} + \frac{2}{3}\int_0^\infty dy \left[n(y) - \theta(y_a - y)\right] \frac{V_{es}(y)}{k_F} \tag{6.8}$$

$$+ \frac{2}{3} y_a \left\{ \frac{2}{q\pi} y_a^2 - \frac{1}{4} y_a - \left[\frac{1}{\pi} + \frac{1}{2} K(0)\right] \right\} \theta(-y_a)$$

$$+ \left\{ \frac{1}{4} + \frac{2}{3\pi} y_a \, \theta(-y_a) \right\} \int_0^1 dq (1-q^2) \frac{\sin^2\delta}{q^2}$$

$$+ \left\{ \frac{2}{3\pi} y_a^2 \, \theta(-y_a) - \left[\frac{1}{\pi} + \frac{1}{2} K(0)\right] \right\} \int_0^1 dq (1-q^2) \frac{\sin 2\delta}{2q}$$

$$- \frac{2}{3\pi} \int_0^1 dq (1-q^2) \frac{1}{q^2} \left\{ y_a + \frac{1}{2q} \left[\sin 2\delta - \sin 2(q y_a + \delta)\right] \right\} \theta(-y_a)$$

$$+ \frac{1}{4\pi} \int_0^1 dq (1-q^2) \int_0^1 dq'^2 (1-q'^2) \left\{ \frac{\sin 2\delta_-}{2q_-} + \frac{\sin 2\delta_+}{2q_+} - \frac{\sin 2\delta'}{q'} \right\}$$

where $K(0) = y_F^{1/3} Ai(0)/Ai'(0)$.

Since by adjusting the field strength parameter the density can be made to vary as rapidly or slowly as desired, and as the exact surface exchange energy as a function of this parameter is known, it is possible to study the convergence properties of the LDA value for this property. This study is presented in Section A where for the first time the local density value of the surface exchange energy is shown

to converge to the exact value as the density becomes slowly varying. In Section B we present rigorous upper bounds for the surface energy of a HF gas and results for the work function employing these energy minimized densities. Finally in Section C we study the effects of introducing correlation on various surface properties such as the work function, surface dipole barrier, and surface energy.

A. Comparison between the Exact and Local Density Approximation for the Surface Exchange Energy

In Fig. 20 we plot the variation of the universal function E_x/k_F^3 as a function of the slope parameter y_F for the exact surface exchange energy. The explicit numerical values (114) are given in Table VIII. The point $y_F=0$ corresponds to the infinite barrier model (IBM) for which the density is most rapidly varying. The density becomes more slowly varying as the value of y_F increases. A study of the graph indicates that over the entire range of y_F considered, the universal function E_x/y_F^3 increases by approximately a factor of six, a result which is substantially different from the conclusions arrived at by Mahan (113). Now in order to determine the variation in the surface exchange energy as a function of the bulk density we must relate the slope parameter to the Wigner-Seitz radius r_s. Such a correspondence, as determined by the constraint set by the BVT for a HF gas is given at the top of Fig. 20. Note that over this range of density ($1\lesssim r_s \lesssim 5$), the exchange energy changes by three orders of magnitude being 63 ergs/cm^2 at $r_s=4.75$ and 39068 ergs/cm^2 at $r_s=1$. For the IBM densities, on the other hand, the results for the surface exchange energy differ by only two orders of magnitude between $r_s=1$ and 6. Thus we note that the use of our more accurate densities leads to considerably different conclusions with regard to the magnitude of the surface exchange energy.

In order to demonstrate the convergence characteristics

TABLE VIII

Values of the universal function for the local density approximation (LDA) and exact surface exchange energies as a function of the slope parameter y_F. The percent error between the LDA and the exact results is quoted in the last column.

Slope Parameter y_F	(Surface Exchange Energy/k_F^3) (10^{-3} a.u.)		Percent Error
	LDA	Exact	
0.0	0.90	0.58	56
0.5	1.08	0.71	52
1.0	1.25	0.87	44
1.5	1.43	1.04	38
2.0	1.61	1.23	31
2.5	1.80	1.42	27
3.0	2.00	1.63	23
3.5	2.21	1.86	19
4.0	2.44	2.09	17
4.5	2.68	2.36	14
5.0	2.92	2.63	11
5.5	3.18	2.90	9.7
6.0	3.44	3.18	8.2
6.5	3.69	3.46	6.6

of the LDA value for the surface exchange energy E_x^{LDA}, we have also plotted in Fig. 20 the variation of the universal function E_x^{LDA}/k_F^3 versus the slope parameter y_F. The precise numerical values are again quoted in Table VIII. The percent error between the LDA and exact values is plotted in Fig. 21. This error monotonically decreases from a maximum of 56% for the rapidly varying IBM density to an error of only 6.6% for the very slowly varying density at $y_F=6.65$. Thus although the LDA value is an overestimate over the entire range of the variational parameter considered it does, as must be the case, asymptotically approach the correct result as the density is made more slowly varying.

B. Rigorous Upper Bounds to the Surface Energy and Calculation of Work Functions.

In this section we present rigorous upper bounds to the surface energy of an inhomogeneous HF gas, and results for the work function as obtained by employing these energy minimized densities and by application of the BVT. The mathematical argument and constraints for the existence of such a bound are discussed below.

The exact total ground state energy E_T of a system of interacting particles with a surface may be written as a sum of the bulk E_b and surface E_s contributions. Now in any Rayleigh-Ritz variational calculation of this energy, the variationally determined value E_T^{var} must be greater than the exact value E_T. i.e.

$$E_T^{var} > E_T, \tag{6.9}$$

or

$$E_b^{var} + E_s^{var} > E_b + E_s, \tag{6.10}$$

where E_b^{var} and E_s^{var} are simply the variationally determined values of E_b and E_s respectively.

For a neutrally charged HF gas with a surface, the components of the bulk and surface energy functionals of the density are known exactly within the Kohn-Sham formalism. Thus

$$E_b = E_{k,b} + E_{x,b} \tag{6.11}$$

and

$$E_s = E_{k,s} + E_{x,s} + E_{es,s} \tag{6.12}$$

where $E_{k,b}$ and $E_{x,b}$ are the bulk contributions to the kinetic and exchange energies, and $E_{k,s}$, $E_{x,s}$, and $E_{es,s}$ the surface kinetic, exchange, and electrostatic contributions. Since the HF wave functions for the homogeneous system are plane waves, the use (in the calculation of the total bulk plus surface energy) of any variational wave functions which are plane waves in the bulk will ensure that

$$E_b^{var} = E_b. \tag{6.13}$$

Therefore, with such a choice of variational wave function

$$E_s^{var} > E_s, \tag{6.14}$$

which proves our contention that variational minimization of the exact energy functional E_s will provide a rigorous upper bound to the surface energy of a HF gas. Furthermore, since it is the variational principle for the energy which is applied, the result for the surface energy will be correct to

$O(\delta^2)$ if trial wave functions or densities correct to $O(\delta)$ are employed. The above arguments of course fail for the case of a fully correlated system since the exact wave function for the homogeneous fully interacting system is unknown. The use of plane waves in the bulk is thus inadequate since the equality of Eq. 6.13 no longer holds.

In Table IX we present rigorous upper bounds to the surface energy of a HF gas over the metallic range (r_s=2-6) by variational minimization of the surface energy functional of Eq. 6.3 with respect to the field strength or slope parameter y_F. The kinetic, electrostatic, and exchange energy components as well as the surface dipole barrier are also quoted in the table. A graph of this HF surface energy as a function of the Wigner-Seitz radius r_s is plotted as curve I in Fig. 22. On the basis of the accuracy of this variational procedure (37) together with that of the wave functions employed, we believe our results for the surface energy to be essentially those that would be obtained by a fully self-consistent non-local calculation such as that originally attempted by Bardeen. In this manner we have thus obviated the necessity of performing that complex numerical calculation. The exact results should lie at most a few ergs/cm^2 below the rigorous bounds quoted in Table IX. Note again, that over the range of densities considered, there is a substantial change in the surface exchange energy component as must be the case. In Fig. 22 we have also plotted (curve II) the bounds obtained by treating the ex-

TABLE IX

Rigorous upper bounds for the surface energy E_s of a Hartree-Fock gas. The slope parameter y_F is determined by minimization of the surface energy functional of Eq. 6.3 and the jellium surface position y_a by the requirement of charge neutrality. The results for the surface dipole barrier $\Delta\phi$ quoted are determined by employing the energy minimized densities.

r_s	y_F	y_a	$\Delta\phi$ (eV)	Surface Energy Components ($ergs/cm^2$)			Surface Energies ($ergs/cm^2$)
				E_k	E_{es}	E_x	E_s
2.0	3.59	1.42	6.58	-5650	1414	2593	-1643
2.5	2.79	1.10	3.77	-1853	444	1077	-332
3.0	2.12	0.83	2.30	-708	168	514	-26
3.5	1.65	0.62	1.54	-309	78	280	49
4.0	1.33	0.47	1.12	-150	43	164	57
4.5	1.10	0.35	0.85	-79	26	108	55
5.0	0.89	0.23	0.66	-42	16	73	47
5.5	0.82	0.19	0.57	-26	12	53	39
6.0	0.64	0.07	0.45	-14	8	39	33

change energy component within the LDA. The fact that these bounds are far inferior is simply a reflection of the poorness of the LDA surface exchange energy functional as discussed in the previous section (see Fig. 20). Meaningful results are obtained only when both exchange as well as correlation are treated locally.

The results for the surface dipole barrier determined by employing the densities obtained by minimizing the exact HF surface energy functional are of course correct only to the same order as that of the wave function employed and not as accurate as the energy. However, as shown in Chap. III, the best method for obtaining accurate dipole barriers in such model potential calculations is by use of the BVT constraint on the electrostatic potential. The results of application of this constraint for the HF gas (i.e. by considering only the kinetic and exchange energies per particle in Eq. 2.32 for the total energy of the homogeneous system) are given in Table X for r_s=1-4.75. For r_s>4.75 the BVT can no longer be satisfied by these wave functions. Based on the proven accuracy of the use of this constraint for this specific property (see Chap. III), we believe our results for the work function of the inhomogeneous HF gas to be most accurate. In this section we have thus presented accurate values for both the surface energy and work function of a HF gas without having solved the problem self-consistently.

TABLE X

Results for metallic and higher density (r_s = 1.00 - 4.75) surface dipole barriers $\Delta\phi$ and work functions Φ of the Hartree-Fock gas. The jellium edge and slope parameters y_a and y_F quoted are determined by application of charge neutrality and the BVT constraint respectively.

r_s	y_F	y_a	Dipole Barrier $\Delta\phi$ (eV)	Work Function Φ (eV)
1.00	6.65	2.65	36.98	3.49
1.50	4.96	1.97	14.63	3.44
2.00	3.83	1.51	7.21	3.00
2.50	2.92	1.16	3.99	2.62
3.00	2.17	0.85	2.35	2.33
3.50	1.51	0.56	1.42	2.08
4.00	0.93	0.25	0.85	1.87
4.50	0.41	-0.12	0.47	1.69
4.75	0.16	-0.42	0.33	1.61

C. Effect of Introducing Correlation on the Surface Properties of a Hartree-Fock gas

In this final section we study the effects of introducing correlation on the surface properties of a HF gas. For the surface dipole barrier and work function we do this by introducing a correlation factor α into the general expression of the BVT. Thus we write

$$\Delta V = V_{es}(y_a) - V_{es}(-\infty) = \bar{\rho}^{d\varepsilon}{}_T/d\bar{\rho}, \qquad (6.15)$$

where

$$\varepsilon_T = \varepsilon_k + \varepsilon_x + \alpha\, \varepsilon_c,$$

and all the other terms are as defined in Chap. II. The value $\alpha=0$ corresponds to the HF gas and $\alpha=1$ to the fully correlated system. The change in the dipole barrier and work function as correlation is introduced can thus be monitored by ensuring that the BVT constraint is satisfied for each value of α as it is varied from 0 to 1. In Fig. 23 we plot the variation of the work function Φ versus the correlation factor α for $r_s=2,2.5,3$ and 4. As may be observed from the figure, the work function for each value of r_s increases by approximately 1 eV as the system changes from a Pauli correlated to a fully correlated one. This increase in work function can be explained by the fact that the total energy of the system is reduced as correlation is intro-

duced. The energy of the Fermi electrons is thus also reduced and therefore the energy required for an electron to escape must increase. The variation of the surface dipole barrier $\Delta\phi$ versus the correlation factor is plotted in Fig. 24. Note that $\Delta\phi$ decreases as correlation effects are enhanced. This decrease, which is about 0.2 eV, is a consequence of the fact that the work function has increased. There is thus less electronic spillover and therefore a decrease in the value of the double layer. The decrease in $\Delta\phi$ may also be explained on the basis of the mathematical statement of the BVT. As more and more correlation is introduced, ΔV decreases, and since ΔV can be a large fraction of the surface dipole barrier, $\Delta\phi$ too must decrease.

The effect of introducing correlation on the surface energy may be best understood by considering the LDA results of Lang and Kohn. These values are also plotted in Fig. 22. As may be observed from the figure, the introduction of correlation increases the surface energy. This is so because correlation lowers the total energy of the crystal, and thus the work required to split it into two must increase.

In conclusion we note that we have studied the surface properties of an inhomogeneous HF gas. We have derived results for the exact surface exchange energy for the accurate set of single-particle wave functions generated by the linear potential model, and demonstrated the convergence of the LDA value of this property as the density profile is

made more slowly varying. Furthermore, we have shown that the surface exchange energy changes by many orders of magnitude as the density profile is changed from one which is slowly varying to one which is rapidly varying. We have also derived rigorous upper bounds for the total surface energy of a HF gas and obtained accurate results for the work function by application of the BVT. In addition, we have plotted the variation of the surface properties of a HF system as correlation is gradually introduced. We have shown that, as must be the case, the introduction of correlation has the effect of increasing the work function, decreasing the surface dipole barrier, and increasing the total surface energy.

APPENDIX A

In this appendix we present the integral expressions involving the Airy functions.

$$\int A_i^2(y)\,dy = y A_i^2(y) - A_i'^2(y)$$

$$\int A_i(y) B_i(y)\,dy = y A_i(y) B_i(y) - A_i'(y) B_i'(y)$$

$$\int y A_i^2(y)\,dy = \frac{1}{3}\left\{ y^2 A_i^2(y) - y A_i'^2(y) + A_i(y) A_i'(y) \right\}$$

$$\int y A_i(y) B_i(y)\,dy = \frac{1}{3}\left\{ y^2 A_i(y) B_i(y) - y A_i'(y) B_i'(y) + \right.$$
$$\left. + \frac{1}{2} A_i(y) B_i'(y) + \frac{1}{2} A_i'(y) B_i(y) \right\}$$

$$\int A_i'^2(y)\,dy = \frac{1}{3}\left\{ 2 A_i(y) A_i'(y) + y A_i'^2(y) - y^2 A_i^2(y) \right\}$$

$$\int A_i'(y) B_i'(y)\,dy = \frac{1}{3}\left\{ A_i(y) B_i'(y) + A_i'(y) B_i(y) - \right.$$
$$\left. - y^2 A_i(y) B_i(y) + y A_i'(y) B_i'(y) \right\}$$

$$\int y^2 A_i^2(y)\,dy = \frac{1}{5}\left\{ y^3 A_i^2(y) - y^2 A_i'^2(y) + 2y A_i(y) A_i'(y) - A_i'^2(y) \right\}$$

$$\int y^2 A_i(y) B_i(y)\,dy = \frac{1}{5}\left\{ y^3 A_i(y) B_i(y) - y^2 A_i'(y) B_i'(y) + y A_i(y) B_i'(y) + \right.$$

$$\left. + y A_i'(y) B_i(y) - A_i(y) B_i(y) \right\}$$

$$\int y A_i'^2(y)\,dy = -\frac{1}{5}\left\{ y^3 A_i^2(y) - y^2 A_i'^2(y) - 3y A_i(y) A_i'(y) + \frac{3}{2} A_i^2(y) \right\}$$

$$\int y A_i'(y) B_i'(y)\,dy = -\frac{1}{5}\left\{ y^3 A_i(y) B_i(y) - y^2 A_i'(y) B_i'(y) - \right.$$

$$\left. - \frac{3}{2}\left[y A_i(y) B_i'(y) + y A_i'(y) B_i(y) - A_i(y) B_i(y) \right] \right\}$$

APPENDIX B

In order to prove the equivalence of the Sugiyama sum rule to the charge neutrality condition, we consider the integral $\int q\delta(q)dq$ of Eq. 3.9. Partial integration yields

$$\int_0^1 q\,\delta(q)dq = 1/2 \int_0^1 dq(1-q^2)\delta'(q)$$

$$= 1/4 \int_0^1 dq(1-q^2)\sin 2\delta(q)/q$$

$$+ 1/2 \int_0^1 dq(1-q^2)qK'(q)/[1+q^2K^2(q)] \qquad (B.1)$$

where we have used the fact that $\delta(0)=0$. From the definition of K(q) (Eq. 3.3), and the identities

$$M(\zeta_b) = Wr(Ai,Bi)/Y(\zeta_b) = 1/[\pi\, Y(\zeta_b)] \qquad (B.2)$$

$$d/[X(\zeta_b)/Y(\zeta_b)]/dq = -\zeta_o/[\pi\, \zeta_b Y^2(\zeta_b)] \qquad (B.3)$$

where Wr(Ai,Bi) is the Wronskian of the Airy functions (91), the derivative $K'(q)=dK(q)/dq$ may be determined so that

$$\int_0^1 q\,\delta(q)dq = -2y_F/15 + 1/4 \int_0^1 dq(1-q^2)\sin 2\delta(q)/q$$

$$- y_F/2 \int_0^1 dq(1-q^2)q^2M^2(\zeta_b)/[\zeta_b^{1/2}\, A(-\zeta_o)]. \qquad (B.4)$$

Using the identity

$$\sin 2\delta(q)/2q = y_F^{1/3}\, M(-\zeta_o)N(-\zeta_o)/\, \Lambda(-\zeta_o), \qquad (B.5)$$

in Eq. B.4 leads to an expression for y_a of Eq. 3.9 which is precisely the same as that of Eq. 3.10, thereby demonstrating that the sum rule and charge neutrality condition are indeed indentical for the FLP model.

APPENDIX C

Consider a jellium of length 2L centered about the origin. The VBT approximation may then be stated as

$$\lim_{L\to\infty} [V_{es}(0)-V_{es}(L)]-[V_{es}(0)-V_{es}(L)] = 0(<L^{-1}).$$

Next consider this slab to be bounded by infinite potential barriers at $\pm$ L' at which points the density vanishes and where L' differs from L by $3\pi/8k_F$. For this model potential, the surface electronic density obtained by a summation over the discrete allowed momenta normal to the surface differs from the value obtained in the continuous case by a term of $0(L'^{-2}) \sim 0(L^{-2})$. On substitution of this density into Eq. 2.22 for the electrostatic potential one obtains that

$$V_{es}(L) = \lim_{L\to\infty} V_{es}(L) + 0(L^{-2}).$$

Thus the VBT condition is reduced to requiring that the electrostatic potential approaches its bulk value faster than L^{-1} as $L \to \infty$. The same arguments may be extended to the case of arbitrary effective potential at the surface if the length L' is considered as the point at which the density is negligible. Since the overall system must be charge neutral, this length can differ from the jellium edge position by only a small amount, and thus the difference between

the electrostatic potential at the surface and its asymptotic value is of $O(L^{-2})$.

Now from Eq. 3.14, the expression for the electrostatic potential $V_{es}(y)$ for large negative y is

$$V_{es}(y)/y_F = 1/\pi + K(0)/2 + y/2 + I/\pi \qquad (C.1)$$

where

$$I = \int_0^1 dq(1-q^2)\sin^2[qy+\delta(q)]/q^2$$

$$= I_1 + I_2 + I_3 + I_4. \qquad (C.2)$$

The asymptotic forms of the integrals I_1, I_2 and I_3 as $y \to -\infty$ are

$$I_1 = \int_0^1 dq(1-q^2)\sin^2 qy/q^2 = -1 - \pi y/2 + O(y^{-2}), \qquad (C.3)$$

$$I_2 = \int_0^1 dq(1-q^2)\sin^2\delta(q)\cos 2qy/q^2 \sim O(y^{-2}), \qquad (C.4)$$

and

$$I_3 = -1/2 \int_0^1 dq \sin 2\delta(q)\sin 2qy$$

$$= 1/4 \sin 2\delta(1)\cos 2y/y + O(y^{-2}). \qquad (C.5)$$

The asymptotic forms of the integrals I_2 and I_3 are obtained by integrating twice by parts and employing the fact that $[(1-q^2)\sin^2\delta(q)]/q^2$ and $\sin 2\delta(q)$ and their first derivatives are continuous and finite for $0 \leq q \leq 1$, and that their second derivatives can thus have, at worst, integrable singularities. We write the integral I_4 as a sum of integrals over two intervals as follows:

$$I_4 = \int_0^1 dq\ \sin 2\delta(q)/2q\ \sin 2qy/q$$

$$I_4 = \int_0^{\epsilon} dq\ \sin 2\delta(q)/2q\ \sin 2qy/q \qquad \text{(C.6)}$$
$$J_0 \quad J_\epsilon \qquad\qquad I_{41} \quad I_{42}$$

where $\epsilon = |y|^{-1/\alpha}$ with $\alpha > 2$. Thus as $y \to -\infty$, $\epsilon \to 0$, $|\epsilon y| \to \infty$, $|\epsilon^{-2}y^{-2}| < |y^{-1}|$, and $|\epsilon^{-1}y^{-2}| < |y^{-1}|$. Since $\sin 2\delta(q)/2q$ is continuous we can then write I_{41} as

$$I_{41} = \sin 2\delta(\epsilon)/(2\epsilon)|_{\epsilon\to 0}\ \mathrm{Si}(2\epsilon y)$$

$$= \sin 2\delta(\epsilon)/(2\epsilon)\Big|_{\epsilon\to 0} \left\{-\frac{\pi}{2} - \frac{\cos 2\epsilon y}{2\epsilon y} + O(y^{-2})\right\} \qquad \text{(C.7)}$$

where $\mathrm{Si}(x) = \int(\sin p/p)dp$ is the sine integral. To solve for I_{42} we integrate by parts and expand the sine integral to obtain

$$I_{42} = \left\{\frac{\sin 2qy}{(2qy)^2}\left[-\frac{\sin 2\delta(q)}{2q} + q\frac{d}{dq}\left(\frac{\sin 2\delta(q)}{2q}\right)\right]\right\}_\epsilon^1$$

$$-\left\{\frac{\sin 2\delta(q)}{2q}\,\frac{\cos 2qy}{2qy}\right\}_{\epsilon}^{1}+L+J \tag{C.8}$$

where L and J are defined below. The first term of Eq. C.8 has the asymptotic form $\sim O(y^{-2})+O(\epsilon^{-1}y^{-2})+O(\epsilon^{-1}y^{-2})$ which from our choice of α goes as $O(<y^{-1})$. The integral L is

$$L=\frac{1}{(2y)^2}\int_{\epsilon}^{1}dq\,\frac{\sin 2qy}{q}\,\frac{d^2}{dq^2}\left(\frac{\sin 2\delta(q)}{2q}\right) \tag{C.9}$$

so that

$$|L|\leq\frac{1}{4\epsilon y^2}\int_{\epsilon}^{1}dq\,\left|\sin 2qy\,\frac{d^2}{dq^2}\left(\frac{\sin 2\delta(q)}{2q}\right)\right| \tag{C.10}$$

from the triangle inequality or since $\epsilon^{-1}\geq q^{-1}$. The integrand of inequality Eq. C.10 has, at worst, integrable singularities so that $|L| \sim O(\epsilon^{-1}y^{-2})=O(<y^{-1})$ as $y\to\pm\infty$. The last term of Eq. C.8 is

$$J=\frac{1}{2y^2}\int_{\epsilon}^{1}dq\,\frac{\sin 2qy}{q^2}\,\frac{d}{dq}\left(\frac{\sin 2\delta(q)}{2q}\right) \tag{C.11}$$

so that

$$|J|\leq\frac{1}{2y^2}\left\{\operatorname*{Max}_{[0,1]}\frac{d}{dq}\left(\frac{\sin 2\delta(q)}{2q}\right)\right\}\int_{\epsilon}^{1}dq\,\frac{1}{q^2}$$

$$\underset{y\to\pm\infty}{\sim} O(\epsilon^{-1}y^{-2})-O(y^{-2})=O(<y^{-1}). \tag{C.12}$$

Thus

$$I_4 = - \pi/2 \sin 2\delta(\varepsilon)/(2\varepsilon)|_{\varepsilon \to 0} - \sin 2\delta(1)/2 \cos 2y/2y \qquad (C.13)$$

and since $[\sin 2\delta(\varepsilon)/2\varepsilon]_{\varepsilon \to 0} = K(0)$ we have, on combining (C.3), (C.5) and (C.13), that

$$I = -1 - \pi y/2 - \pi K(0)/2 + 0(<y^{-1}). \qquad (C.14)$$

Further substitution of Eq. C.14 into Eq. C.1 yields, as y goes to $- \infty$,

$$V_{es}(y)/k_F \sim 0 + 0(<y^{-1}), \qquad (C.15)$$

thus demonstrating that the electrostatic potential generated by the FLP model conforms to the VBT requirement that it tends to its asymptotic value inside the medium faster than y^{-1}. We note, however, that although this property of the electrostatic potential has been derived for the FLP model, it also holds true for the step and linear potential models since only the phase shifts are different and factors involving them either vanish or are cancelled out.

APPENDIX B

For the model effective potential of Eq. 3.1 the three constraints of the BVT, self-consistency of $\Delta\phi$ and charge neutrality can be satisfied exactly for all $r_s \leq 4.3$. For a given density in the present calculations, the jellium edge position y_a is determined by the charge neutrality condition, the barrier height parameter y_b by the self-consistency of $\Delta\phi$ and the field strength or slope parameter y_F by the constraint set on the electrostatic potential by the BVT. The values of the barrier height and slope parameters thus determined are, however, unique in that precisely the same values are obtained when the barrier height is adjusted to satisfy the BVT and the field strength varied till the dipole barrier is self-consistent. In Fig. 10 we plot the variation of the universal function $\Delta\phi / k_F$ versus the slope parameter y_F (for self-consistently obtained barrier height parameter y_b) with the value of r_s for a specific y_F determined via the BVT. This graph differs from the universal curves of Fig. 3 in that now a specific constraint, viz the BVT, is being applied to relate the slope parameter to the density. The non-linear relationship between r_s and y_F through the sum rule, and the corresponding variation of the self-consistent y_b versus y_F are plotted in Fig. 11. Thus, for a given density, it is possible to determine from these graphs the value of the slope parameter y_F which satisfies the BVT, the self-consistently determined barrier height

parameter y_b, and the corresponding value of the surface dipole barrier for this choice of y_F.

For $r_s>4.3$ no choice of parameters can satisfy all three constraints simultaneously. However, it is possible to satisfy the two requirements of self-consistency of the barrier height and charge neutrality exactly for all lower densities since at $r_s=4.3$ the model effective potential employed changes continuously to the step potential model. The self-consistency procedure for this potential is particularly straightforward since analytic expressions for both the surface dipole barrier and jellium edge position as functions of the barrier height parameter $\beta=k_F/(2V)^{1/2}$ have been derived (34). As the density is decreased, the self-consistently obtained barrier height increases till in the limit of vanishing density the potential reduces to the infinite barrier model. In Fig. 12 we plot the variation of the universal function $\Delta\phi/k_F$ for the step model versus the barrier height parameter β . The corresponding non-linear relationship between the density and self-consistent barrier height is also given in the same graph. It is evident from this figure that one may substitute infinite barrier model results for very low densities without giving rise to any significant error.

APPENDIX E

As indicated in Chap. V, the single-particle wave function constituting the trial wave function ψ_{0T} are of the form

$$\psi_{\vec{k}}(\vec{r}_i) = {}_k(x_i)\ \exp[i(k_y y_i + k_z z_i)], \tag{E.1}$$

where the $\psi_k(x_i)$ are chosen to be those generated by the LP model. Thus

$$\psi_k(x_i) = \begin{cases} (2/L)^{1/2}\ \sin[kx_i+\delta(k)] & \text{for} \quad x_i \leq 0 \\ (2/L)^{1/2}\ \sin\delta\, Ai(\zeta_i)/Ai(-\zeta_o) & \text{for} \quad x_i \geq 0 \end{cases} \tag{E.2}$$

where $\zeta_i = x_i k_F y_F^{-1/3} - \zeta_o$, $\zeta_o = y_F^{2/3} k^2/k_F^2$, y_F is the slope parameter and $\delta(k)$ the phase shift as defined is Chap. IV.

Defining $g_i(x_i) = df(x_i)/dx_i$, the differential equation 5.21 for the components of the auxiliary function reduces to a first order differential equation

$$\frac{dg_i}{dx_i} + \frac{2g_i(x_i)}{\psi_k(x_i)} \frac{d\psi_k}{dx_i} = \delta(x_i - x). \tag{E.3}$$

We label the regions coresponding to $x_i \geq 0$ and $x_i \leq 0$ as I and II respectively. Since Eq. 5.21 is a second order differential equation and as there are two regions of space to be considered, we apply the folowing boundary conditions for

its solution :

(a) the functions $g_i^I(x_i)$ and $g_i^{II}(x_i)$ be continuous at $x_{i=0}$

(b) the functions $f_i^I(x_i)$ and $f_i^{II}(x_i)$ be continuous at $x_{i=0}$

(c) the auxiliary function and thus each component of it vanish far outside the surface so that these is no contribution to the correction term from there i.e.

$$\lim f_i^I(x_i)\psi_k(x_i) = 0$$

(d) that $f_i^{II}(x_i)\psi_k^2(x_i)$ oscillate and vanish about zero as x_i goes to $-\infty$.

This last condition ensures that the contribution of $f_i(x_i)\psi_k^2(x_i)$ to the correction term $\rho_1(x)$ is merely a constant, thus permitting the elimination of the $\overline{\delta V}_i$ term in Eq. 5.15 since the latter vanishes as x^{-1} as x goes to $-\infty$.

Consider first region I. Substituting $\psi_k(x_i)$ from Eq. E.1 into Eq. E.3 we have

$$\frac{dg_i}{dx_i} + 2\, g_i(\beta_i)\frac{A_i'(\beta_i)}{A_i(\beta_i)} = \delta(\beta_i - \beta) \qquad (E.4)$$

The integral factor (IF) of the above differential equation is

$$IF = e^{\int_0^{x_i} dx_i' \, 2\frac{A_i'(\beta_i')}{A_i(\beta_i')}} = \frac{A_i^2(\beta_i)}{A_i^2(-\beta_0)} \qquad (E.5)$$

Multiplying both side of Eq. E.4 by the IF and integrating we obtain

$$g_i^I \frac{A_i^2(\vartheta_i)}{A_i^2(-\vartheta_0)} = \int_{-\vartheta_0}^{\vartheta_i} d\vartheta_i' \frac{A_i^2(\vartheta_i')}{A_i^2(-\vartheta_0)} \delta(\vartheta_i' - \vartheta) + C_I$$

$$= \frac{A_i^2(\vartheta)}{A_i^2(-\vartheta_0)} \theta(\vartheta_i - \vartheta) + C_I \qquad \text{(E.6)}$$

so that

$$g_i^I(\vartheta_i) = \frac{A_i^2(\vartheta)}{A_i^2(\vartheta_i)} \theta(\vartheta_i - \vartheta) + C_I \frac{A_i^2(-\vartheta_0)}{A_i^2(\vartheta_i)} \qquad \text{(E.7)}$$

The function $f_i^I(x_i)$ may be determined by substituting $g_i^I(x_i)$ into the expression

$$f_i^I(x_i) = \int_0^{x_i} g_i^I(x_i')\, dx_i' + C_I' \qquad \text{(E.8)}$$

and noting that

$$\frac{d}{d\vartheta_i}\left[\frac{B_i(\vartheta_i)}{A_i(\vartheta_i)}\right] = \frac{A_i B_i' - B_i A_i'}{A_i^2} = \frac{W\{A_i, B_i\}}{A_i^2} = \frac{1}{\pi^2 A_i^2} \qquad \text{(E.9)}$$

where W{Ai,Bi} is the Wronskian of the Airy functions Ai and Bi. Thus

$$f_i^I(\vartheta_i) = \pi k_F^{-1} \mu_F^{1/3} \left\{ A_i^2(\vartheta) \left[\frac{B_i(\vartheta_i)}{A_i(\vartheta_i)} - \frac{B_i(\vartheta)}{A_i(\vartheta)}\right] \theta(\vartheta_i - \vartheta) \right. \qquad \text{(E.10)}$$

$$+ C_I A_i^2(-\zeta_0)\left[\frac{B_i(\zeta_i)}{A_i(\zeta_i)} - \frac{B_i(-\zeta_0)}{A_i(-\zeta_0)}\right]\Bigg\} + C_I'$$

For the solution of Eq. E.3 in region II we make a change of variables to $y_i = k_F x_i$ and $k = k_F q$. Thus Eq. E.3 may be written as

$$\frac{dg_i^{II}}{dy_i} + 2q\cot(qy_i+\delta)\, g_i^{II}(y_i) = \delta(y_i - y) \qquad (E.11)$$

and its solution is

$$g_i^{II}(y_i) = -\frac{\sin^2(qy+\delta)}{\sin^2(qy_i+\delta)}\,\theta(y-y_i) + C_{II}\frac{\sin^2\delta}{\sin^2(qy_i+\delta)} \qquad (E.12)$$

Integrating Eq. E.12 we obtain

$$f_i^{II}(y_i) = \frac{\sin^2(qy+\delta)}{k_F q}\Big\{\cot(qy_i+\delta) - \cot(qy+\delta)\Big\}\theta(y-y_i) \qquad (E.13)$$

$$- C_{II}\frac{\sin^2\delta}{k_F q}\Big\{\cot(qy_i+\delta) - \cot\delta\Big\} + C_{II}'$$

where C_{II}' is the constant of intrgration. We next apply the boundary conditions (BC) in order to determine the various constants in the above expressions. On application of BC (c) we have

$$C_I = -Ai^2(\zeta)/Ai^2(-\zeta_0), \qquad (E.14)$$

where the continuity of the g_i functions leads to

$$C_{II} = \frac{\sin^2(qy+\delta)}{\sin^2\delta}\,\theta(y) - \frac{A_i^2(\xi)}{A_i^2(-\xi_0)}\,\theta(\xi+\xi_0) \tag{E.15}$$

Next the application of BC (d) yields

$$C'_{II} = \frac{1}{2k_F q}\left\{\sin 2(qy+\delta) - C_{II}\sin 2\delta\right\} \tag{E.16}$$

and finally, the requirement of the continuity of the f_i functions gives rise to

$$C'_I = \frac{\sin^2(qy+\delta)}{k_F q}\left\{\cot\delta - \cot(qy+\delta)\right\}\theta(y) \tag{E.17}$$

$$- \pi k_F^{-1} y_F^{1/3} A_i^2(\xi)\left\{\frac{B_i(-\xi_0)}{A_i(-\xi_0)} - \frac{B_i(\xi)}{A_i(\xi)}\right\}\theta(-\xi_0-\xi)$$

$$+ C'_{II}$$

Substitution of Eqs. E.14-E.17 into Eqs. E.10 and E.13 yields Eq. 5.23.

APPENDIX F

In the determination of the surface exchange energy within the LP approximation we follow the method of Harris and Jones (66), and Mahan (113). However, in our calculations we consider a semi-infinite lattice and not a finite box as have these other authors. The normalization constants are thus the same as in Chap. IV. Another consequence of considering a semi-infinite lattice is that we no longer require to make an Euler-Maclaurin expansion in our calculations in order to obtain the various surface contributions to the energy.

The exchange energy is defined as

$$E_x = -\frac{1}{4}\int d\vec{r}\int d\vec{r}'\,\frac{1}{|\vec{r}-\vec{r}'|}\,|\rho(\vec{r},\vec{r}')|^2 \qquad \text{(F.1)}$$

where $\rho(\vec{r},\vec{r}')=2\sum_{\vec{k}}\psi_{\vec{k}}(\vec{r})\psi^*_{\vec{k}}(\vec{r}')$ is the single-particle density matrix. The general form of the single-particle wave function within the jellium approximation is

$$\psi_{\vec{k}}(\vec{r}) = \psi_k(x)\,\exp[i(\vec{k}_{\parallel}\cdot\vec{x}_{\parallel}], \qquad \text{(F.2)}$$

where $\vec{k}_{\parallel}$ and $\vec{x}_{\parallel}$ are the electronic momentum and position vectors in a plane parallel to the surface, and k and x the corresponding quantities perpendicular to the surface. With

a change of variables to $\vec{P}=\vec{k}_{\parallel}-\vec{k}_{\parallel}'$, $\vec{R}=\vec{x}_{\parallel}-\vec{x}_{\parallel}'$, and $X=x-x'$, substitution of Eq. F.2 into F.1 leads to

$$E_x=-\frac{1}{4}\int dx\int dx'\,\psi_k^*(x)\psi_{k'}^*(x)\psi_k(x')\psi_{k'}(x')\int d\vec{x}_{\parallel}\int d\vec{x}_{\parallel}'\frac{e^{i\vec{P}\cdot\vec{R}}}{\sqrt{X^2+R^2}} \qquad (F.3)$$

We first consider the integral

$$I=\int d\vec{x}_{\parallel}\frac{e^{i\vec{P}\cdot\vec{R}}}{\sqrt{X^2+R^2}}=\int_0^{\infty}R\,dR\int_{-\pi}^{+\pi}d\theta\,\frac{e^{iPR\cos\theta}}{\sqrt{X^2+R^2}} \qquad (F.4)$$

$$=2\pi\int_0^{\infty}R\,dR\,\frac{J_0(PR)}{\sqrt{X^2+R^2}}$$

where J_0 is the zeroth order Bessel function of the first kind. With a change of variable to $s=[1+(R^2/X^2)]^{1/2}$ we have

$$I=2\pi X\int_1^{\infty}ds\,J_0(PX\sqrt{s^2-1})=2\pi X\sqrt{\frac{2}{\pi}}\frac{K_{\frac{1}{2}}(PX)}{\sqrt{PX}} \qquad (F.5)$$

$$=\frac{2\pi}{P}e^{-PX}$$

where $K_{1/2}=(\pi/2z)^{1/2}\exp(-z)$ is the half integer modified Bessel function of the second kind. The integral of Eq. F.5 is given in Gradshteyn and Ryzhik (115). Thus, with the definition $P^2=[(k_y-k_y')^2+(k_z-k_z')^2]$, and $k_x=k$, $k_x'=k'$ we have

$$E_x=-\frac{2\pi}{A}\sum_{\vec{k}_{\parallel},k}\sum_{\vec{k}_{\parallel}',k'}\theta(\epsilon_F-\epsilon_{\vec{k}_{\parallel},k})\,\theta(\epsilon_F-\epsilon_{\vec{k}_{\parallel}',k'})\cdot G(P,k,k') \qquad (F.6)$$

where

$$G(P,k,k') = \frac{1}{P}\int_{-\infty}^{+\infty} dx \int_{-\infty}^{+\infty} dx'\; e^{-P|x|}\, \psi_k^*(x)\psi_k^*(x')\psi_{k'}(x)\psi_{k'}(x') \qquad (F.7)$$

Now it can be shown that (66,113)

$$\sum_{\vec{k}_{\parallel}} \sum_{\vec{k}'_{\parallel}} \theta(\epsilon_F - \epsilon_{\vec{k}_{\parallel}})\,\theta(\epsilon_F - \epsilon_{\vec{k}'_{\parallel}}) = \frac{A^2}{(2\pi)^3}\int_0^{2k_F} dP\, P\, H(P,k,k') \qquad (F.8)$$

where

(F.9)

$$H(P,k,k') = \begin{cases} \pi\,(k'^2 - k^2) & \text{for } \gamma^2 \geq k_F^2 - k'^2 \text{ and } \gamma > 0 \\ \pi\left[(k_F^2 - k'^2) + (k_F^2 - k^2)\right] & \text{for } \gamma^2 \geq k_F^2 - k'^2 \text{ and } \gamma < 0 \\ -2\left[(k_F^2 - k'^2)\sin^{-1}\dfrac{\gamma}{\sqrt{k_F^2 - k'^2}} + \gamma\sqrt{k_F^2 - k'^2 - \gamma^2}\right] + \pi(k_F^2 - k^2) & \text{for } \gamma^2 < k_F^2 - k'^2 \end{cases}$$

$$\gamma = \frac{1}{2P}(P^2 + k^2 - k'^2)$$

Thus Eq. F.6 can be expressed as

$$E_x = -A/(2\pi)^2 \sum_{kk} \int_0^{2k_F} PH(P,k,k')G(P,k,k')dP. \qquad (F.10)$$

For the determination of G(P,k,k') of Eq. F.7 we employ the

single-particle wave functions generated by the linear potential model (Eq. 6.5). Defining

$$g(P,k,k') = G(P,k,k')/B^4 \ , \tag{F.11}$$

where B is the normalization constant, we rewrite Eq. F.10 as

$$E_x = -A/(2\pi)^2 \sum_k B^2 \sum_k B^2 \int_0^{2k_F} PH(P,k,k')g(P,k,k')dP. \tag{F.12}$$

Since

$$\sum_k = L/\pi \int_0^{k_F} dk, \tag{F.13}$$

we have

$$\sum_k B^2 = 2/\pi \int_0^{k_F} dk, \tag{F.14}$$

so that we now have

$$E_x = -A/\pi^4 \int_0^{2k_F} dP \int_0^{k_F} dk \int_0^{k_F} dk' PH(P,k,k')g(P,k,k'). \tag{F.15}$$

In order to determine $g(P,k,k')$ we split this integral into three parts corresponding to the contributions for $x \geq 0$ (region 1), $x \leq 0$ (region2), and the cross terms, thus

$$g(P,k,k')=g^{(1)}(P,k,k')+g^{(2)}(P,k,k')+g^{(12)}(P,k,k'), \qquad (F.16)$$

where the superscripts (1), (2), and (3) correspond to contributions from the different regions and the cross term respectively. For the calculation of region 1 we have

$$g^{(1)}(P,k,k') = \frac{1}{P}\frac{1}{B^4}\int_0^\infty dx \int_0^x dx' \, e^{-P|x|} \psi_k^*(x)\psi_{k'}^*(x)\psi_k(x')\psi_{k'}(x') . \qquad (F.17)$$

For the LP model wave functions the indefinite integrals in $g^{(1)}$ cannot be done analytically since they involve products of Airy functions of different arguments and hence must be performed numerically. Thus the contribution to E_x from region 1 requires a five fold numerical computation. However, $g^{(1)}$ can be obtained entirely analytically for the wave functions of the step potential model. Next we have

$$g^{(2)}(P,k,k') = \frac{1}{P}\frac{1}{B^4}\int_{-\infty}^0 dx \int_{-\infty}^0 dx' \, e^{-P|x|} \psi_k^*(x)\psi_{k'}^*(x) \cdot \psi_k(x')\psi_{k'}(x') . \qquad (F.18)$$

In performing the the above integrals we replace the lower limit by -L and then take the limlt as L goes to ∞ at a later stage of the calculation. Thus we obtain

(F.19)

$$g^{(2)}(P,k,k') = \frac{L}{4}\left(\frac{1}{P^2+k_-^2}+\frac{1}{P^2+k_+^2}\right)+\frac{1}{8(P^2+k_+^2)}\left\{\frac{1}{k_+}\left[\sin 2\delta_+ + \sin 2(k_+L-\delta_+)\right]\right.$$

$$\left.-\frac{1}{k}\left[\sin 2\delta + \sin 2(kL-\delta)\right]-\frac{1}{k'}\left[\sin 2\delta' + \sin 2(k'L-\delta')\right]\right\}+$$

$$+\frac{1}{8(P^2+k_-^2)}\left\{\frac{1}{k_-}\left[\sin 2\delta_- + \sin 2(k_-L-\delta_-)\right]-\frac{1}{k}\left[\sin 2\delta +\right.\right.$$

$$\left.\left.+\sin 2(kL-\delta)\right]-\frac{1}{k'}\left[\sin 2\delta' + \sin 2(k'L-\delta')\right]\right\}+$$

$$+\frac{1}{4P}\left[\frac{k_-\sin\delta_-}{P^2+k_-^2}-\frac{k_+\sin\delta_+}{P^2+k_+^2}\right]^2-\frac{P}{4}\left[\frac{\cos\delta_-}{P^2+k_-^2}-\frac{\cos\delta_+}{P^2+k_+^2}\right]^2$$

where $k_\pm = k \pm k'$, $\delta_\pm = \delta \pm \delta'$, $\delta = \delta(k)$, and $\delta' = \delta(k')$. This expression is of course the same for the step, linear, and finite linear potential models since in region 2 the wave functions are in all cases simply oscillatory functions. Only the explicit values for the phase shift are different. Finally we have

$$g^{(12)}(P,k,k') = \frac{2}{P}\frac{1}{B^4}\int_0^\infty dx\, e^{-Px}\,\psi_k(x)\psi_{k'}(x)\cdot\int_{-\infty}^0 dx'\, e^{Px'}\cdot \qquad (F.20)$$

$$\cdot\,\psi_k(x')\psi_{k'}(x').$$

The contribution from region 2 to the above integral is easily obtained and is the same for all the model potentials. Thus

$$\frac{1}{B^2}\int_{-\infty}^{0} dx' \, e^{px'} \psi_k(x')\psi_{k'}(x') = \frac{1}{2(p^2+k_-^2)}(p\cos\delta_- + k_-\sin\delta_-) \qquad (F.21)$$

$$- \frac{1}{2(p^2+k_+^2)}(p\cos\delta_+ + k_+\sin\delta_+)$$

For the LP model wave functions, the contribution from region 1 to Eq. F.20 cannot be done analytically. The integral can be performed for the step model. Thus the contribution of $g^{(12)}$ to E_x for the former set of wave functions reduces to a four fold integral. Corresponding to regions 1, and 2, and the cross term contributions, we then write

$$E_x = E_x^{(1)} + E_x^{(2)} + E_x^{(12)}, \qquad (F.22)$$

where

$$E_x^{(1)} + E_x^{(12)} = -\frac{A}{\pi^4}\int_0^{2k_F} dp \int_0^{k_F} dk \int_0^{k_F} dk' \; p\,H(p,k,k') \cdot \qquad (F.23)$$

$$\cdot \left[g^{(1)}(p,k,k') + g^{(12)}(p,k,k')\right]$$

Eq. F.23 cannot be simplified any further. However,

$$E_x^{(2)} = -\frac{A}{\pi^4}\int_0^{2k_F} dp \int_0^{k_F} dk \int_0^{k_F} dk' \; p\,H(p,k,k')\, g^{(2)}(p,k,k') \qquad (F.24)$$

can be further simplified. Substituting Eq. F.19 into Eq. F.24 we have

$$E_x^{(2)} = K + J + I, \tag{F.25}$$

where

$$K = -\frac{AL}{4\pi^4}\int_0^{2k_F} dP \int_0^{k_F} dk \int_0^{k_F} dk'\, P\, H(P,k,k') \left\{ \frac{1}{P^2+k_+^2} + \frac{1}{P^2+k_-^2} \right\} \tag{F.26}$$

$$\begin{aligned} J = -\frac{A}{4\pi^4}\int_0^{2k_F} dP \int_0^{k_F} dk \int_0^{k_F} dk'\, P\, H(P,k,k') \Bigg\{ & \frac{1}{P^2+k_+^2}\left(\frac{\sin 2\delta_+}{2k_+} - \frac{\sin 2\delta}{2k} - \frac{\sin 2\delta'}{2k'}\right) \\ & + \frac{1}{P^2+k_-^2}\left(\frac{\sin 2\delta_-}{2k_-} - \frac{\sin 2\delta}{2k} - \frac{\sin 2\delta'}{2k'}\right) + \frac{1}{P}\left(\frac{k_-\sin\delta_-}{P^2+k_-^2} - \frac{k_+\sin\delta_+}{P^2+k_+^2}\right)^2 \\ & - P\left(\frac{\cos\delta_-}{P^2+k_-^2} - \frac{\cos\delta_+}{P^2+k_+^2}\right)^2 \Bigg\} \end{aligned} \tag{F.27}$$

$$\begin{aligned} I = -\frac{A}{4\pi^4}\int_0^{2k_F} dP \int_0^{k_F} dk \int_0^{k_F} dk'\, P\, H(P,k,k') \Bigg\{ & \frac{1}{P^2+k_+^2}\left[\frac{\sin 2(k_+L-\delta_+)}{2k_+}\right. \\ & \left. - \frac{\sin 2(kL-\delta)}{2k} - \frac{\sin 2(k'L-\delta')}{2k'}\right] + \frac{1}{P^2+k_-^2}\left[\frac{\sin 2(k_-L-\delta_-)}{2k_-}\right. \\ & \left. - \frac{\sin 2(kL-\delta)}{2k} - \frac{\sin 2(k'L-\delta')}{2k'}\right] \Bigg\} \end{aligned} \tag{F.28}$$

The expression for the integrals K and J cannot be simplified any further and thus three fold integrals have to be performed to determine their contribution to E_x. However, the last integral I can be simplified in the limit as L goes to ∞ . We consider here only a typical term of I such as

$$I_6 \sim \int_0^{k_F} dk' \frac{H(P,k,k')}{P^2+k^2} \cdot \frac{\sin 2(k'L-\delta')}{2k'} \tag{F.29}$$

For $k\neq 0$, and L very large, $k'L \gg \delta'$, and $\sin 2(k'L-\delta')$ is a very rapidly oscillating functions. Thus the integral vanishes for all $k' \neq 0$ and the only contribution occurs when k' goes to 0. Thus we may write

$$I_6 \sim \int_0^{k_F} dk' \frac{H(P,k,0)}{P^2+k^2} \frac{\sin 2k'L}{2k'} \tag{F.30}$$

$$= \frac{H(P,k,0)}{2(P^2+k^2)} S_i(2k_FL)$$

Note that in the above expression we have dropped the δ' term. This is reasonable since $\lim_{k\to 0} \delta(k)=0$. Thus

$$\sin 2(kL-\delta) \underset{k\to 0}{\sim} \sin 2kL(1-2k^2) - k\cos 2kL \tag{F.31}$$

which with a change of variable to $2kL=x$ is

$$\sin 2(kL-\delta) \underset{\substack{k\to 0 \\ x\to 0}}{\sim} \sin x\left(1-\frac{x^2}{L^2}\right) - \frac{x}{L}\cos x \underset{\substack{x\to 0 \\ L\to\infty}}{\sim} \sin x \tag{F.32}$$

Therefore

$$I_6 \underset{L\to\infty}{\sim} \frac{H(P,k,0)}{2(P^2+k^2)} \frac{\pi}{2} \qquad (F.33)$$

Performing the integrals for the remaining terms in a similiar manner and employing the conditions $H(P,k,-k)=H(P,k,k)$ and $H(P,k_F,k_F)=0$ we have

$$I = -\frac{A}{(2\pi)^3}\int_0^{2k_F} dP \int_0^{k_F} dk\, P\left\{\frac{1}{P^2}H(P,k,k) - \frac{1}{P^2+k^2}\left[H(P,k,0)+H(P,0,k)\right]\right\} \qquad (F.34)$$

With the jellium edge defined at 'a', the volume of the crystal is

$$\Omega = (L+a)A = AL + Aa. \qquad (F.35)$$

Now it can be shown that the total exchange energy per unit volume for the uniform electron gas system is (66)

$$E_{x,b} = -\frac{1}{4\pi^4}\int_0^{2k_F} dP \int_0^{k_F} dk \int_0^{k_F} dk'\, P\, H(P,k,k')\left\{\frac{1}{P^2+k_+^2}+\frac{1}{P^2+k_-^2}\right\} = -\frac{3k_F}{4\pi}\bar{\rho} \qquad (F.36)$$

where $\bar{\rho}$ is the number of electrons per unit volume. The above integral is the same as that which appears in Eq. F.26 for K. Thus Eq. F.26 for K is

$$K = \Omega E_{x,b} - AaE_{x,b} \qquad (F.37)$$

and

$$E_x^{(2)} = \Omega E_{x,b} - AaE_{x,b} + J + I. \qquad (F.38)$$

Therefore the total (bulk + surface) exchange energy (Eq. F.22) is

$$E_x = \Omega E_{x,b} - AaE_{x,b} + J + I + E_x^{(1)} + E_x^{(12)}$$

$$= \Omega E_{x,b} + AE_{x,s}. \qquad (F.39)$$

The surface contribution to the exchange energy per unit area of the surface is then

$$E_{x,s} = -aE_{x,b} + [J+I+E_x^{(1)}+E_x^{(12)}]/A.$$

$$E_{x_s} = -\frac{3k_F}{4\pi}\bar{\rho}\,a - \frac{1}{4\pi^4}\int_0^{2k_F} dp \int_0^{k_F} dk \int_0^{k_F} dk'\; p\, H(p,k,k') \cdot \qquad (F.40)$$

$$\cdot \left\{ \frac{1}{p^2+k_+^2}\left(\frac{\sin 2\delta_+}{2k_+} - \frac{\sin 2\delta}{2k} - \frac{\sin 2\delta'}{2k'}\right) + \frac{1}{p^2+k_-^2}\left(\frac{\sin 2\delta_-}{2k_-} - \frac{\sin 2\delta}{2k} - \frac{\sin 2\delta'}{2k'}\right) \right.$$

$$\left. + \frac{1}{p}\left(\frac{k_- \sin\delta_-}{p^2+k_-^2} - \frac{k_+ \sin\delta_+}{p^2+k_+^2}\right)^2 - p\left(\frac{\cos\delta_-}{p^2+k_-^2} - \frac{\cos\delta_+}{p^2+k_+^2}\right)^2 \right\}$$

$$- \frac{1}{(2\pi)^3}\int_0^{2k_F} dp \int_0^{k_F} dk\; p \left\{ \frac{H(p,k,k)}{p^2} - \frac{H(p,k,0)+H(p,0,k)}{p^2+k^2} \right\}$$

$$-\frac{1}{\pi^4}\int_0^{2k_F} dP \int_0^{k_F} dk \int_0^{k_F} dk' \, H(P,k,k') \left\{ P \frac{\cos\delta_-}{P^2+k_-^2} - P \frac{\cos\delta_+}{P^2+k_+^2} + \right.$$

$$\left. + k_- \frac{\sin\delta_-}{P^2+k_-^2} - k_+ \frac{\sin\delta_+}{P^2+k_+^2} \right\} \frac{1}{B^2} \int_0^\infty dx \, e^{-Px} \psi_k(x) \psi_{k'}(x)$$

$$-\frac{1}{\pi^4}\int_0^{2k_F} dP \int_0^{k_F} dk \int_0^{k_F} dk' \, H(P,k,k') \frac{1}{B^4} \int_0^\infty dx \int_0^\infty dx' \, e^{-P|x-x'|} \cdot$$

$$\cdot \psi_k(x) \psi_k(x') \psi_{k'}(x) \psi_{k'}(x') .$$

Substituting the LP wave functions of Eq. 6.5 into the above equation and factoring out the k_F dependence by changing the variables to $y=xk_F$, $q=kk_F$, and $q'=k'k_F$ we obtain the universal function Eq. 6.8 of Chap. VI.

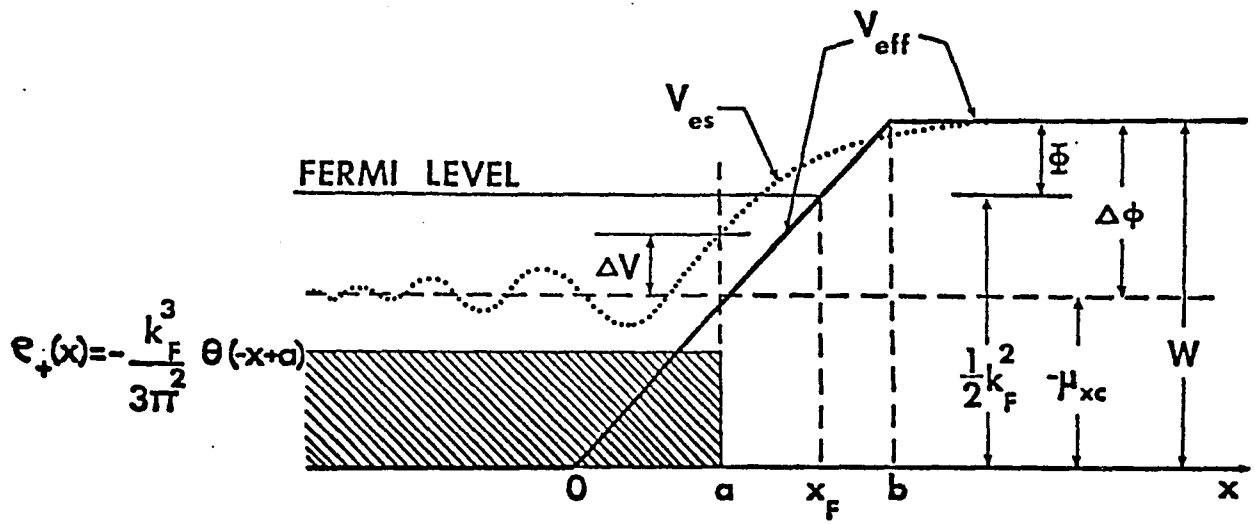

Fig. 1.

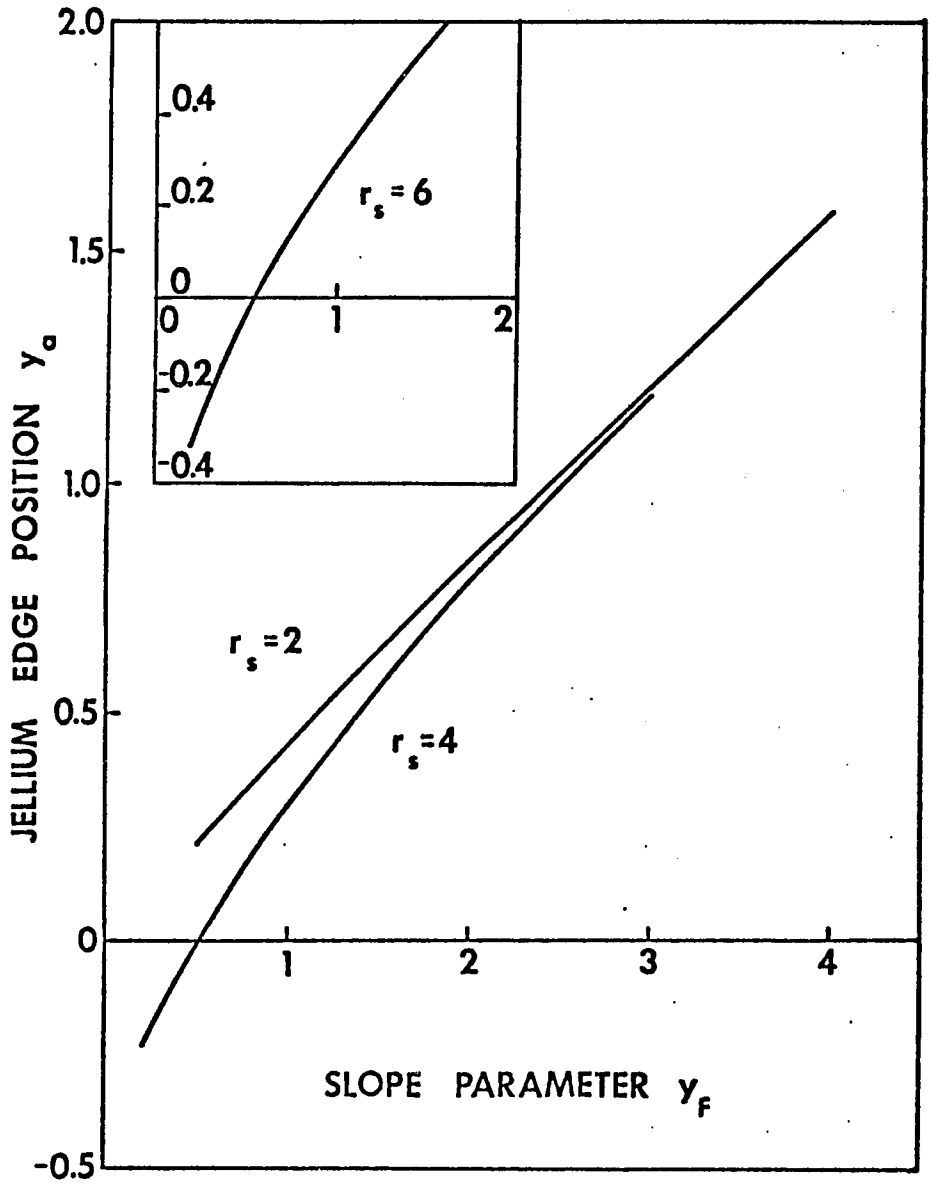
2.0
1.5
1.0
0.5
0
-0.5
JELLIUM EDGE POSITION y_a
0.4
0.2
0
-0.2
-0.4
0
1
2
$r_s = 6$
$r_s = 2$
$r_s = 4$
1
2
3
4
SLOPE PARAMETER y_F

Fig. 2.

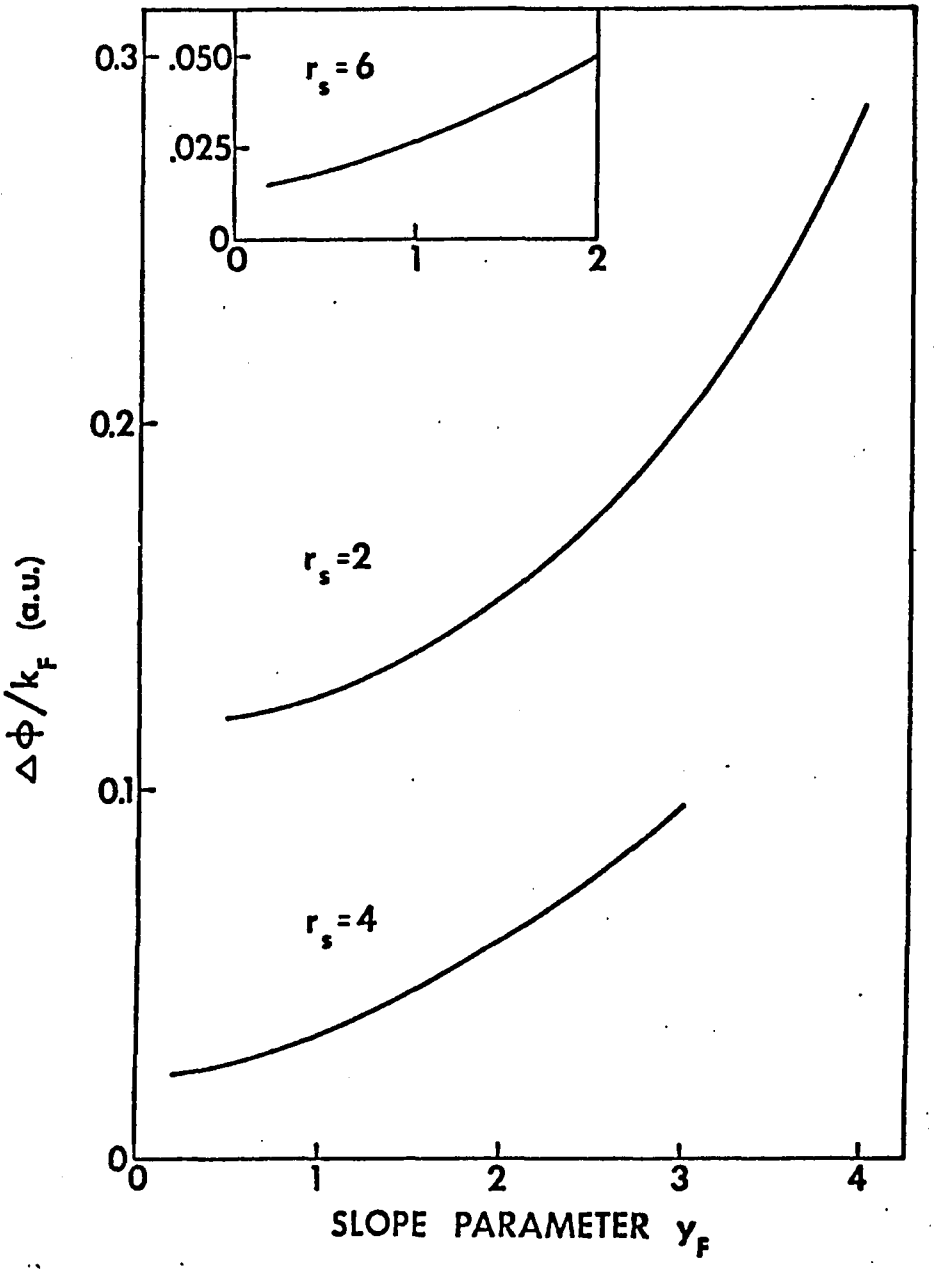
0.3
.050
.025
0
0
1
2
$r_s = 6$
0.2
$r_s = 2$
0.1
$r_s = 4$
0
0
1
2
3
4
$\Delta\phi/k_F$ (a.u.)
SLOPE PARAMETER y_F

Fig. 3.

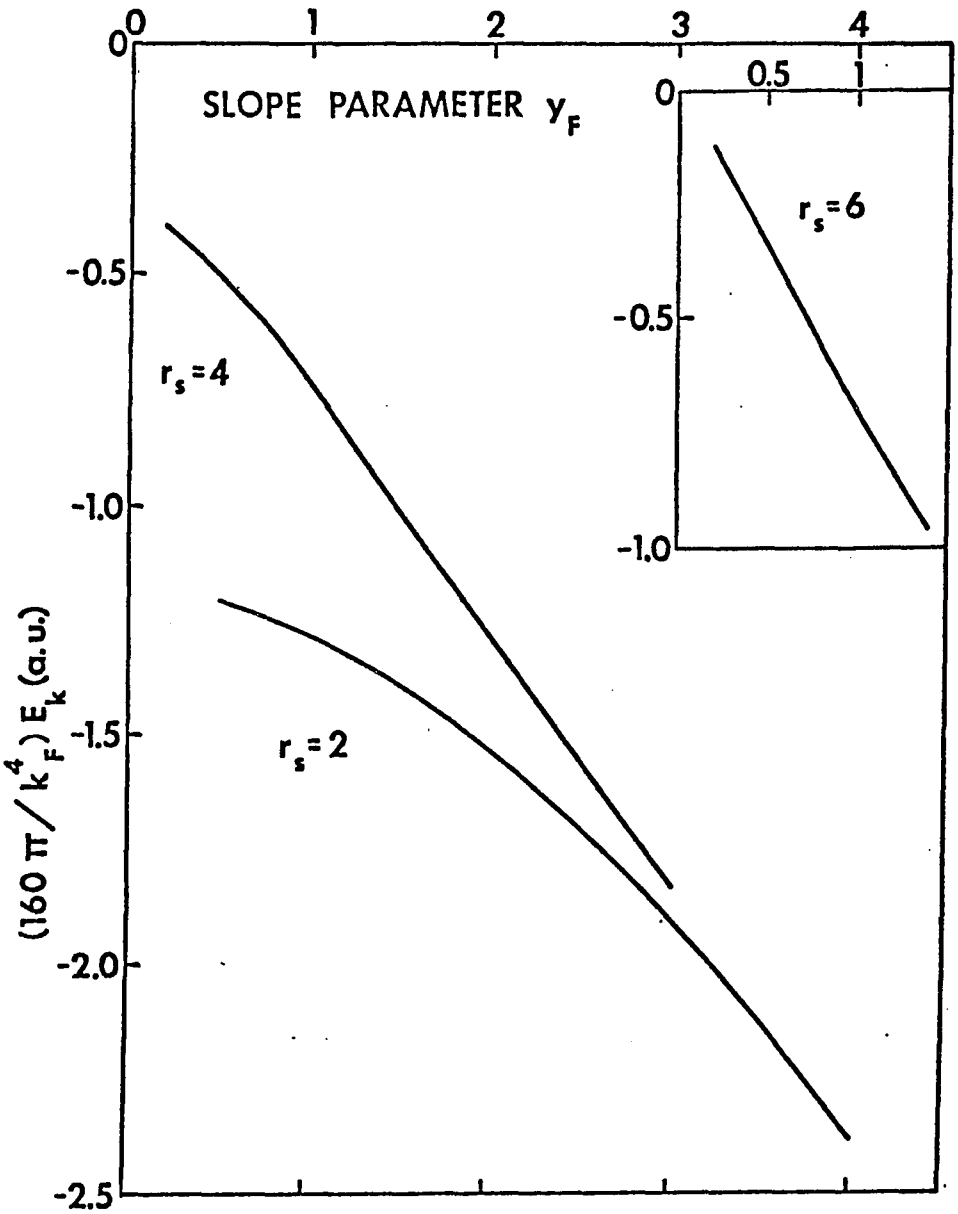
0
1
2
3
4
SLOPE PARAMETER y_F
0
0.5
1
$r_s=6$
-0.5
-1.0
$r_s=4$
$r_s=2$
-0.5
-1.0
-1.5
-2.0
-2.5
$(160\pi/k_F^4)E_k$ (a.u.)

Fig. 4.

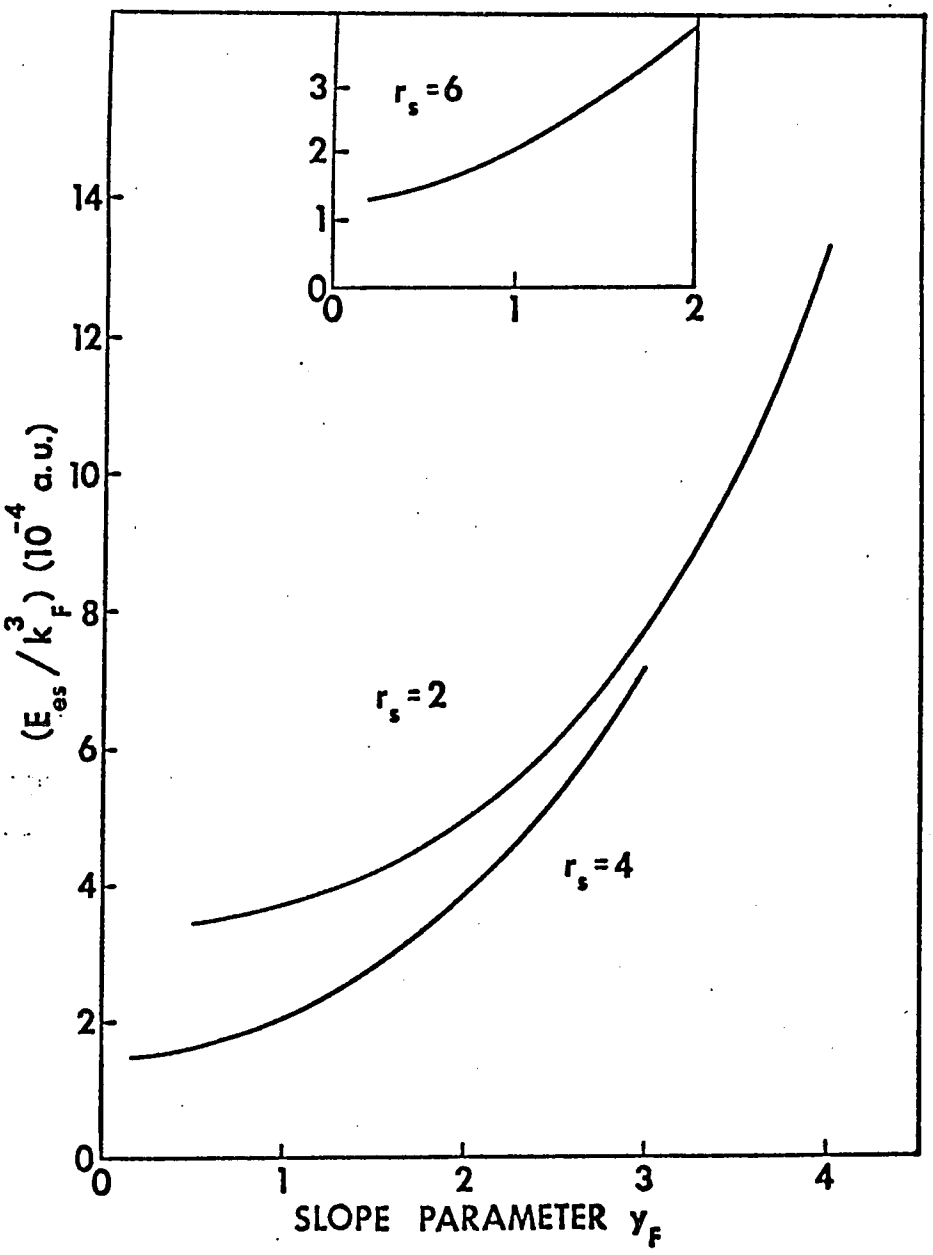

Fig. 5.

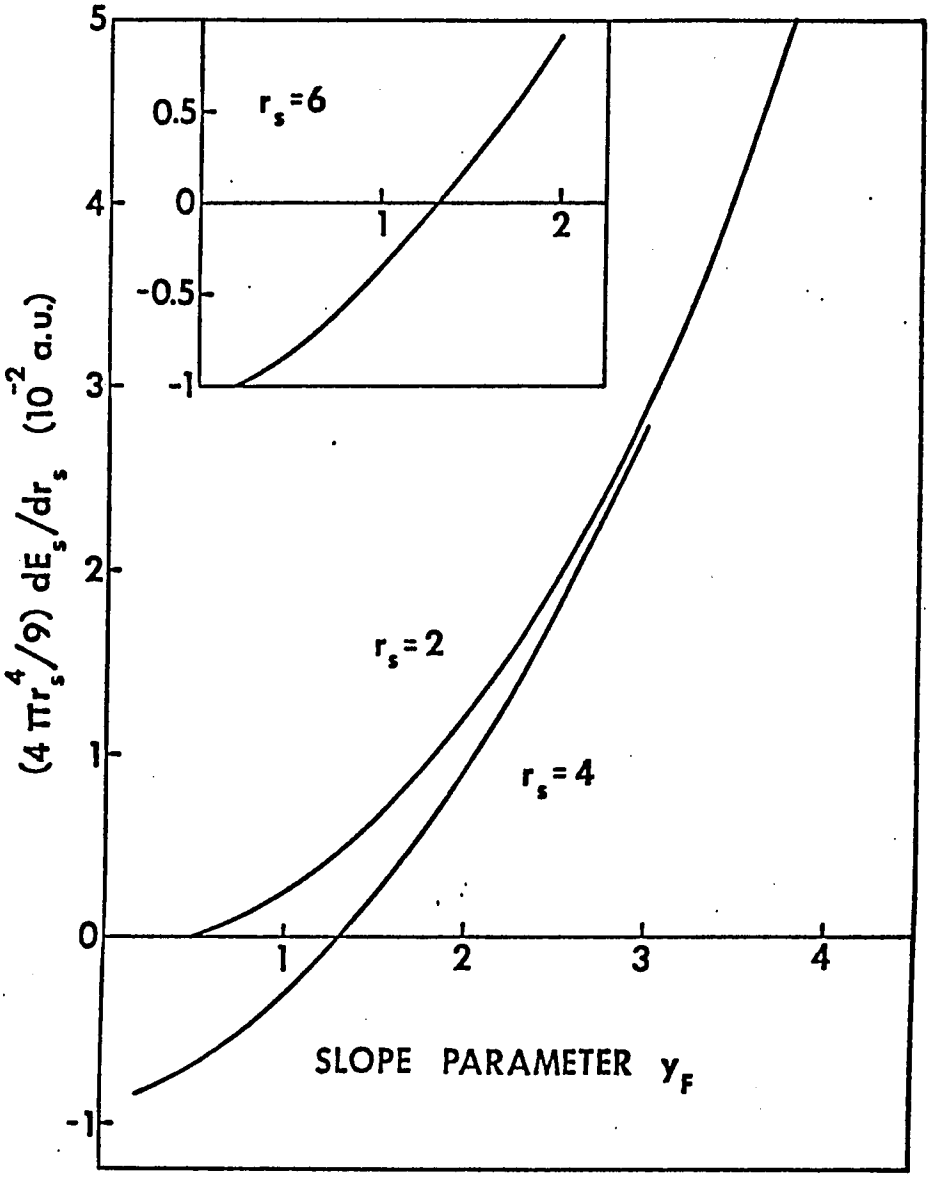
$(4\pi r_s^4/9)\, dE_s/dr_s$ $(10^{-2}$ a.u.)
SLOPE PARAMETER y_F
$r_s = 2$
$r_s = 4$
$r_s = 6$
5
4
3
2
1
0
-1
0.5
0
-0.5
-1
1
2
3
4

Fig. 6.

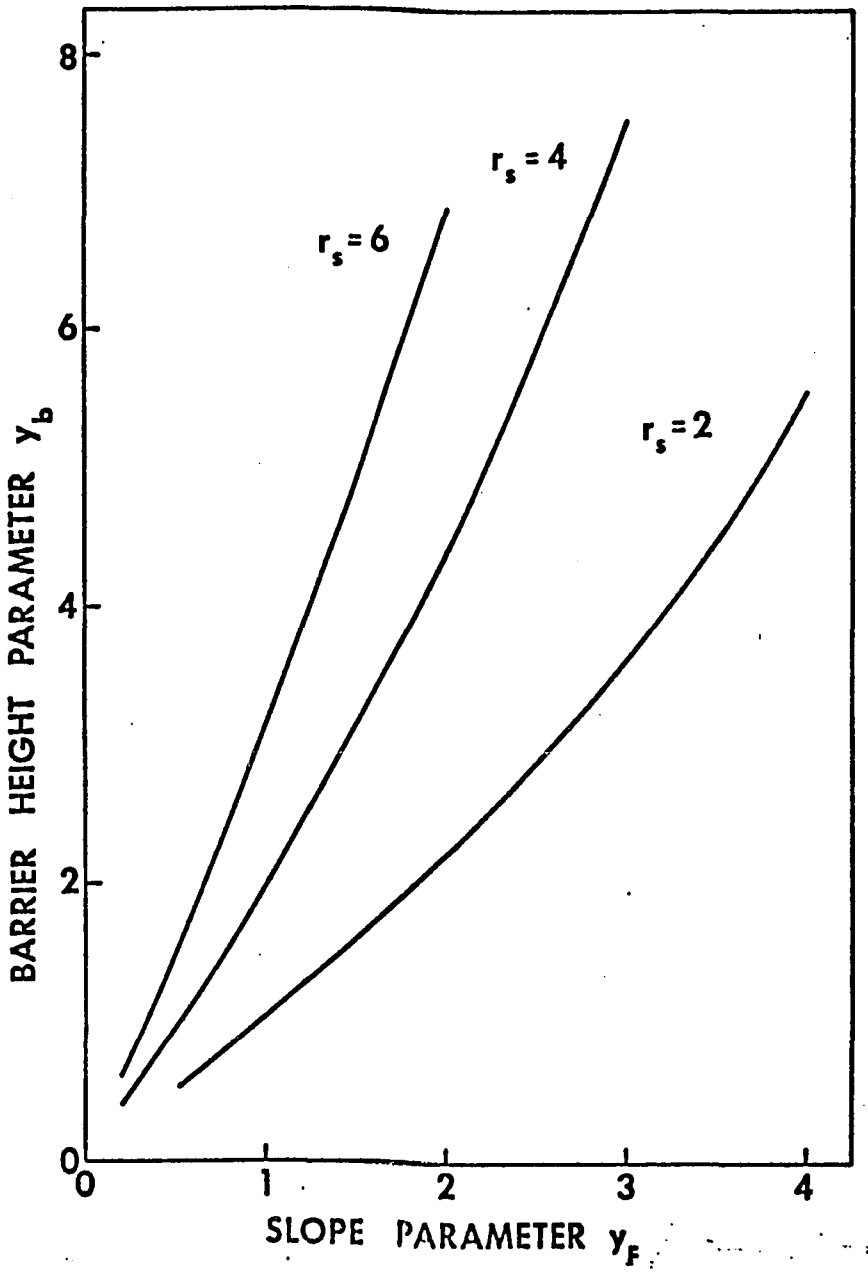
8
6
4
2
0
0
1
2
3
4
$r_s = 4$
$r_s = 6$
$r_s = 2$
BARRIER HEIGHT PARAMETER y_b
SLOPE PARAMETER y_F

Fig. 7.

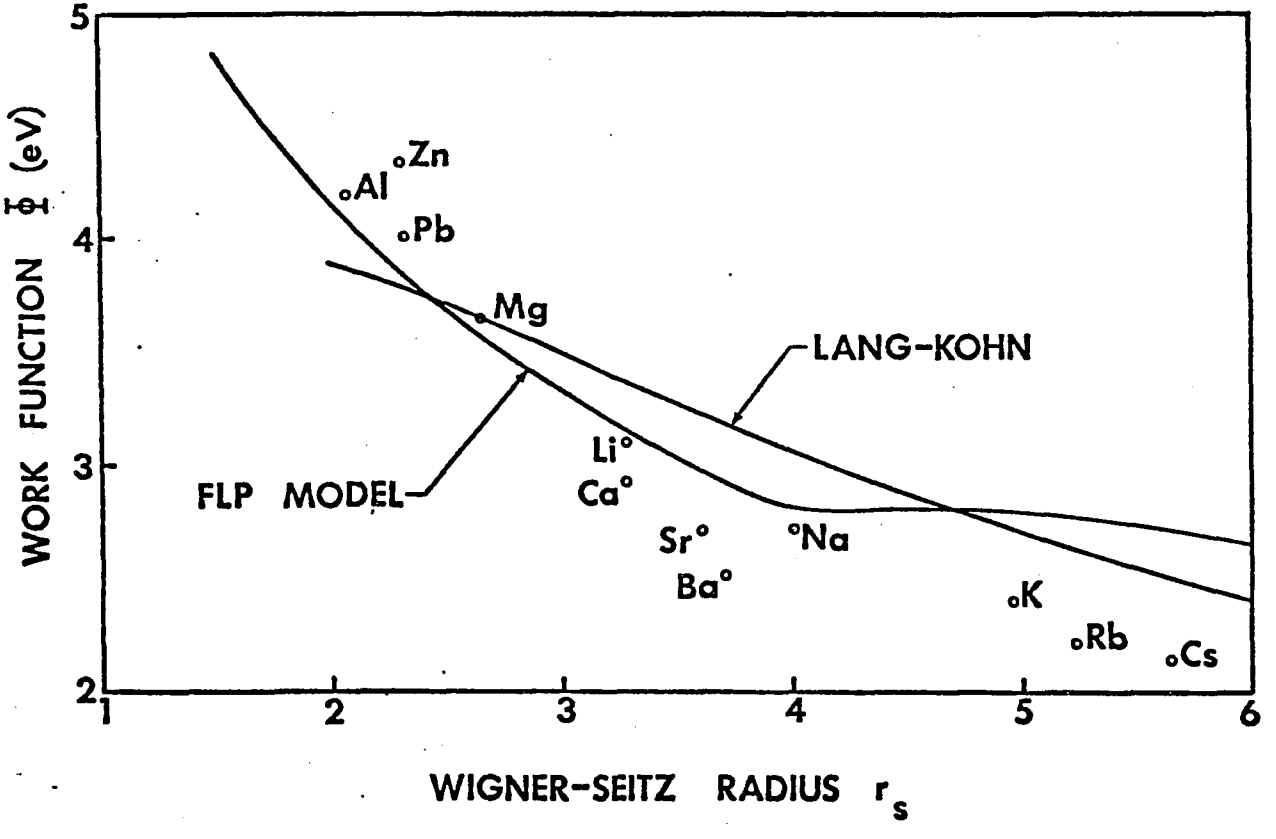
WORK FUNCTION Φ (eV)
WIGNER-SEITZ RADIUS r_s
LANG-KOHN
FLP MODEL
Zn
Al
Pb
Mg
Li
Ca
Sr
Na
Ba
K
Rb
Cs
5
4
3
2
1
2
3
4
5
6

Fig. 8.

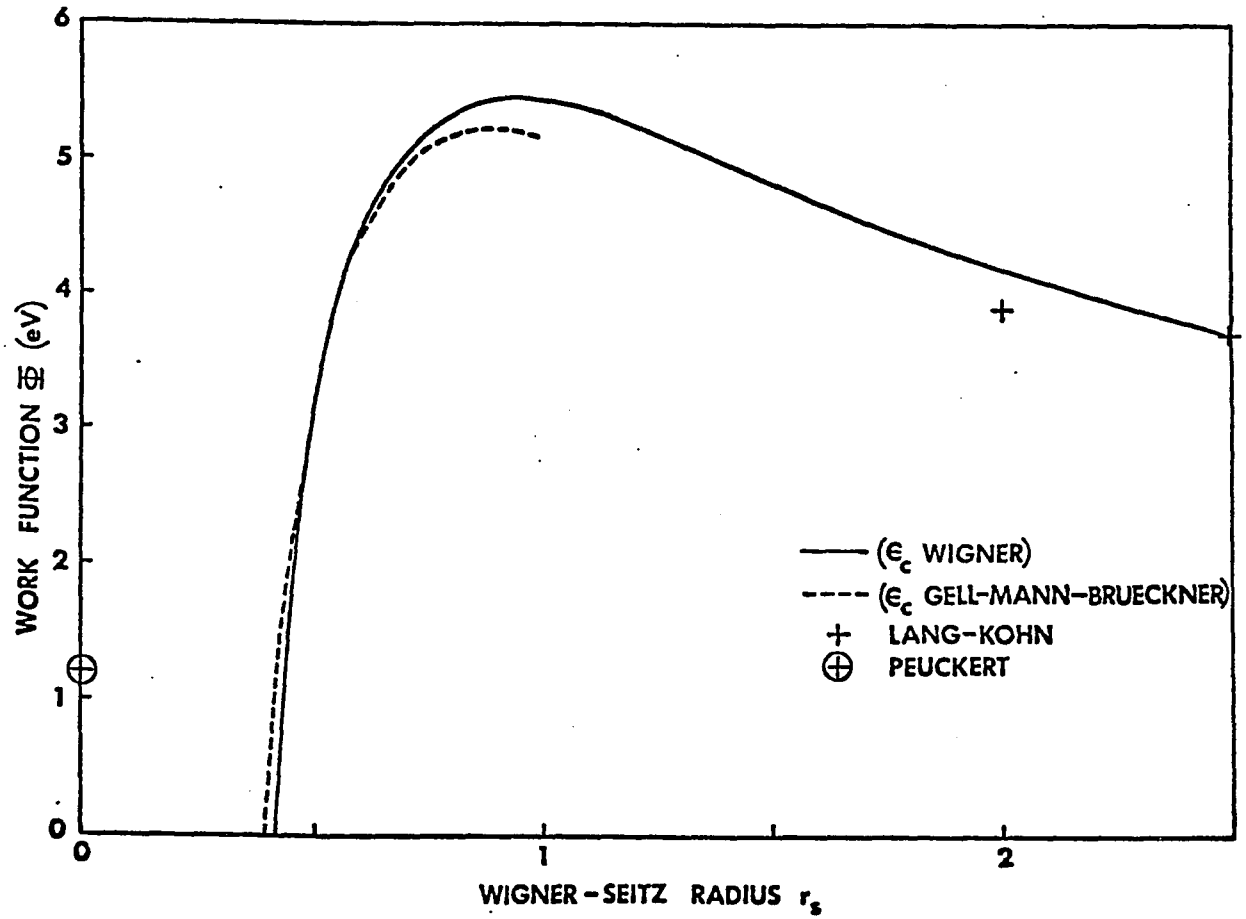
6
5
4
3
2
1
0
0
1
2
WORK FUNCTION Φ (eV)
WIGNER-SEITZ RADIUS r_s
(ϵ_c WIGNER)
(ϵ_c GELL-MANN-BRUECKNER)
LANG-KOHN
PEUCKERT

Fig. 9.

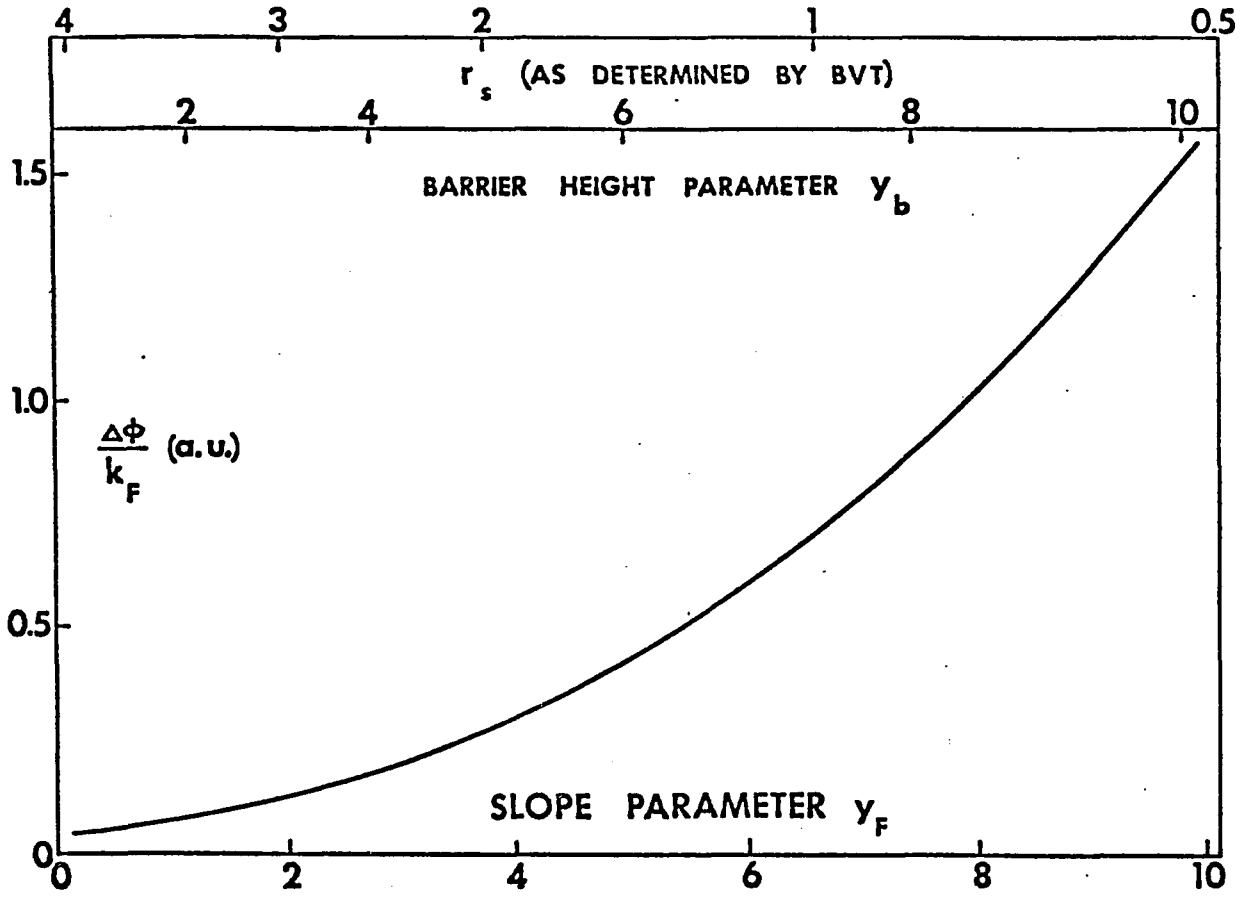
4
3
2
1
0.5
r_s (AS DETERMINED BY BVT)
2
4
6
8
10
BARRIER HEIGHT PARAMETER y_b
1.5
1.0
0.5
0
$\frac{\Delta\Phi}{k_F}$ (a.u.)
SLOPE PARAMETER y_F
0
2
4
6
8
10

Fig. 10.

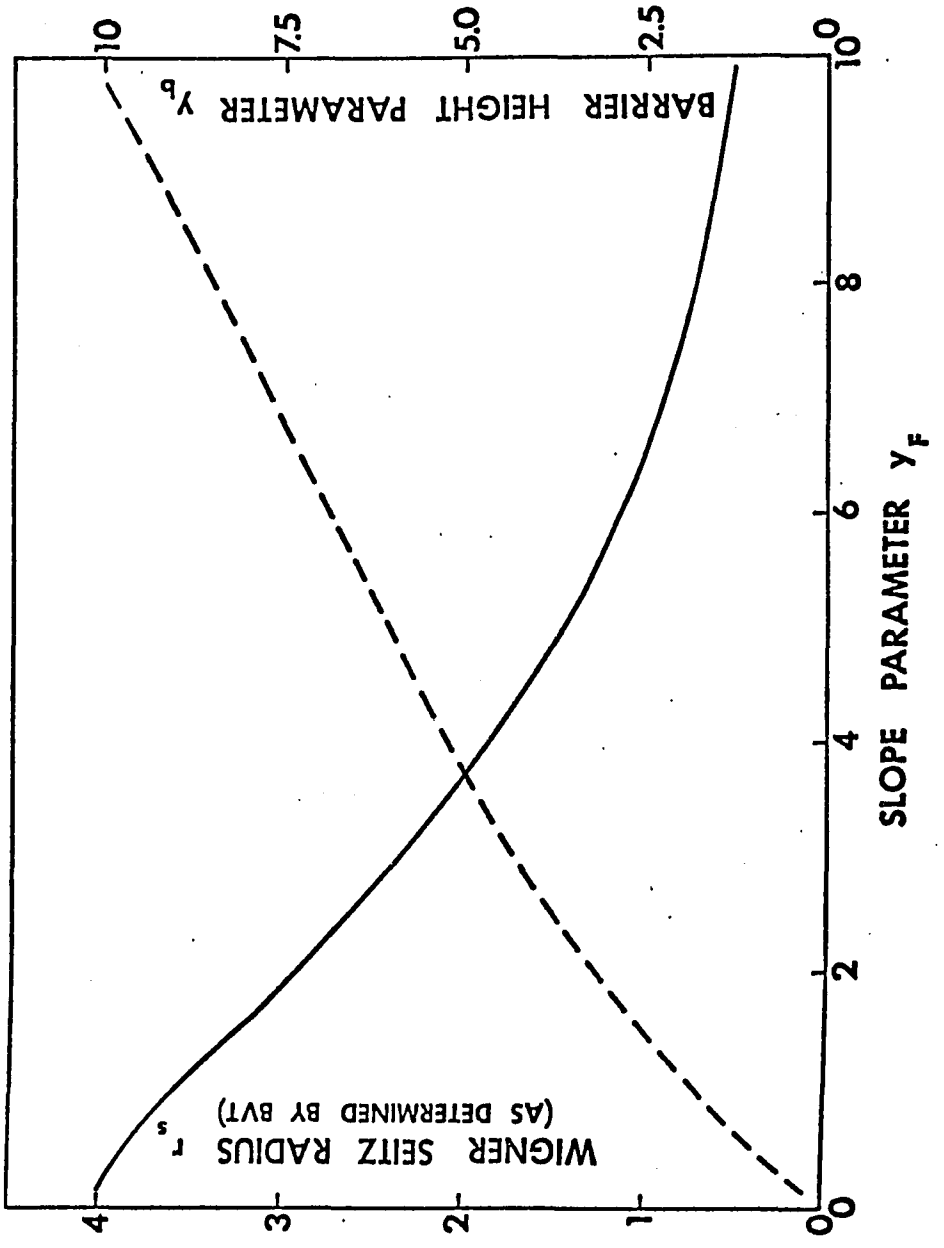
BARRIER HEIGHT PARAMETER y_b
10
7.5
5.0
2.5
0
WIGNER SEITZ RADIUS r_s
(AS DETERMINED BY BVT)
4
3
2
1
0
0
2
4
6
8
10
SLOPE PARAMETER y_F

Fig. 11.

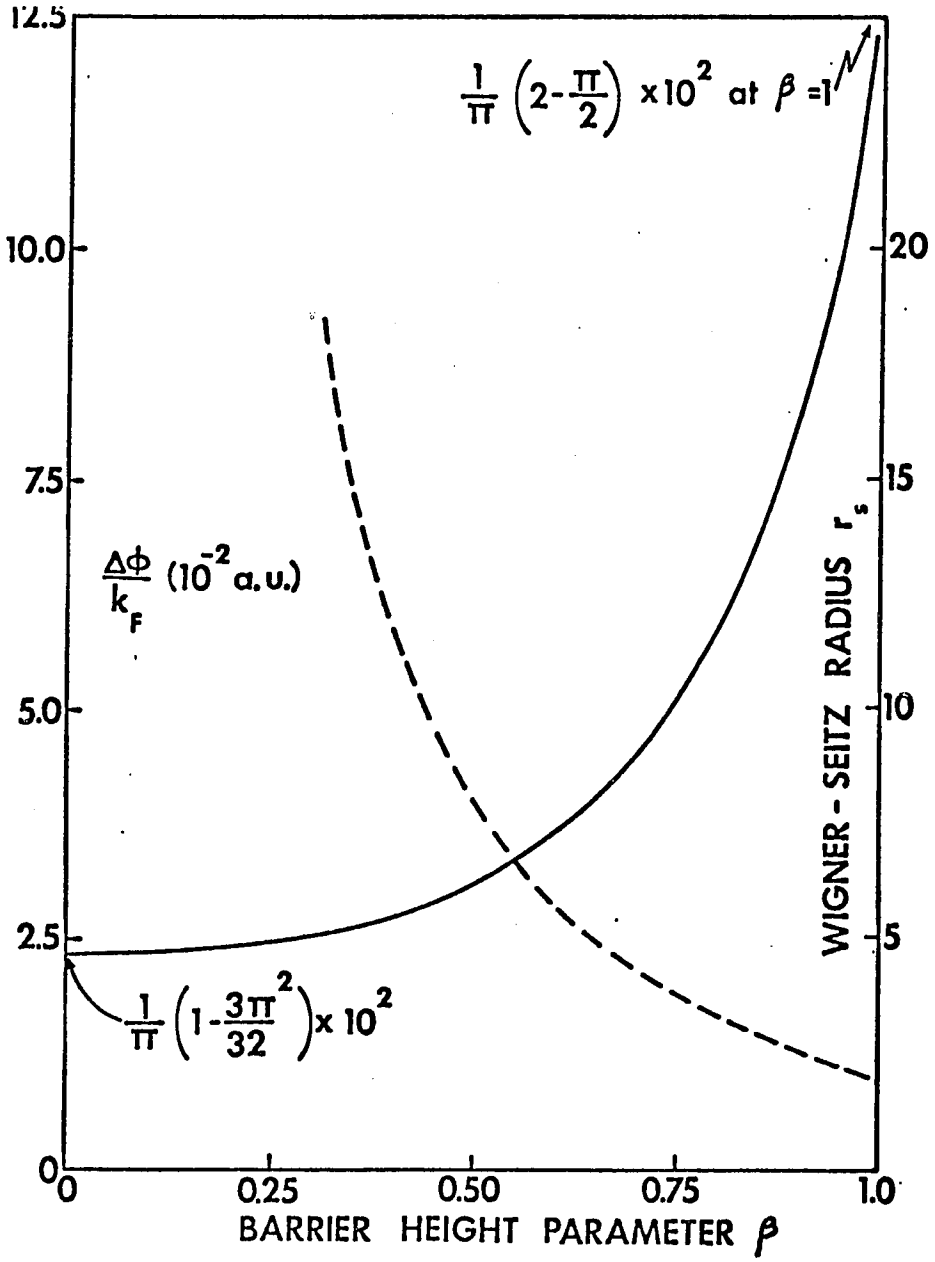
12.5
10.0
7.5
5.0
2.5
0
0
0.25
0.50
0.75
1.0
BARRIER HEIGHT PARAMETER β
$\frac{1}{\pi}\left(2-\frac{\pi}{2}\right)\times10^{2}$ at β =1
$\frac{\Delta\phi}{k_F}$ (10^{-2} a.u.)
$\frac{1}{\pi}\left(1-\frac{3\pi^2}{32}\right)\times10^{2}$
WIGNER - SEITZ RADIUS r_s
20
15
10
5

Fig. 12.

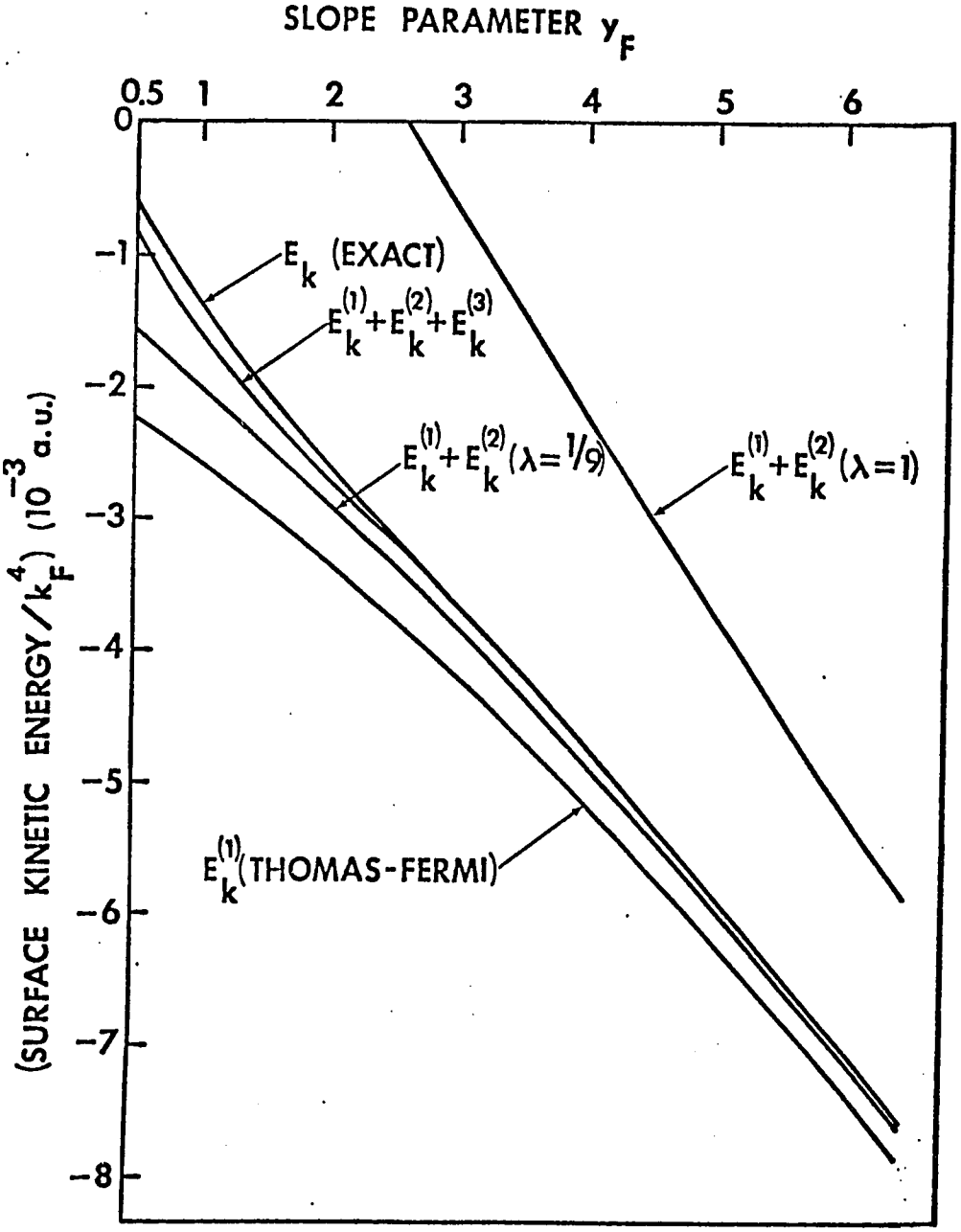
SLOPE PARAMETER y_F
0.5
1
2
3
4
5
6
0
−1
−2
−3
−4
−5
−6
−7
−8
(SURFACE KINETIC ENERGY / k_F^4) (10^{-3} a.u.)
E_k (EXACT)
$E_k^{(1)}+E_k^{(2)}+E_k^{(3)}$
$E_k^{(1)}+E_k^{(2)}(\lambda=1/9)$
$E_k^{(1)}+E_k^{(2)}(\lambda=1)$
$E_k^{(1)}$(THOMAS-FERMI)

Fig. 13.

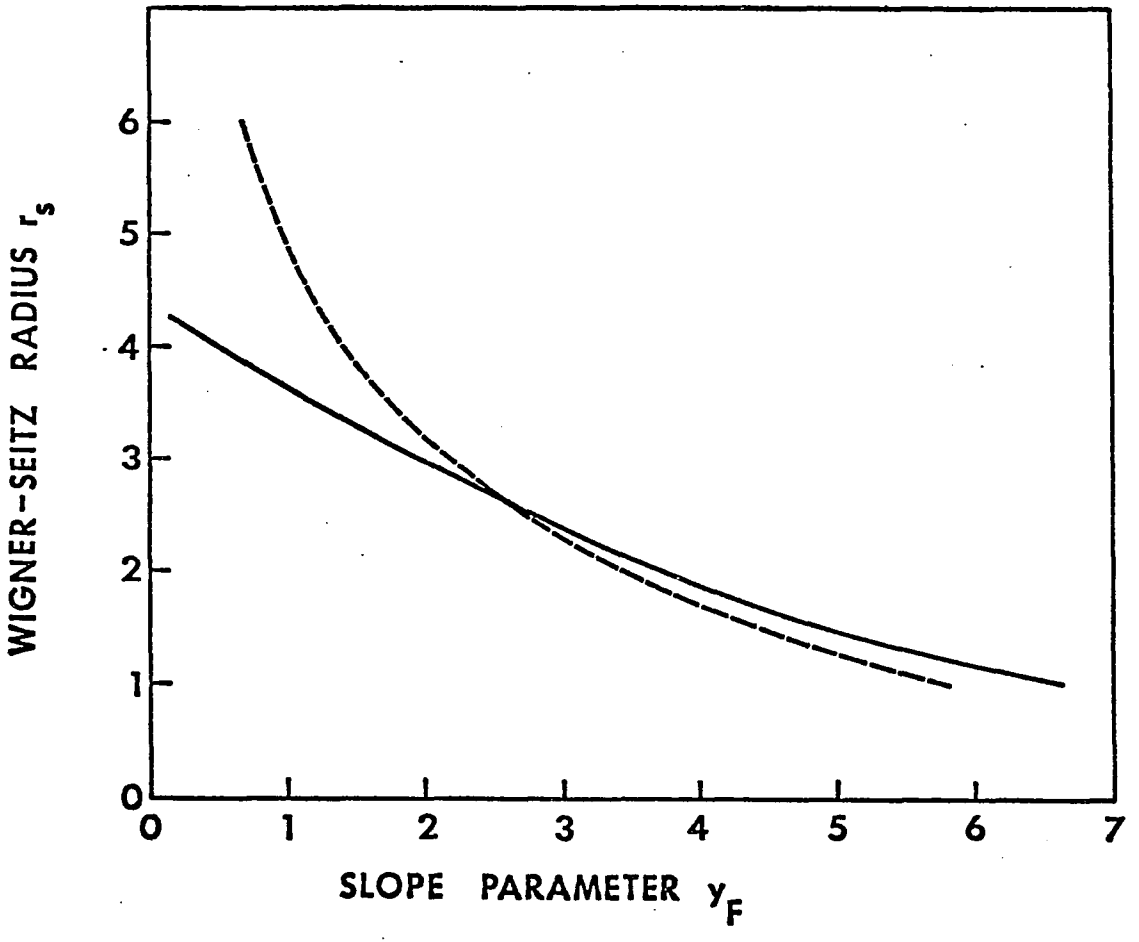

Fig. 14.

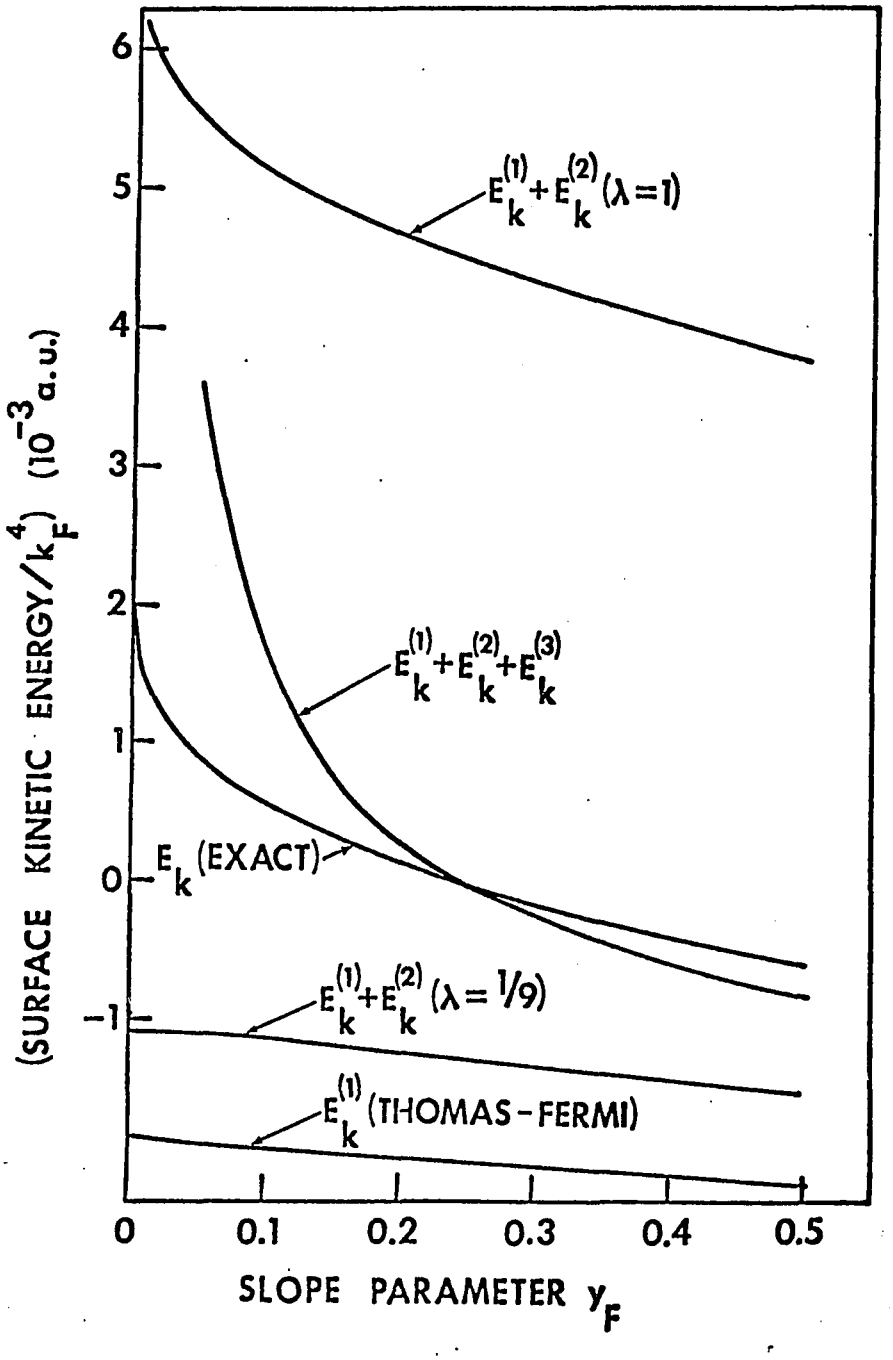
6
5
4
3
2
1
0
−1
$E_k^{(1)}+E_k^{(2)}(\lambda=1)$
$E_k^{(1)}+E_k^{(2)}+E_k^{(3)}$
E_k (EXACT)
$E_k^{(1)}+E_k^{(2)}(\lambda=1/9)$
$E_k^{(1)}$ (THOMAS-FERMI)
(SURFACE KINETIC ENERGY/k_F^4) (10^{-3} a.u.)
0
0.1
0.2
0.3
0.4
0.5
SLOPE PARAMETER y_F

Fig. 15.

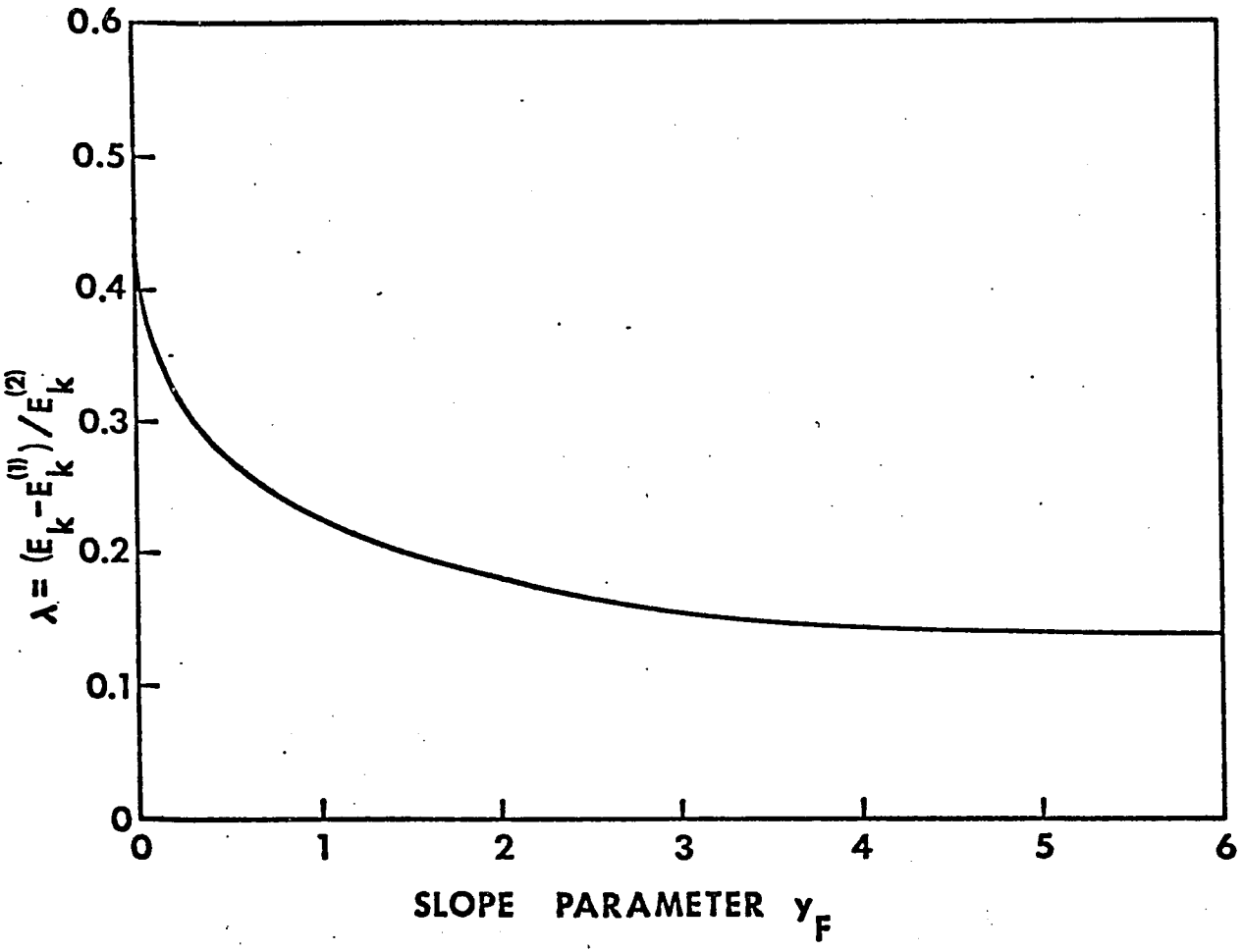
0.6
0.5
0.4
0.3
0.2
0.1
0
$\lambda = (E_k - E_k^{(1)})/E_k^{(2)}$
0
1
2
3
4
5
6
SLOPE PARAMETER y_F

Fig. 16.

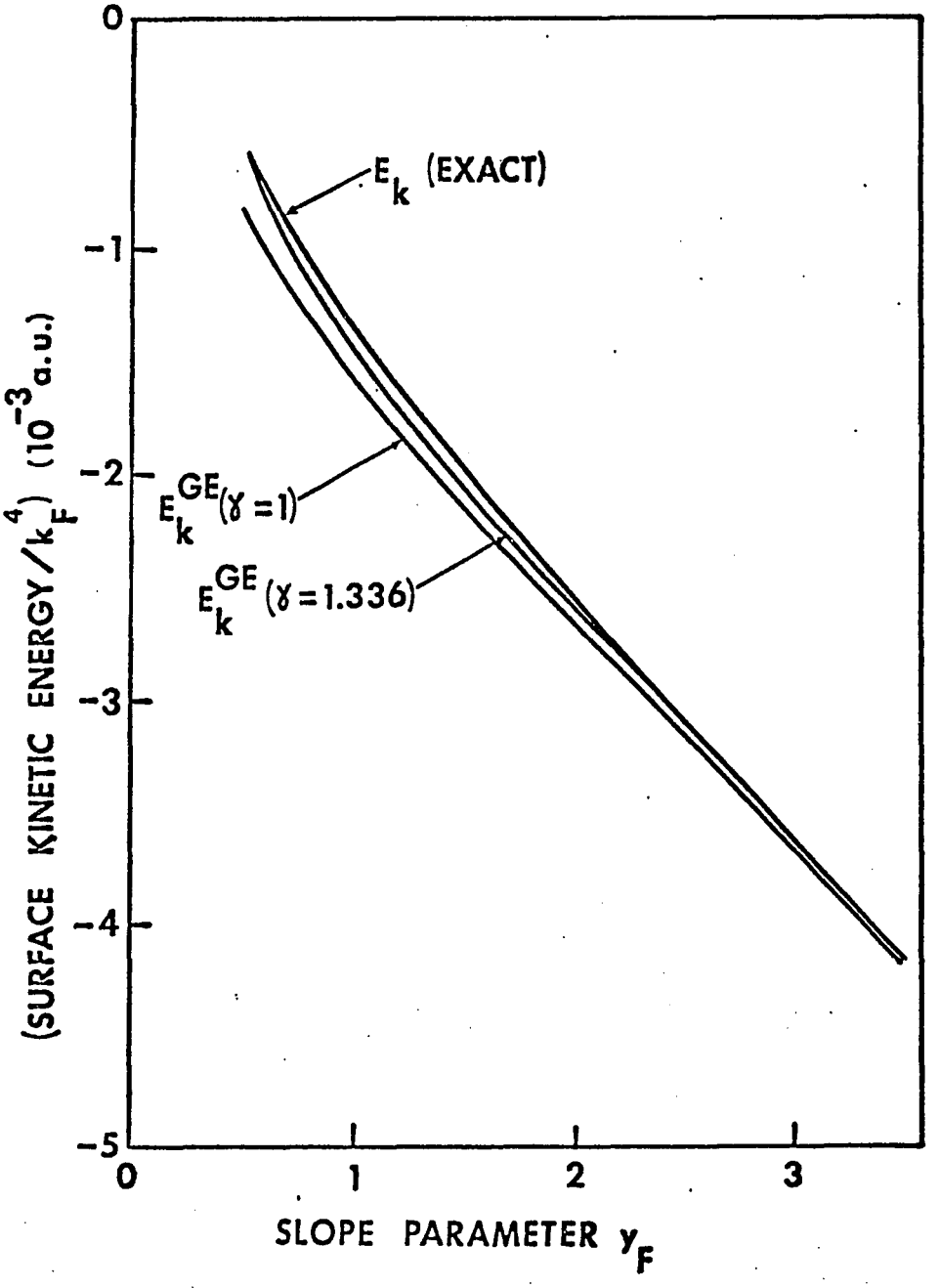
0
-1
-2
-3
-4
-5
0
1
2
3
E_k (EXACT)
$E_k^{GE}(\gamma = 1)$
$E_k^{GE}(\gamma = 1.336)$
(SURFACE KINETIC ENERGY / k_F^4) (10^{-3} a.u.)
SLOPE PARAMETER y_F

Fig. 17.

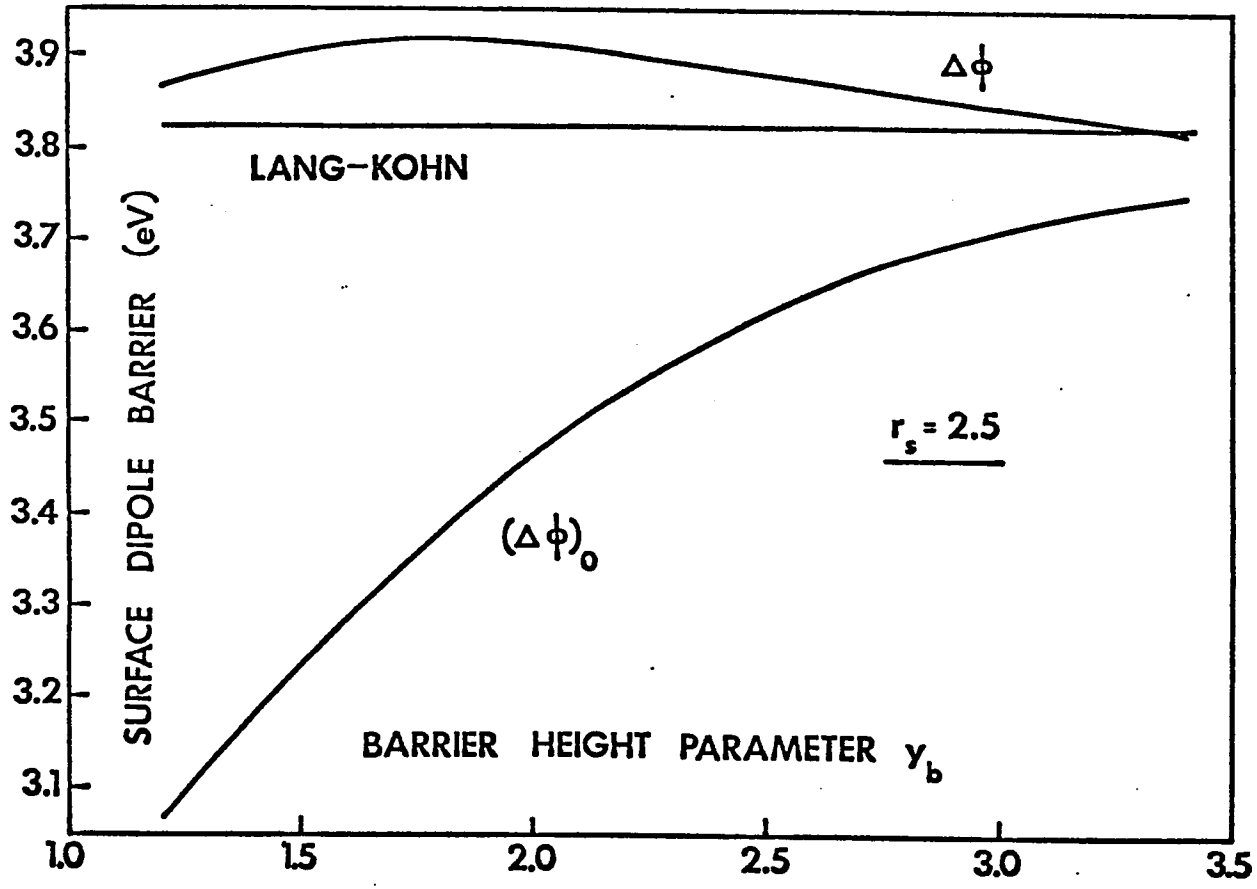
3.9
3.8
3.7
3.6
3.5
3.4
3.3
3.2
3.1
SURFACE DIPOLE BARRIER (eV)
Δϕ
LANG-KOHN
r_s = 2.5
(Δϕ)_0
BARRIER HEIGHT PARAMETER y_b
1.0
1.5
2.0
2.5
3.0
3.5

Fig. 18.

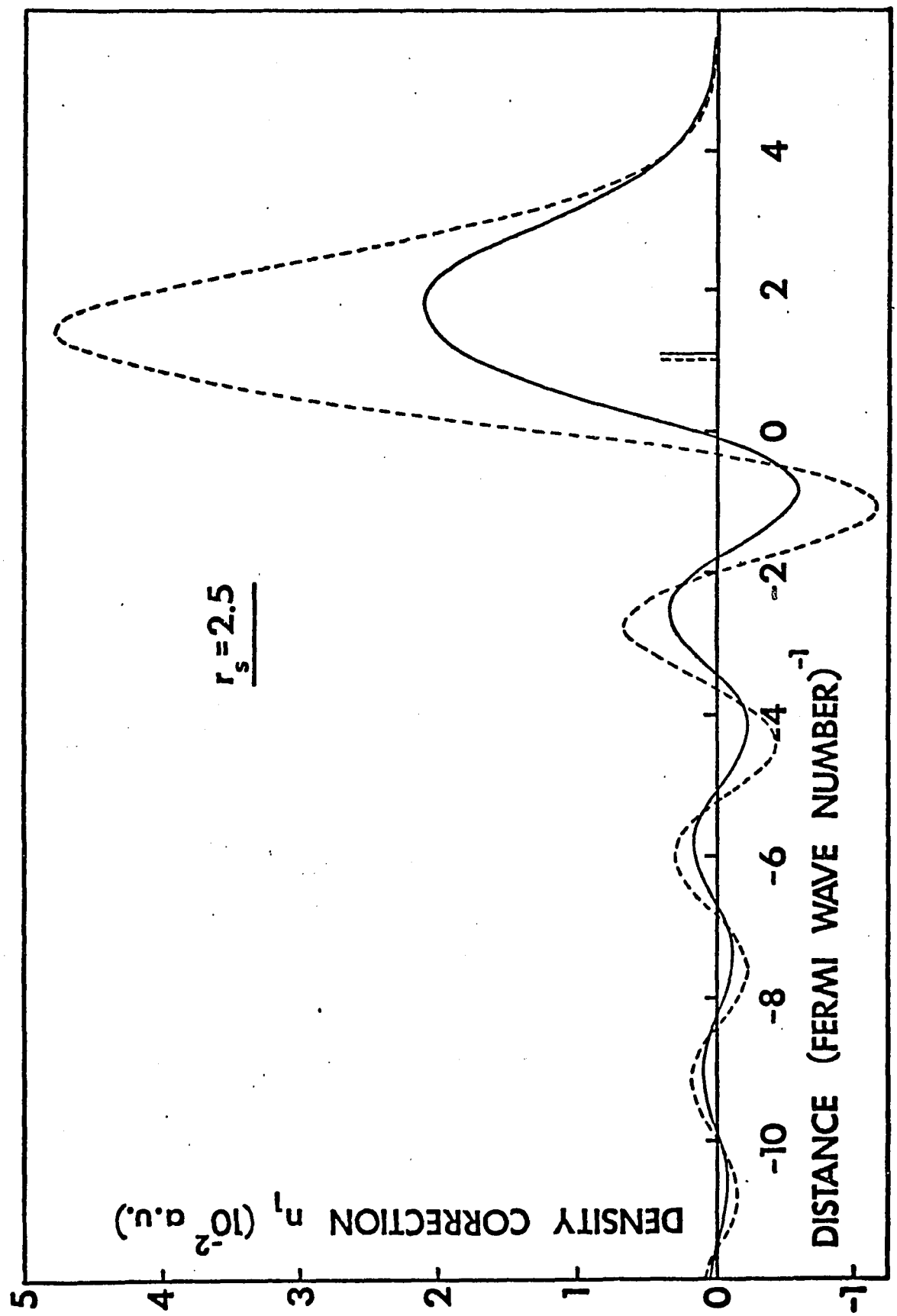
r_s=2.5
DENSITY CORRECTION n_1 (10^{-2} a.u.)
DISTANCE (FERMI WAVE NUMBER)$^{-1}$
5
4
3
2
1
0
-1
-10
-8
-6
-4
-2
0
2
4

Fig. 19.

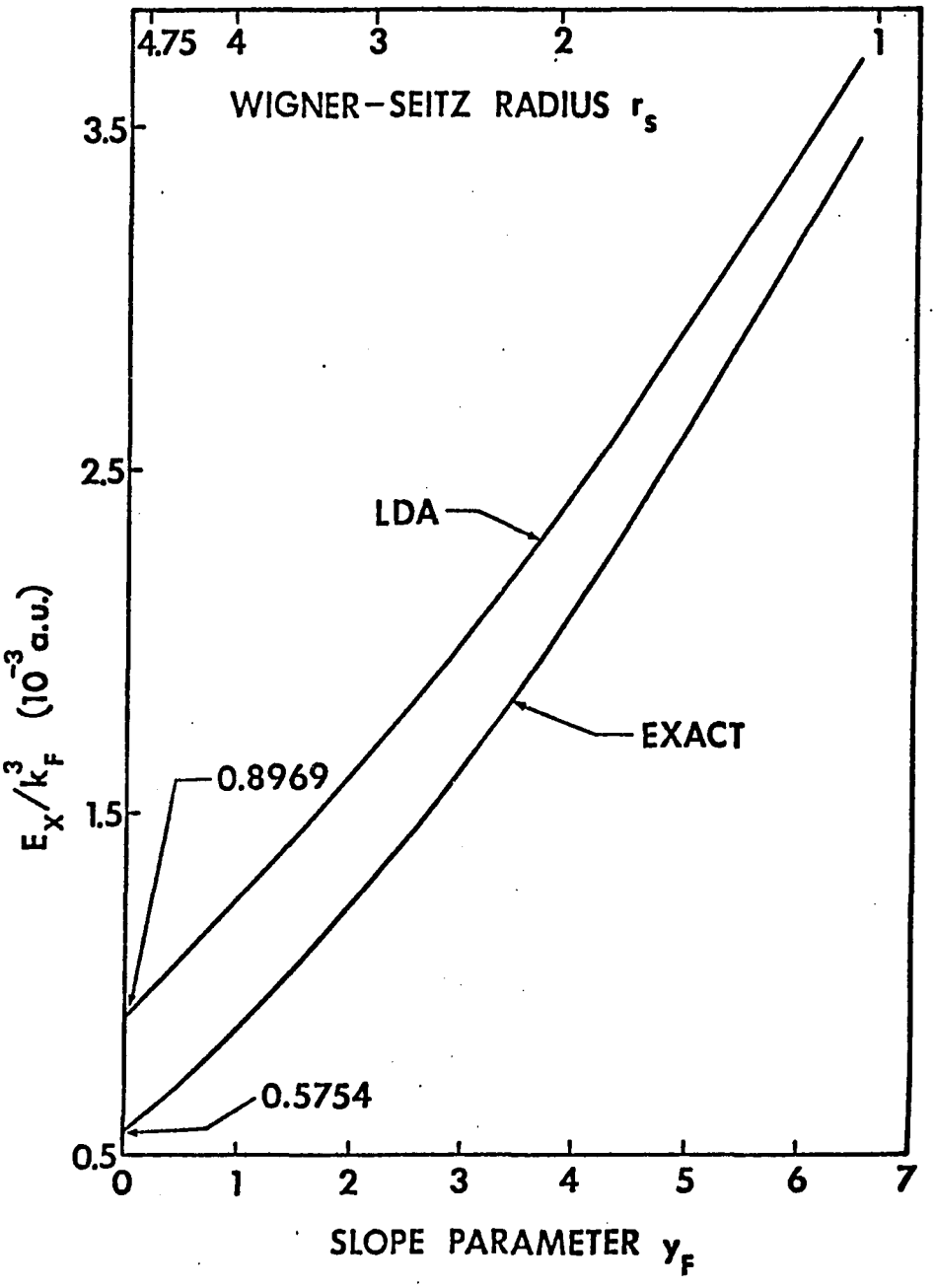
4.75
4
3
2
1
WIGNER–SEITZ RADIUS r_s
3.5
2.5
1.5
0.5
E_X/k_F^3 (10^{-3} a.u.)
LDA
EXACT
0.8969
0.5754
0
1
2
3
4
5
6
7
SLOPE PARAMETER y_F

Fig. 20.

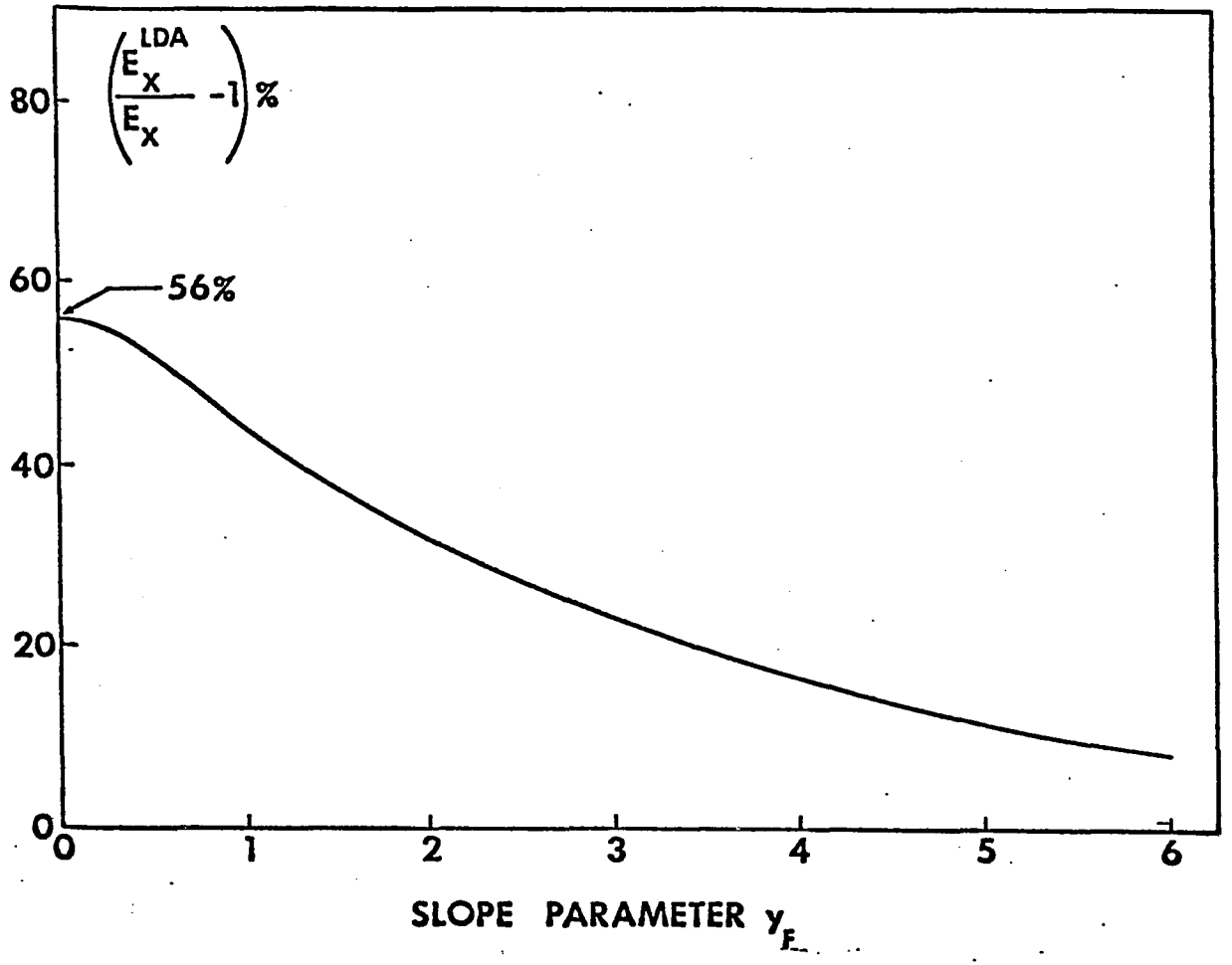
$\left(\frac{E_X^{LDA}}{E_X} - 1\right)\%$
80
60
40
20
0
56%
0
1
2
3
4
5
6
SLOPE PARAMETER y_F

Fig. 21.

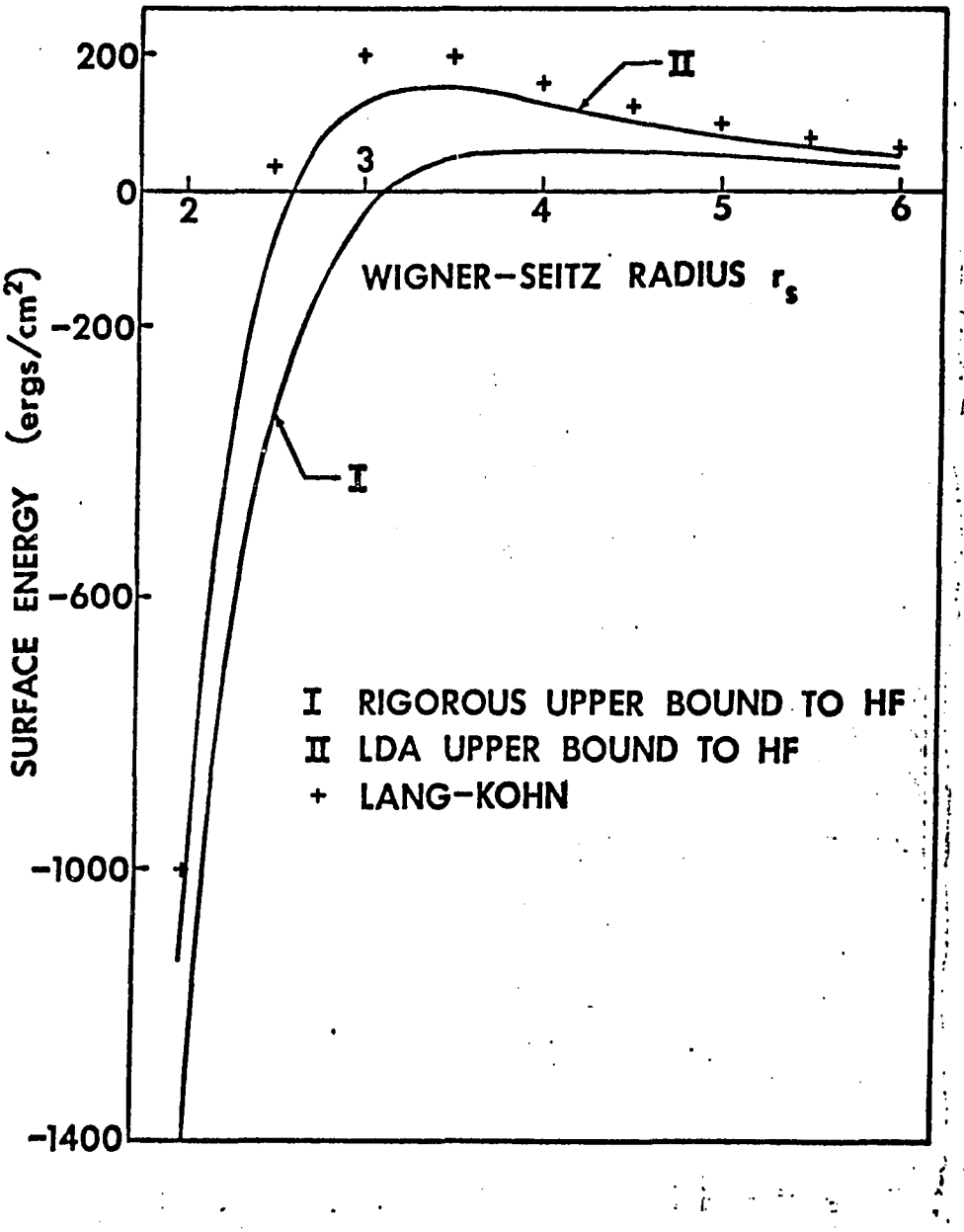
200
0
-200
-600
-1000
-1400
2
3
4
5
6
II
I
WIGNER–SEITZ RADIUS r_s
SURFACE ENERGY (ergs/cm^2)
I RIGOROUS UPPER BOUND TO HF
II LDA UPPER BOUND TO HF
+ LANG–KOHN

Fig. 22.

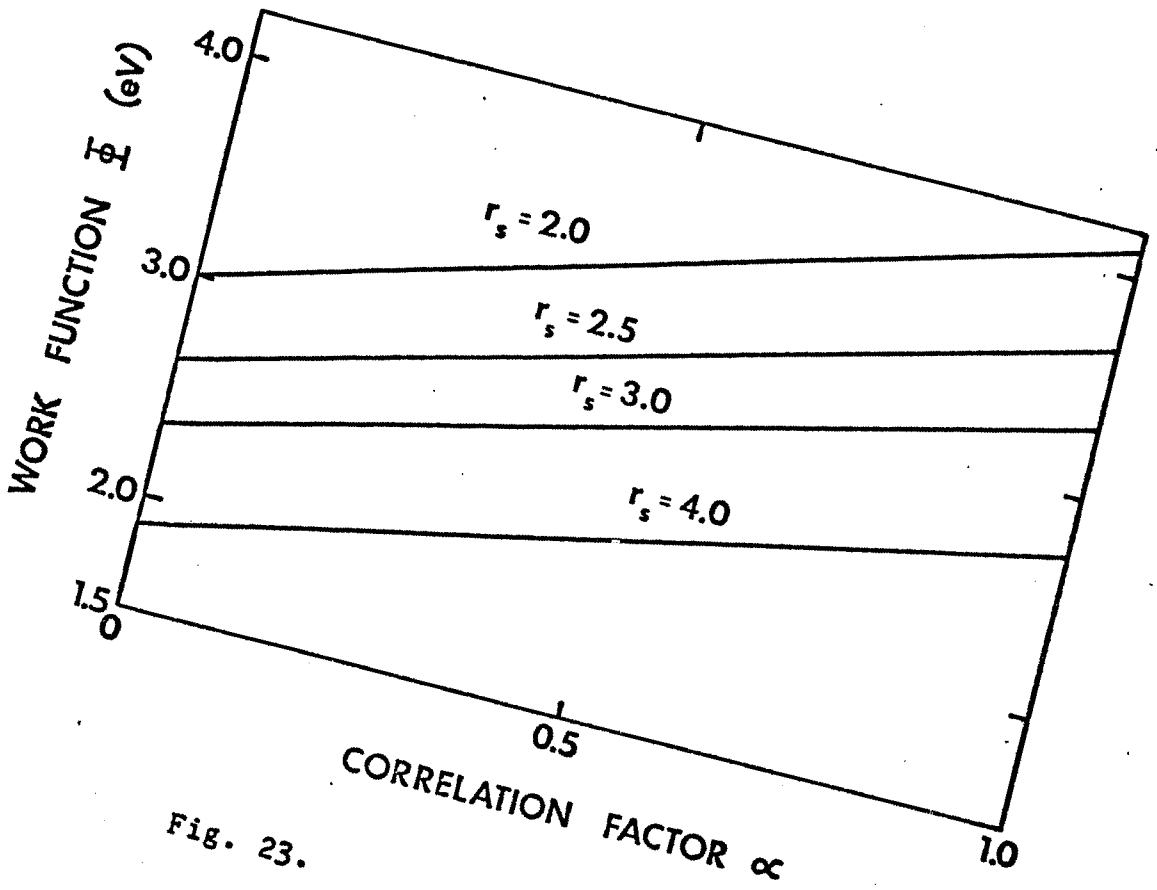
WORK FUNCTION Φ (eV)
4.0
3.0
2.0
1.5
0
0.5
1.0
CORRELATION FACTOR α
$r_s = 2.0$
$r_s = 2.5$
$r_s = 3.0$
$r_s = 4.0$

Fig. 23.

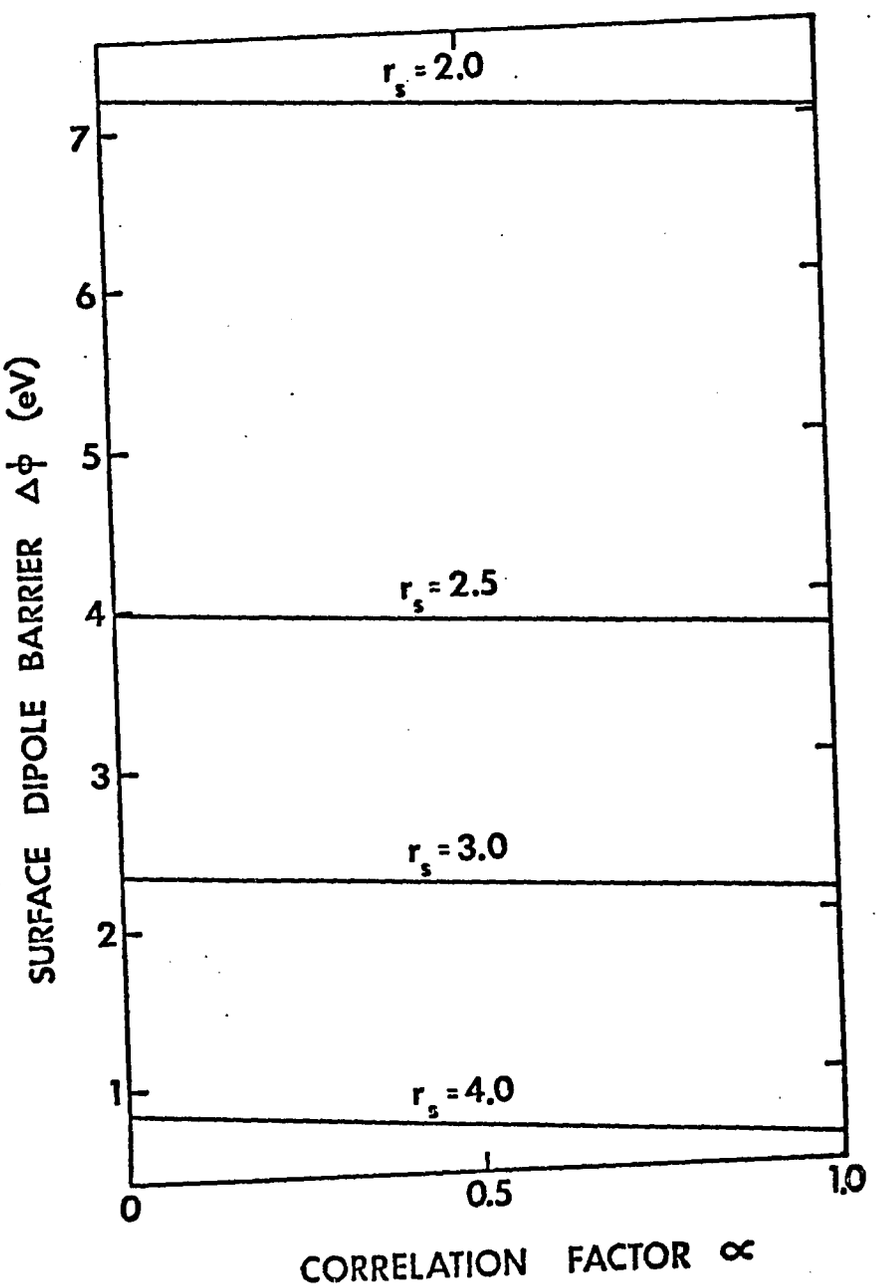
$r_s = 2.0$
$r_s = 2.5$
$r_s = 3.0$
$r_s = 4.0$
7
6
5
4
3
2
1
0
0.5
1.0
SURFACE DIPOLE BARRIER $\Delta\phi$ (eV)
CORRELATION FACTOR α

Fig. 24.

BIBLIOGRAPHY

1. E. Wigner and J. Bardeen, Phys. Rev. 48 , 84 (1935).
2. J. Bardeen, Phys. Rev. 49 , 653 (1936).
3. R. Smoluchowski, Phys. Rev. 60 , 661 (1941).
4. H.B. Huntington, Phys. Rev. 81 , 1035 (1951).
5. A. Sugiyama, J. Phys. Soc. Jpn. 15 , 965 (1960).
6. R.M. Stern and H. Taub, CRC Critical Reviews in Solid State Science 1 , 221 (1970).
7. P.J. Estrup and E.G. McRea, Surface Science 25 , 1 (1971).
8. J. Flamholz and J.B. Krieger, J. Chem. Phys. 56 , 5843 (1972).
9. D.S. Boudreaux, Surface Science 28 , 344 (1971).
10. E. Caruthers, L. Kleinman, and G.P. Alldredge, Phys. Rev. B 10 , 1252 (1974).
11. P. Hohenberg and W. Kohn, Phys. Rev. 136 , B864 (1964).
12. W. Kohn and L.J. Sham, Phys. Rev. 140 , A1133 (1965).
13. N.D. Lang and W. Kohn, Phys. Rev. B 1 , 4555 (1970).
14. N.D. Lang and W. Kohn, Phys. Rev. B 3 , 1215 (1971).
15. J.A. Appelbaum and D.R. Hamann, Phys. Rev. B 6 , 2166 (1972); Phys. Rev. Lett. 32 , 225 (1974).
16. G.P. Alldredge and L. Kleinman, Phys. Rev. Lett. 28 , 1264 (1972); Phys. Rev. B 10 , 559 (1974).
17. E. Caruthers, L. Kleinman, and G.P. Alldredge, Phys. Rev. B 8 , 4570 (1973); B 9 , 3330 (1974); B 9 , 3325

(1974).

18. R.W. Hardy and R.E. Allen, Solid State Commun. 19 , 1 (1976); Surface Science 61 , 177 (1976).

19. J.R. Chelikowsky, M. Shulter, S.G. Louie and M. Cohen, Solid State Commun. 17 , 1103 (1975).

20. J.G. Gay, J.R. Smith and F.J. Arlinghaus, Phys. Rev. Lett. 38 , 561 (1977).

21. J.A. Appelbaum and D.R. Hamann, Solid State Commun. 27 , 881 (1978).

22. G.P. Kerker, K.M. Ho, and M.L. Cohen, Phys. Rev. B (to be published).

23. J.R. Smith, Phys. Rev. 181 , 522 (1969).

24. G. Paasch and M. Heitschold, Phys. status Solidi. (b) 67 , 743 (1975).

25. D.S. Boudreaux and H.J. Juretschke, in Structure and Properties of Metal Surfaces (Honda Memorial Series on Materials Science, No. 1, Tokyo, Japan, 1973), p. 94.

26. N.D. Lang, in Solid State Physics, Advances in Research and Applications , edited by H. Ehrenreich, F. Seitz and D. Turnbull (Academic New York, 1973), Vol. 28, p. 243.

27. A.J. Bennett, CRC Critical Review in Solid State Science 4 , 261 (1974).

28. S. Lundqvist, in Surface Science , Vol. 1 , (International Atomic Energy Agency, Vienna, 1975), p. 331.

29. J.R. Smith, in Topics in Applied Physics , Vol. 4 , (Springer-Verlag, 1975), p. 1.

30. N.D. Lang, in Electronic Structure and Reactitivity of Metal Surfaces , edited by E.G. Derouane and A.A. Lucas (Plenum, New York, 1976), p. 81.

31. J.A. Appelbaum and D.R. Hamann, Rev. Mod. Phys. 48 , 479 (1976).

32. H.F. Budd and J. Vannimenus, Phys. Rev. Lett. 31 , 1218 (1973); 31 , 1430(E) (1973).

33. B.L. Moisewitsch, Variational Principles (Interscience, New York, 1966), p. 153.

34. V. Sahni, J.B. Krieger and J. Gruenebaum, Phys. Rev. B 12 , 3505 (1975).

35. V. Sahni and J. Gruenebaum, Phys. Rev. B 15 , 1929 (1977).

36. V. Sahni, J.B. Krieger and J. Gruenebaum, Phys. Rev. B 15 , 1941 (1977).

37. V. Sahni and J. Gruenebaum, Solid State Commun. 21 , 463 (1977).

38. J. Vannimenus and H.F. Budd, Solid State Commun. 15 , 1739 (1974).

39. A.S. Kompaneets and E.S. Pavolovskii, Sov. Phys. JETP 4 , 328 (1957).

40. D.A. Kirzhnits, Sov. Phys. JETP 5 , 64 (1957).

41. K.L. Le Couteur, Proc. Phys. Soc. 84 , 837 (1964).

42. J.C. Stoddart, A.M. Beattie, and N.H. March, Int. J. Quantum Chem. Symposium Supplement 4s , 35 (1970).

43. C.H. Hodges, Can. J. Phys. 51 , 1428 (1973).

44. J.R. Smith, S.C. Ying, and W. Kohn, Phys. Rev. Lett.

30 , 610 (1973).

45. D.J. Kim, H.C. Praddaude, and B.B. Schwartz, Phys. Rev. Lett. 23 , 419 (1969); D.J. Kim, B.B. Schwartz, and H.C. Praddaude, Phys. Rev. B 7 , 205 (1973).

46. M.M. Pant and A.K. Rajagopal, Solid State Commun. 10 , 1157 (1972).

47. R.L. Kautz and B.B. Schwartz, Phys. Rev. B 14 , 2017 (1976).

48. C.Q. Ma and V. Sahni, Phys. Rev. B 16 , 4249 (1977).

49. C.Q. Ma and V. Sahni, "Statistical Calculation of Jellium Surface Properties", Phys. Rev. B (to be published).

50. N.H. March, Adv. in Physics 6 , 1 (1957).

51. V. Sahni and J.B. Krieger, Int. J. Quantum Chem. Symposium 5 , 47 (1971).

52. J.B. Krieger and V. Sahni, Phys. Rev. A 6 , 919 (1972).

53. V. Sahni and J.B. Krieger, Phys. Rev. A 6 , 928 (1972).

54. V. Sahni and J.B. Krieger, Int. J. Quantum Chem. Symposium 6 , 103 (1972).

55. V. Sahni and J.B. Krieger, Phys. Rev. A 8 , 65 (1973).

56. V. Sahni and J.B. Krieger, Phys. Rev. A 11 , 409 (1975).

57. V. Sahni, J.B. Krieger and J. Gruenebaum, Phys. Rev. A 12 , 768 (1975).

58. R.T. Brown, Phys. Rev. A 1 ,1342 (1970); E.G.G. Technical Report Nos. E.G.G. 1183-1453 and 1183-1458 (1969) (unpublished).

59. Y.K. Kim and M. Inokuti, Phys. Rev. 165 , 39 (1968).

60. V. Sahni, Ph.D. thesis (Polytechnic Institute of Brooklyn, 1972) (unpublished).

61. C.L. Pekeris, Phys. Rev. 115 , 1216 (1959); 126 , 1470 (1962).

62. B.Y. Tong and L.J. Sham, Phys. Rev. 144 , 1 (1966).

63. H.B. Shore, J.H. Rose, and E. Zaremba, Phys. Rev. B 15 , 2858 (1977).

64. P. Eisenberger and P.M. Platzman, Phys. Rev. A 2 , 415 (1970).

65. C.L. Pekeris, Phys. Rev. A 4 , 516 (1971).

66. J. Harris and R.O. Jones, J. Phys. F 4 , 1170 (1974).

67. E. Wikborg and J.E. Inglesfield, Solid State Commun. 16 , 335 (1975).

68. A.K. Gupta and K.S. Singwi, Phys. Rev. B 15 , 1801 (1977).

69. S. Raimes, Wave Mechanics of Electrons in Metals (North-Holland, Amsterdam, 1961), p. 177.

70. D. Pines, Elementary Excitations in Solids (Benjamin, New York, 1963), p. 94.

71. N.D. Lang and L.J. Sham, Solid State Commun. 16 , 581 (1975).

72. D.C. Langreth and J.P. Perdew, Solid State Commun. 17 , 1425 (1975).

73. D.C. Langreth and J.P. Perdew, Phys. Rev. B 15 , 2884 (1977).

74. V. Sahni and C.Q. Ma, Bull. Am. Phys. Soc. 23 , 259 (1978).

75. D.J.W. Geldart and M. Rasolt, Phys. Rev. B 13 , 1477 (1976); M. Rasolt and D.J.W. Geldart, Phys. Rev. Lett. 35 , 1234 (1975); Solid State Commun. 18 , 549 (1976).

76. P. Vashista and K.S. Singwi, Phys. Rev. B 6 , 875 (1972).

77. D.J.W. Geldart, M. Rasolt, and R. Taylor, Solid State Commun. 10 , 279 (1972).

78. K.H. Lau and W. Kohn, J. Phys. Chem. Solids 37 , 99 (1976).

79. J.P. Perdew, D.C. Langreth, and V. Sahni, Phys. Rev. Lett. 38 , 1030 (1977).

80. V. Sahni and J. Gruenebaum, "Rayleigh-Ritz Variational Calculations of Real Metal Surface Properties", Phys. Rev. B (to be published).

81. J.A. Alonso and L.A. Girifalco, Solid State Commun. 24 , 135 (1977); Phys. Rev. B 17 , 3735 (1978).

82. O. Gunnarsson, M. Jonson, and B. Lundqvist, Solid State Commun. 24 , 765 (1977).

83. Atomic units are used here: $|e|=\hbar=m=1$. The unit of energy is 27.21 eV.

84. A. Sugiyama, J. Phys. Soc. Jpn. 16 , 1327 (1961).

85. D.C. Langreth, Phys. Rev. B 5 , 2842 (1972).

86. G.D. Mahan and W.L. Schaich, Phys. Rev. B 10 , 2647 (1974).

87. V. Sahni (private communication).

88. R. Monnier, J.P. Perdew, D.C. Langreth, and J.W. Wil-

kins, Phys. Rev. B 18 , 656 (1978).

89. J.P. Perdew and V. Sahni, "Accurate and Easy Method for Work Function Calculations" (to be published).

90. M. Gell-Mann and K.A. Brueckner, Phys. Rev. 106 , 364 (1957).

91. M. Abramowitz and I.A. Stegun, Handbook of Mathematical Functions (Dover, New York, 1965), p. 446.

92. V. Peuckert, J. Phys. C 7 , 2221 (1974).

93. Figure 4 of Ref. 30 shows that the work function has a maximum of ≃ 4eV for r_s between 1.5 and 2.0. More recently a fully self-consistent calculation (J.P. Perdew, private communication) in the local density approximation using the von Barth-Hedin (J. Phys. C 5 , 1629 (1972)) parameterization of the RPA exchange-correlation energy indicates the same high density behaviour of the work function as in Fig. 9 of the text. A maximum of 4.3 eV for the work function occurs at r_s=1.75, the work function vanishing at r_s ≃ 0.6. Thus although the model potential calculation produces very accurate high density dipole barriers, any small error is magnified in the results for the work function since the latter is obtained as a cancellation between two very large numbers as r_s becomes small. Furthermore, since the Thomas-Fermi, Thomas-Fermi-Dirac and Thomas-Fermi-Dirac-Gombas work functions (J.R. Smith, Ph.D. thesis, Ohio State University, Columbus, 1968, unpublished, and Ref. 26) are

respectively 0, 1.3 and 2.3 eV independent of r_s and do involve a precise cancellation of the divergent terms as $r_s \to 0$, we have extended the statistical calculations of Smith (Ref. 23) including the first density gradient correction to the kinetic energy to the high density region. Precisely the same behavicur for the high density work function is again observed with a maximum of 4.05 eV occuring at $r_{s=1.3}$, and rapidly vanishing at $r_s \simeq 0.57$.

94. C. Warner, in Thermionic Conversion Specialists Conference , San Diego, 10 , 170 (1971).

95. W. Jones and W.H. Young, J. Phys. C 4 , 1322 (1971).

96. W. Jones, Phys. Lett. 34A , 351 (1971).

97. N.H. March and W.H. Young, Proc. Phys. Soc. 72 , 182 (1958).

98. J. Goodisman, Phys. Rev. A 1 , 1574 (1970).

99. J. Shy-Yih Wang and M. Rasolt, Phys. Rev B 13 , 5330 (1976).

100. C. Moller and M.S. Plesset, Phys. Rev. 46 , 618 (1934).

101. L.M. Delves, Nucl. Phys. 41 , 497 (1963); 45 , 313 (1963); Math. Comput. 91 , 380 (1965).

102. C. Schwartz, Ann. Physics (N.Y.) 2 , 170 (1959).

103. S. Aranoff and J. Percus, Phys. Rev. 166 , 1255 (1968).

104. L.M. Delves, Proc. Phys. Soc. (London) 92 , 55 (1967).

105. A. Dalgarno and A.L. Stewart, Proc Roy. Soc. (London) 85 , 399 (1965).

106. V. Heine, Phys. Rev. 153 , 673 (1967).

107. J. Hubbard, Proc. Phys. Soc. (London) 92 , 921 (1967).

108. L. Hodges, R.E. Watson, and H. Ehrenreich, Phys. Rev. B 5 , 3953 (1972).

109. N.W. Ashcroft, Phys. Lett. 23 , 48 (1966).

110. J.P. Perdew and R. Monnier, Phys. Rev. Lett. 37 , 1286 (1976); R. Monnier and J.P. Perdew, Phys. Rev. B 17 , 2595 (1978).

111. G. Paasch and M. Heitschold, Phys. Status Solidi (b) 83 , 209 (1977).

112. C.Q. Ma and V. Sahni (unpublished).

113. G.D. Mahan, Phys. Rev. B 12 , 5585 (1975).

114. In obtaining the numerical values of the exact surface exchange energy, we have performed multi-dimensional (up to 5-dimensional, see Appendix F) integrations employing an iterative and adaptive Monte Carlo scheme with a new algorithm, see G.P. Lepage, J. Comput. Phys. 27 , 192 (1978).

115. I.S. Gradshteyn and I.M. Ryzhik, Tables of Integrals Series and Products (Academic Press, New York, 1965), p. 721.